Foraging in a Complex World: From Individual Flight Performance to Collective Behavior in Bumblebees (Bombus Impatiens)

Foraging in a complex world: from individual flight performance to collective behavior in bumblebees (*Bombus impatiens*)

A dissertation presented by

James DeWitt Roberts Crall

to

The Department of Organismic and Evolutionary Biology

in partial fulfillment of the requirements
for the degree of

Doctor of Philosophy

in the subject of

Biology

Harvard University
Cambridge, MA
March 2017

Dissertation Advisor: Dr. Naomi Pierce James DeWitt Roberts Crall

Foraging in a complex world: from individual flight performance to collective behavior in bumblebees (*Bombus impatiens*)

Abstract

Foraging is a crucial and remarkably complex behavior that is key to survival. For social insects such as bumblebees, successful foraging depends on a combination of individual traits (e.g. physiological and biomechanical performance of individual workers) and collective behavioral strategies for regulating food intake at the colony level. Here, I use foraging behavior in bumblebees as a lens to explore how insects cope with challenging, natural environments, scaling from individual performance to group dynamics. First, I explore how bumblebee foragers cope with structural clutter, with particular emphasis on the allometry of maneuverability and flight performance (Chapter 1). Next, I investigate how the variable, turbulent wind flows that characterize natural environments affect flight stability (Chapter 2) and landing behavior (Chapter 3) of bumblebee foragers. Moving from the individual to the colony level, I then develop an automated, high throughput behavioral tracking system (Chapter 4) capable of following uniquely identified individuals in visually complex environments, and use this system to explore the distribution and regulation of foraging activity across entire bumblebee colonies (Chapter 5). Finally, I use this same tracking system to examine the effects of exposure to a common neonicotinoid pesticide (imidacloprid) encountered during foraging, and show that it disrupts aspects of social behavior and communication in bumblebee colonies (Chapter 6).

Contents

Acknowledgements

The work presented throughout this thesis was made possible only through the wisdom, support, and effort of innumerable incredible people, a small portion of whom are listed here. For those omitted, please know that I appreciate your help and support.

I am grateful to have received generous funding support from sources both within the Harvard community (the Department of Organismic and Evolutionary Biology, the Mind, Brain, and Behavior Initiative, the Museum of Comparative Zoology, and the David Rockefeller Center for Latin American Studies), and beyond (the National Science Foundation, the Organization for Tropical Studies, and the Company of Biologists).

I have also benefitted from incredible institutional support, and thank members of the support, cleaning, and administrative staff from the Harvard Forest, the Center for Brain Science, STRI at Barro Colorado Island, OTS at Las Cruces Biological Station (in particular Rodolfo Quiros and Randy Figueroa), and the Museum of Comparative Zoology for supporting my work. I owe an especially heavy debt to the incredible support staff at the Concord Field Station, including Ken (the Man) Wilcox, Pedro Ramirez, Lisa Litchfield, Andra Hollis, and Somer O'Brien for their support (and patience) over the years.

I am fortunate to have had the opportunity of working during my PhD research with so many brilliant and inspiring fellow students, mentees, and collaborators, including Dominic Akandwanaho, Maude Baldwin, Leonora Bittleston, Julia Brokaw, Lettie Cabot, Jeremy Chang, Glenna Clifton, Mark Cornwall, Rod Eastwood, Susie Gagliardi, Nick Gravish, Sawyer Hescock, Jay Iwasaki, Sarah Kocher, Mirko Kovac, Kelsey McKenna, Nora Mishanec, Talia Moore, Andrew Mountcastle, Anita Murrell, Jake Peters, Sridhar Ravi, Ivo Ros, Daniel Rundle, Mary Salcedo, Mariah Slone, Andre Souffrant, and Callin Switzer. You have shaped how I think about the world and how I do science, so thank you.

I thank my Dissertation Advisory Committee, Andy Biewener, Elizabeth Crone, and Benjamin de Bivort, for their support and contributions to my work, as well as my thesis advisors, Stacey Combes and Naomi Pierce, for encouraging my scientific explorations and continuously inspiring my curiosity about the natural world.

Finally, I owe an immense debt of gratitude to my community outside of OEB (especially the Guira Woods crew) and my family, Blake and Oliver, for filling my life with so much joy and laughter during the long road of this PhD.

For Oliver and Blake

And to a world filled with more knowledge and compassion

Introduction

Natural environments are highly complex. Resources are distributed patchily in both space and time, and abiotic conditions such as temperature, light, and wind shift dramatically on timescales from seconds to seasons, and on spatial scales from patches of grass to entire mountain ranges.

For social insects, the challenge of coping with environmental complexity is twofold: First, individual workers must be physiologically, biomechanically, and behaviorally capable of performing daily activities such as gathering food, finding mates, and escaping predators. In addition, social insects (i.e. ants, bees, wasps, and termites) live in groups where the fitness of individual workers is tightly linked to the success of the group (Hölldobler & Wilson, 2009) and work is performed by many individuals in concert (Oster & Wilson, 1978). As a consequence, social insects must also have collective behavioral strategies for coping with rapid, and often drastic, changes in the environment, in addition to adaptations at the individual, organismal level. Social insects must be robust to environmental perturbations as both individuals, and as groups.

Foraging behavior provides a powerful example of this dynamic. In social insects, developing brood within the nest depend on the intake of resources (i.e. nectar and pollen in the case of bumblebees) that are physically separated from the nest, and foragers provide the sole link between growth within the nest and resources in the environment.

For a foraging bee, gathering resource form the outside world and bringing them back to nest requires a remarkable combination of organismal traits; she must draw on

substantial energy reserves to fuel metabolically costly flight (Heinrich, 1975), use this energy to power wing movements that keep her aloft and generate maneuvers and accelerations (Dudley, 2002), and use sophisticated visual odometry systems and landmark learning (Degen et al., 2016) to navigate and control flight through a complex visual landscape. At the colony level, there must be efficient and robust systems for maintaining a consistent flux of resources into the colony while allocating workers to multiple tasks (e.g. nursing, nest defense, and maintenance, in addition to foraging), all of which are vital to colony growth and survival. Colonies must also be able to cope with environmental perturbations such as resource scarcities, or loss of foragers to predation. Finally, all of this must occur in the absence of any central control.

In this thesis, I explore foraging behavior in bumblebee (*Bombus impatiens*) colonies, with a particular focus on how both individual workers (Chapters 1-3) and colonies as integrated units (Chapter 4-6) cope with the challenges posed by natural environmental variation.

In Chapter 1 (Crall, Ravi, Mountcastle, & Combes, 2015b), I explore a key component of environmental complexity facing foraging bumblebees: structural clutter. Despite significant progress in our understanding of the biomechanics and aerodynamics of insect flight, maneuverability and its importance for flight performance in real-world environments is less well understood. Foraging bees must maneuver through clutter on a daily basis to access floral resources. By training bees to maneuver through a constricted flight tunnel that forces them to maneuver vertically and laterally, I show that flight performance is reduced in larger bees. Contrary to predictions,

however, the observed allometry of flight performance is not driven by the scaling of acceleration capacity. Instead, decreased flight performed in larger bees appears to result from the scaling of collision risk, rather than fundamental biomechanical or physiological limitations on acceleration.

In Chapter 2, I explore the effects of variable wind environments on flight performance and stability in bumblebees. First, using an automated, radio-frequency identification system paired with detailed wind measurements in an outdoor environment, I measure wind speeds and environmental turbulence experienced by foraging bumblebees in natural environments. Then, I recreate these flow conditions in a wind tunnel to assess the impacts of turbulence on flight performance. I find that field-realistic turbulence negatively impacts flight stability of bees, and identity kinematic parameters that bumblebees use to mitigate the effects of this turbulence, in particular shifts in wingbeat frequency and stroke amplitude.

In Chapter 3 (Chang, Crall, & Combes, 2016), I investigate how wind impacts landing, a behavior that bees must perform successfully hundreds to thousands of times daily. Specifically, I test the effects of wind on an established visual landing strategy (Baird, Boeddeker, Ibbotson, & Srinivasan, 2013) that allows for smooth deceleration when approaching looming objects. While bumblebees decelerate smoothly during landing in still air, as predicted by the model, in the presence of a headwind bees show no deceleration, resulting in high impact collisions upon landing. I provide evidence that, instead of abandoning this visual control strategy, bees may be prevented from decelerating by local flow conditions around flowers. These results highlight the

importance of robust morphological designs that can provide robust fail-safes to sophisticated control mechanisms in challenging environmental conditions.

Turning to the group level, in Chapter 4 (Crall, Gravish, Mountcastle, & Combes, 2015a), I develop a low-cost, image based technique for tracking uniquely identified tags in visually complex scenes. This technique has the advantages of being capable of tracking multiple individuals simultaneously on heterogeneous backgrounds, and maintains identity even if tracking is interrupted, making it well-suited to long-term studies of individual behavior in animal groups. As a proof-of-principle, I use this technique to follow the movement paths of uniquely-identified workers within bee colonies. Finally, I develop an open-source software package in Matlab to make this technique freely available to researchers.

In Chapter 5, I use this technique to explore the extent and importance of inter-individual behavioral variation within bumblebee colonies, focusing on how colonies regulate foraging activity in response to disturbance (i.e. forager predation). I find that foraging activity is highly skewed within bumblebee colonies, with a small number of workers performing the majority of foraging work. I find that colonies actively regulate the total amount of foraging activity and its distribution across workers at the colony level. I also find evidence for widespread behavioral idiosyncrasy among workers in every behavioral trait I measure, and that this idiosyncrasy plays a key role in determining patterns of task switching under colony perturbation. These results provide evidence for a key role of spatial heterogeneity on information flow within nests and

provide insight into the dynamic regulation of collective behavior in social insect colonies.

In Chapter 6, I explore the effects of exposure to a common neonicotinoid pesticide (imidacloprid) encountered during foraging in agricultural and residential environments on collective behavior in bumblebee colonies. Using a split-colony design, with different treatment groups within each colony, I show that exposure to field-realistic, brief doses of imidacloprid reduces rates of nest care and alters patterns of social interaction within bumblebee colonies. These results provide evidence for a previously unknown behavioral mechanism by which neonicotinoid pesticides may impact bee colony growth (Whitehorn, O'Connor, Wackers, & Goulson, 2012).

In the Appendix (Crall et al., 2016), I explore the dynamics of collective light avoidance in a gregarious cockroach, *Blaberus discoidalis*. While groups of cockroaches perform better than individuals at collectively avoiding a mobile light stimulus, individual cockroaches show consistent individual variation in performance at this task, and that this variation is robust to group composition. Individual performance in groups shows no correlation to performance in a solitary context, however, suggesting that social plays an important role in modulating individual variation in behavior in these groups.

References

Baird, E., Boeddeker, N., Ibbotson, M. R., & Srinivasan, M. V. (2013). A universal strategy for visually guided landing. *Proceedings of the National Academy of Sciences of the United States of America*, *110*(46), 18686–18691. http://doi.org/10.1073/pnas.1314311110

Chang, J. J., Crall, J. D., & Combes, S. A. (2016). Wind alters landing dynamics in bumblebees. *The Journal of Experimental Biology*, *219*(Pt 18), 2819–2822. http://doi.org/10.1242/jeb.137976

Crall, J. D., Gravish, N., Mountcastle, A. M., & Combes, S. A. (2015a). BEEtag: A Low-Cost, Image-Based Tracking System for the Study of Animal Behavior and Locomotion. *PLoS ONE*, *10*(9), e0136487–13. http://doi.org/10.1371/journal.pone.0136487

Crall, J. D., Ravi, S., Mountcastle, A. M., & Combes, S. A. (2015b). Bumblebee flight performance in cluttered environments: effects of obstacle orientation, body size and acceleration. *The Journal of Experimental Biology*, *218*(Pt 17), 2728–2737. http://doi.org/10.1242/jeb.121293

Crall, J. D., Souffrant, A. D., Akandwanaho, D., Hescock, S. D., Callan, S. E., Coronado, W. M., et al. (2016). Social context modulates idiosyncrasy of behaviour in the gregarious cockroach Blaberus discoidalis. *Animal Behaviour*, *111*(C), 297–305. http://doi.org/10.1016/j.anbehav.2015.10.032

Degen, J., Kirbach, A., Reiter, L., Lehmann, K., Norton, P., Storms, M., et al. (2016). Honeybees Learn Landscape Features during Exploratory Orientation Flights. *Current Biology*, 1–6. http://doi.org/10.1016/j.cub.2016.08.013

Dudley, R. (2002). The Biomechanics of Insect Flight. Princeton University Press.

Heinrich, B. (1975). Energetics of pollination. *Annual Review of Ecology and Systematics*, *6*(1), 139–170. http://doi.org/10.1146/annurev.es.06.110175.001035

Hölldobler, B., & Wilson, E. O. (2009). The Superorganism. W. W. Norton & Company.

Oster, G. F., & Wilson, E. O. (1978). Caste and Ecology in the Social Insects.

Whitehorn, P. R., O'Connor, S., Wackers, F. L., & Goulson, D. (2012). Neonicotinoid pesticide reduces bumble bee colony growth and queen production. *Science*, *336*(6079), 351–352. http://doi.org/10.1126/science.1215025

Chapter 1: Bumblebee flight performance in cluttered environments: Effects of obstacle orientation, body size, and acceleration

Reprinted from:
Crall, J. D., Ravi, S., Mountcastle, A. M., & Combes, S. A. (2015). Bumblebee flight performance in cluttered environments: effects of obstacle orientation, body size and acceleration. *The Journal of Experimental Biology*, *218*(Pt 17), 2728–2737. http://doi.org/10.1242/jeb.121293

© 2015. Published by The Company of Biologists Ltd | The Journal of Experimental Biology (2015) 218, 2728-2737 doi:10.1242/jeb.121293

RESEARCH ARTICLE

Bumblebee flight performance in cluttered environments: effects of obstacle orientation, body size and acceleration

James D. Crall[1,*], Sridhar Ravi[2], Andrew M. Mountcastle[1] and Stacey A. Combes[1]

ABSTRACT

Locomotion through structurally complex environments is fundamental to the life history of most flying animals, and the costs associated with movement through clutter have important consequences for the ecology and evolution of volant taxa. However, few studies have directly investigated how flying animals navigate through cluttered environments, or examined which aspects of flight performance are most critical for this challenging task. Here, we examined how body size, acceleration and obstacle orientation affect the flight of bumblebees in an artificial, cluttered environment. Non-steady flight performance is often predicted to decrease with body size, as a result of a presumed reduction in acceleration capacity, but few empirical tests of this hypothesis have been performed in flying animals. We found that increased body size is associated with impaired flight performance (specifically transit time) in cluttered environments, but not with decreased peak accelerations. In addition, previous studies have shown that flying insects can produce higher accelerations along the lateral body axis, suggesting that if maneuvering is constrained by acceleration capacity, insects should perform better when maneuvering around objects laterally rather than vertically. Our data show that bumblebees do generate higher accelerations in the lateral direction, but we found no difference in their ability to pass through obstacle courses requiring lateral versus vertical maneuvering. In sum, our results suggest that acceleration capacity is not a primary determinant of flight performance in clutter, as is often assumed. Rather than being driven by the scaling of acceleration, we show that the reduced flight performance of larger bees in cluttered environments is driven by the allometry of both path sinuosity and mean flight speed. Specifically, differences in collision-avoidance behavior underlie much of the variation in flight performance across body size, with larger bees negotiating obstacles more cautiously. Thus, our results show that cluttered environments challenge the flight capacity of insects, but in surprising ways that emphasize the importance of behavioral and ecological context for understanding flight performance in complex environments.

KEY WORDS: Insect flight, Collision avoidance, *Bombus impatiens*, Clutter, Environmental complexity, Locomotion

INTRODUCTION

Natural environments are highly variable over space and time, and this complexity has important consequences for animal locomotion (Combes and Dudley, 2009; Dickinson et al., 2000). The variable costs and constraints associated with locomotion in complex habitats affect broad ecological patterns of animal movement and habitat use (Combes and Dudley, 2009; Dickinson et al., 2000; Hadley and Betts, 2009; Shepard et al., 2013), as well as biotic interactions (Morice et al., 2013). Determining how environmental complexity affects and limits locomotion is thus key to understanding the ecology and evolution of animals whose fitness is tied to movement through natural environments.

Flying insects must negotiate three-dimensional clutter consisting of biological features such as grass, shrubs and trees, as well as man-made structures such as buildings and cars. Successful navigation through cluttered environments results from a remarkable integration of sensory perception, control strategies, and physiological and morphological adaptations for producing aerodynamic forces and torques (Dudley, 2002b; Lin et al., 2014). The costs associated with moving through structurally complex environments may be particularly acute for flying animals, given the high metabolic costs of flight, particularly at low speeds (Dudley, 2002b).

Historically, the ability to navigate through cluttered environments has been attributed to 'maneuverability', but the definition of this term is problematic. Interpretations can generally be divided into two broad categories: (1) narrower, physiological or mechanical definitions [e.g. minimum radius of curvature (Norberg and Rayner, 1987) or acceleration capacity (i.e. axial agility) (Buchwald and Dudley, 2010; Dillon and Dudley, 2004; Dudley, 2002a)] and (2) broader, integrative definitions [e.g. the ability to avoid collisions in cluttered environments (Stockwell, 2001; Swaddle and Witter, 1998) or the ability to evade a predator (Combes et al., 2012; Domenici, 2001)] that focus on successful performance of a complex task requiring turns and accelerations.

Much of the previous quantitative work on maneuverability has focused on the narrower, physiological and mechanical concepts because these are easier to measure in the laboratory, and because integrative definitions of maneuverability are likely to be context specific (Dudley, 2002a); however, the connections between isolated maneuvers performed in the lab and complex tasks performed in natural environments are not always clear. For example, while both higher acceleration capacity and the ability to fly through cluttered environments are intuitively associated with maneuverability, it is not clear whether the former directly determines the latter.

Despite a wealth of biomechanical and ecomorphological hypotheses, few studies exist that directly link biomechanical flight performance to navigation through clutter. For example, one common prediction is that higher maximum acceleration capacity (including both changes in velocity along a linear path and turning or radial accelerations) should allow for sharper turns and a lower minimum turning radius (Aldridge and Brigham, 1988; Andersson and Norberg, 1981; Thomas, 1996), thus improving biomechanical flight performance in cluttered environments (Norberg and Rayner,

[1]Concord Field Station, Department of Organismic and Evolutionary Biology, Harvard University, 100 Old Causeway Rd, Bedford, MA 01730, USA. [2]School of Aerospace Mechanical and Manufacturing Engineering, RMIT University, Melbourne, VIC 3001, Australia.

*Author for correspondence (james.crall@gmail.com)

Received 17 February 2015; Accepted 30 June 2015

The Journal of Experimental Biology

The Journal of Experimental Biology (2015) 218, 2728-2737 doi:10.1242/jeb.121293

1987; Thomas and Balmford, 1995). This simple prediction assumes that animals flying through clutter regularly operate near the limits of their acceleration capacity, an assumption that remains almost entirely untested for most taxa. One goal of the current study was therefore to provide direct, empirical data on flying bumblebees that reveal which aspects of biomechanical flight performance are most relevant to the task of successfully navigating through complex environments. We used the length of time required to traverse a cluttered environment (i.e. transit time) as our metric of flight performance. Because energy consumption is largely independent of flight speed in bumblebees (Dudley and Ellington, 1990; Ellington et al., 1990), time spent in flight is closely correlated with total energy consumption, which is at the heart of nearly all foraging decisions in bumblebees (Heinrich, 2004); thus, transit time is likely to be an ecologically relevant feature of flight performance in natural environments.

One salient component of environmental clutter is obstacle orientation. Whereas obstacles in the natural world can occur in any orientation, flying insects are unlikely to have equivalent capacities for maneuvering in all directions. Rotational moments of inertia differ among the three body axes, and flapping wings play a larger role in resisting rotations around some axes (e.g. flapping counter-torque; Hedrick et al., 2009). These differences are likely to affect an insect's ability to generate changes in body position or orientation along various axes, as well as to resist changes imposed by external perturbations. Recent work has shown that bumblebees flying in unsteady flow experience the greatest rotational instabilities around the roll axis and the greatest translational instabilities in the lateral direction, regardless of whether the oncoming flow disturbances are oriented vertically or horizontally (Ravi et al., 2013). This directional instability may arise from the body having a lower rotational moment of inertia around the roll axis than around the pitch or yaw axes. At the same time, decreased inertia around the roll axis could make it easier for bees to initiate voluntary rotations around the roll axis and to move laterally, suggesting that vertically oriented obstacles (which require lateral maneuvers in order to avoid them) may be easier for bees to negotiate than horizontal ones. Despite this potential anisotropy in maneuvering performance, previous studies have focused almost exclusively on lateral maneuvering, in the context of both flight performance (Stockwell, 2001; Swaddle and Witter, 1998) and visual responses to obstacles (Kern et al., 2012).

Body size is also hypothesized to affect flight performance in clutter, and this assertion is supported by at least one previous study, which showed that larger bats experience more collisions when flying through an obstacle course (Stockwell, 2001). Mechanistic explanations for the hypothesis that larger animals perform more poorly in cluttered environments often invoke the predicted decrease in mass-specific force production (and thus acceleration) with increased body size (Vogel, 1994). Maximum mass-specific force production does decrease with body size in bees (Buchwald and Dudley, 2010; Dillon and Dudley, 2004) (although perhaps not across insects more broadly; see Marden, 1987), and there is some evidence that accelerations during free flight decrease with body size in midges (Crompton et al., 2003). Limits to acceleration capacity may reduce an animal's ability to rapidly change its speed and/or direction to avoid collisions, and may also impose limits on flight speed through cluttered environments, as increased speed along a curved path requires higher radial acceleration. Therefore, if bees do rely on maximum acceleration to maneuver through cluttered environments, the predicted negative allometry of acceleration capacity should restrict larger bees to moving more slowly through these environments.

To examine the influence of body size and obstacle orientation on flight performance in cluttered environments, and to determine which aspects of performance are most critical for traversing these environments, we filmed bumblebees (*Bombus impatiens* Cresson 1863) flying through obstacle courses requiring either lateral or vertical maneuvers and reconstructed their three-dimensional flight paths. We analyzed these flight paths to investigate (a) whether flight performance through clutter is impaired in larger bees, (b) whether this effect is due to limitations on maximum acceleration, and (c) whether obstacle orientation affects flight performance in complex environments.

RESULTS

Maximum flight speed in a wind tunnel

To investigate the relationship between body size and maximum flight speed in the absence of obstacles, we tested the maximum flight speed of 19 bumblebee (*B. impatiens*) foragers (ranging from 72 to 260 mg in mass) from a single hive in a wind tunnel. Top flight speed increased significantly with body mass [maximum velocity (m s^{-1}) versus body mass (g), $y=10.48+5.59\times\log_{10}(x)$, $P=0.0007$, $R^2=0.468$; supplementary material Fig. S1).

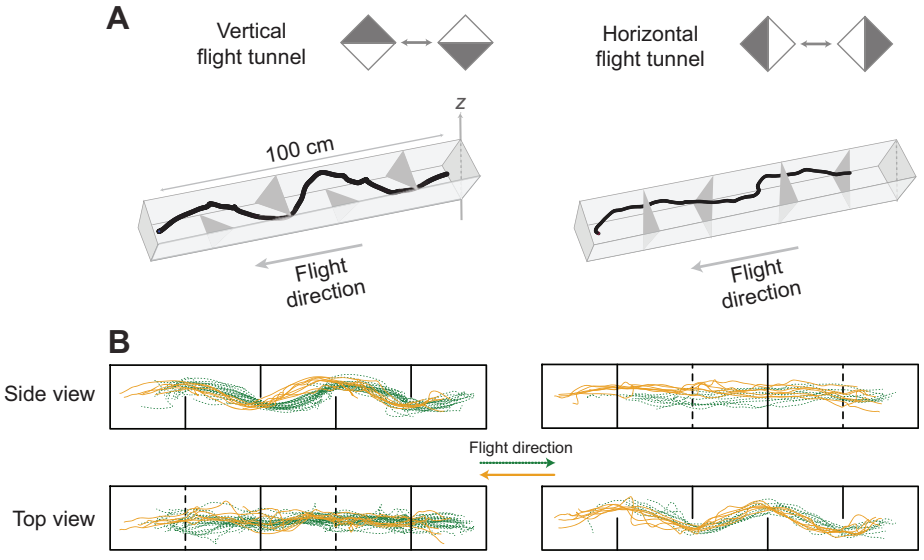

Fig. 1. Flight tunnels with obstacles for testing flight performance in cluttered environments. (A) Schematic diagram of vertical and horizontal flight tunnels. Tunnels had a diamond-shaped cross-section with obstacles alternately occluding either the top and bottom halves of the tunnel to induce vertical maneuvering (vertical flight tunnel, left) or the left and right halves to induce lateral maneuvering (horizontal flight tunnel, right). Sample three-dimensional flight paths through each tunnel are shown below. (B) Flight paths of all bees flying to the right (green dashed line, entering the hive) or to the left (solid yellow line, exiting the hive), through the vertical and horizontal flight tunnels.

The Journal of Experimental Biology (2015) 218, 2728-2737 doi:10.1242/jeb.121293

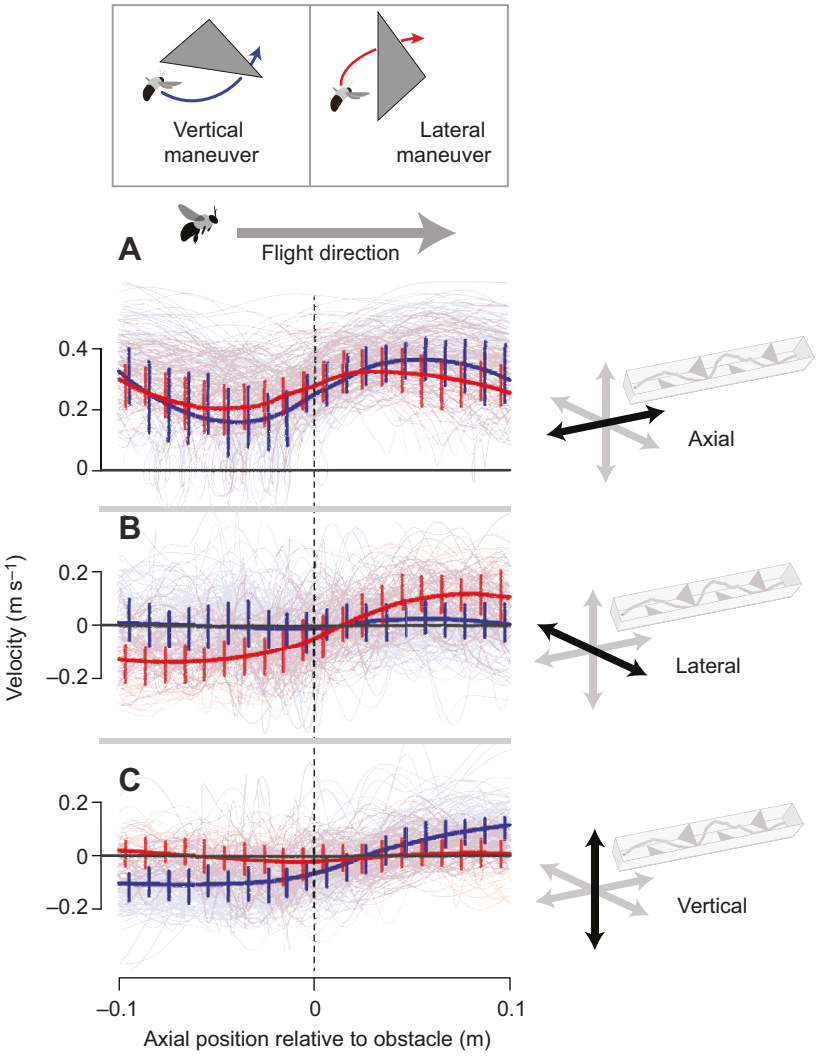

Fig. 2. Flight velocity versus position relative to the obstacle for vertical and lateral maneuvers. (A) Axial, (B) lateral and (C) vertical flight velocity. Thin, transparent traces show raw data for all maneuvers (blue, vertical; red, lateral) in all bees. Solid lines show local regression-smoothed average traces for each type of maneuver, and vertical bars represent interquartile range for spatially binned data at 1 cm intervals.

Flight performance in clutter

To investigate flight performance of bumblebees in cluttered environments, we recorded voluntary flight trajectories (N=56) of individual bumblebees either leaving or returning to the hive through one of two flight tunnels. One flight tunnel required the bees to maneuver vertically to avoid obstacles (referred to as the 'vertical' flight tunnel, N=37), while the other required the bees to maneuver laterally (the 'horizontal' flight tunnel, N=19; Fig. 1A). Bees followed a roughly sinusoidal path in the direction of obstacle avoidance (i.e. maneuvering up/down in the vertical flight tunnel and left/right in the horizontal flight tunnel) while maintaining a relatively straight flight path along the other axis (Fig. 1B). Flight paths for bees entering and exiting the hive were qualitatively similar. Median axial velocity (i.e. flight speed along the major axis of the flight tunnel) across trials was 0.28±0.06 m s^{-1}, in close agreement with (and not significantly different from, t=−1.75, d.f.= 55, P=0.09) previously reported bumblebee flight speeds of 0.29±0.05 m s^{-1} in an obstacle-free flight tunnel with similar dimensions and strong optic flow (Baird et al., 2010).

In both obstacle courses, bees reduced axial velocity before passing obstacles and increased velocity afterwards (Fig. 2A). Lateral and vertical velocity profiles of flights in the two obstacle courses closely mirrored each other. Bees executing vertical maneuvers showed a distinct sign change in vertical velocity before and after passing obstacles (i.e. flying up/down to avoid obstacles and then in the opposite direction to return to their original height), while showing no clear changes in lateral velocity as they passed obstacles; bees executing lateral maneuvers showed the opposite trend, with distinct sign changes in lateral velocity as they maneuvered left/right before and after passing obstacles, with no change in vertical velocity (Fig. 2B,C).

Maximum acceleration differed significantly with direction (i.e. between the axial, vertical and horizontal axes) but not between the two obstacle courses. Overall, maximum lateral acceleration (i.e. acceleration in the horizontal plane, perpendicular to the long axis of the tunnel; Fig. 3A) was higher than maximum vertical acceleration (Fig. 3A; a_{lat}–a_{vert}: t=9.82, d.f.=55, P≪0.01), and both lateral and vertical acceleration were higher than axial acceleration (i.e. acceleration along the long axis of the flight tunnel; Fig. 3A; a_{lat}–a_{ax}: t=10.29, d.f.=55, P≪0.01; a_{vert}–a_{ax}: t=4.08, d.f.=55, P≪0.01). Despite this difference in acceleration across axes, there was no difference in transit time between the vertical and horizontal flight tunnel (Fig. 3B; t=0.94, d.f.=32.5, P=0.35).

Body size had a strong effect on many aspects of flight performance in clutter (Fig. 4). Transit time through the obstacle course increased significantly with body size (Fig. 4A, Table 1). Maximum total acceleration (i.e. three-dimensional acceleration) showed no significant relationship with body size, and had a slightly positive trend towards increasing rather than decreasing with body

The Journal of Experimental Biology (2015) 218, 2728-2737 doi:10.1242/jeb.121293

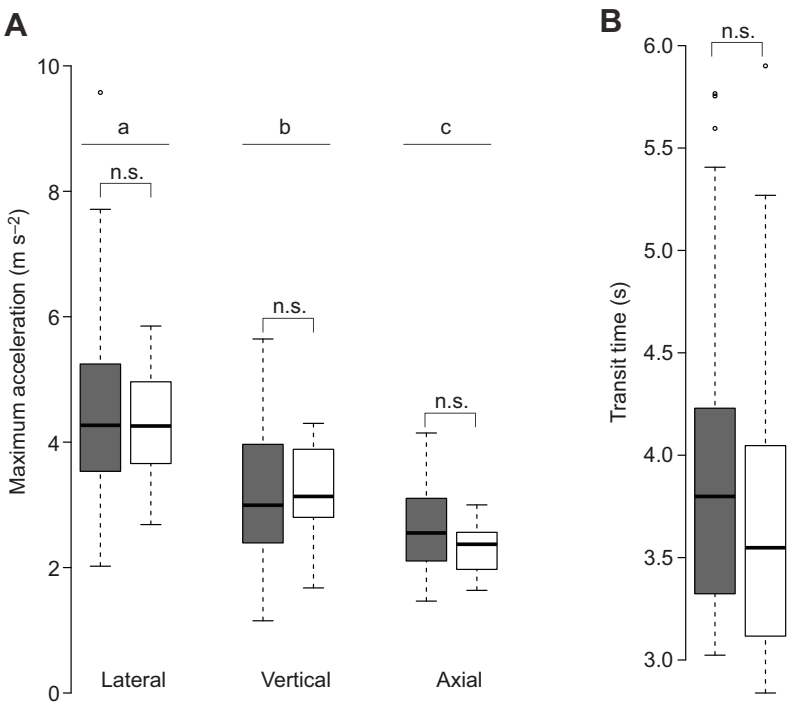

Fig. 3. Maximum acceleration and normalized transit time in the flight tunnels. (A) Maximum acceleration in the lateral, vertical and axial directions in the vertical (gray) and horizontal (white) flight tunnels. Letters denote significant differences between groups for α=0.05. n.s. denotes non-significant differences. (B) Normalized transit time in the vertical (gray) and horizontal (white) flight tunnels.

size (Fig. 4B, Table 1). Path sinuosity increased significantly with body size (Fig. 4C, Table 1) while median flight speed decreased with body size (Fig. 4D, Table 1).

Maximum acceleration had little direct effect on any aspect of flight performance measured. Acceleration had a significant but weak effect on sinuosity (Fig. 5C, y=1.106+0.022x, t=2.53, d.f.=54, P=0.01, R^2=0.09), but no significant effect on either median flight speed (Fig. 5B, y=0.30+0.0050x, t=1.16, d.f.=54, P=0.25) or transit time through the course (Fig. 5A, y=3.78+0.020x, t=0.281, d.f.=54, P=0.78).

Impaired performance at larger body sizes was driven in part by an increase in corrective maneuvering in large bees. The number of corrective maneuvers (quantified as the total number of times bees reversed axial direction to avoid an obstacle) increased significantly with body length (Fig. 6A; $y=e^{-2.19+129.7x}$, z=3.3, d.f.=53, $P\ll0.01$), and had a significant, positive relationship with both path sinuosity (Fig. 6B; y=1.17+0.070x, t=7.2, d.f.=53, $P\ll0.01$, R^2=0.48) and flight speed (Fig. 6C; y=0.346−0.019x, t=−3.3, d.f.=53, $P\ll0.01$, R^2=0.15), both of which in turn directly affected transit time through the obstacle course (Fig. 4C,D).

DISCUSSION

The role of acceleration in flight performance through clutter

Our results show that larger bumblebees move more slowly through structural clutter (Fig. 4A), despite being capable of faster top flight speeds in a wind tunnel. While such impaired maneuverability at large body size is often attributed to the scaling of maximum acceleration capacity, we found no evidence to support this hypothesis for bumblebees.

First, we found a statistically insignificant positive trend in the relationship between maximum observed acceleration and body size in bumblebees (Fig. 4B; supplementary material Fig. S2), whereas a negative relationship is expected from both theoretical and empirical results for bees (Buchwald and Dudley, 2010; Dillon and Dudley, 2004). While this could potentially be due to methodological differences (e.g. measuring accelerations in free-flight versus load-lifting experiments), we believe a more parsimonious explanation is that the behavioral context presented here (voluntarily maneuvering around obstacles) does not elicit or require maximum acceleration from bumblebees. However, data on maximum acceleration in free flight are rare, and further experiments directly comparing maximum free-flight acceleration across behavioral contexts would be valuable for interpreting different assays of maximum flight performance.

A second, more direct line of evidence supporting the conclusion that scaling of maximum acceleration is not responsible for the flight performance trends we observed is that maximum acceleration had no direct effect on median flight speed (Fig. 5B), and only a weak effect on path sinuosity (Fig. 5A). Median flight speed and path sinuosity explain nearly all (~96%) of the variance in transit time (data not shown), and thus our results provide no evidence that maximum acceleration contributes directly to transit time through an obstacle course (Fig. 5C).

Finally, bumblebees in our flight trials exhibited anisotropy in maximum acceleration along different axes, with lateral accelerations being significantly higher than vertical accelerations (Fig. 3A). If maximum acceleration capacity limited transit time through an obstacle course, we would predict that transit time in the vertical obstacle course (which requires vertical movements to traverse) would be longer than in the horizontal obstacle course; however, there was in fact no difference in transit time between the two obstacle courses (Fig. 3C).

Alternative mechanisms for the effects of body size on flight performance

Although we found no evidence that maximum acceleration limits flight performance in cluttered environments, we did find that body size has a significant effect on both sinuosity and flight speed, the two fundamental components of transit time, suggesting that these variables may be more important in understanding limitations to flight in clutter than maximum acceleration capacity.

The Journal of Experimental Biology (2015) 218, 2728-2737 doi:10.1242/jeb.121293

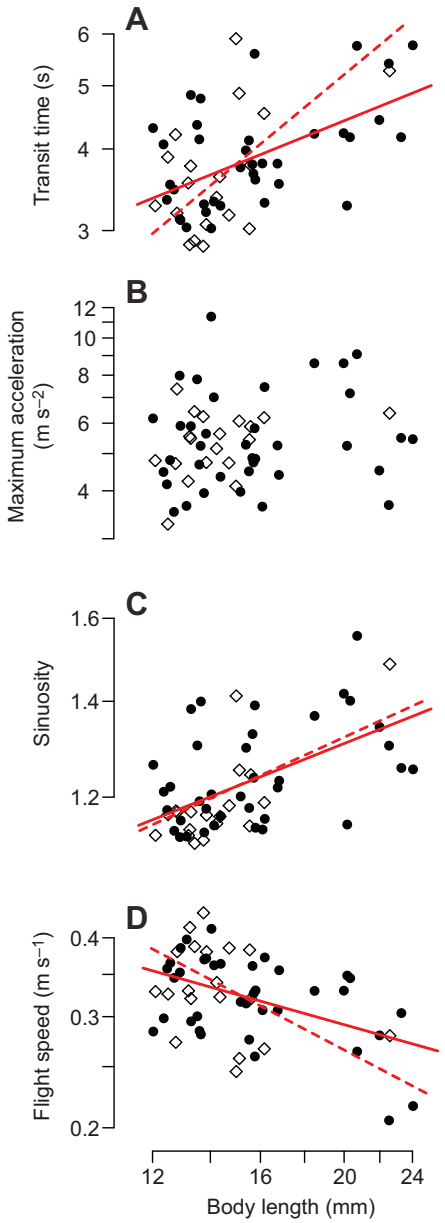

Fig. 4. Effect of body size on flight performance across trials in the flight tunnels. Log-transformed (A) transit time, (B) maximum acceleration, (C) sinuosity and (D) flight speed data versus body length for the vertical flight tunnel (filled circles) and horizontal flight tunnel (open diamonds). Red lines show results of ordinary least squares (solid) and major axis (dashed) regression for variables where body length has a significant effect at the α=0.05 level (Table 1).

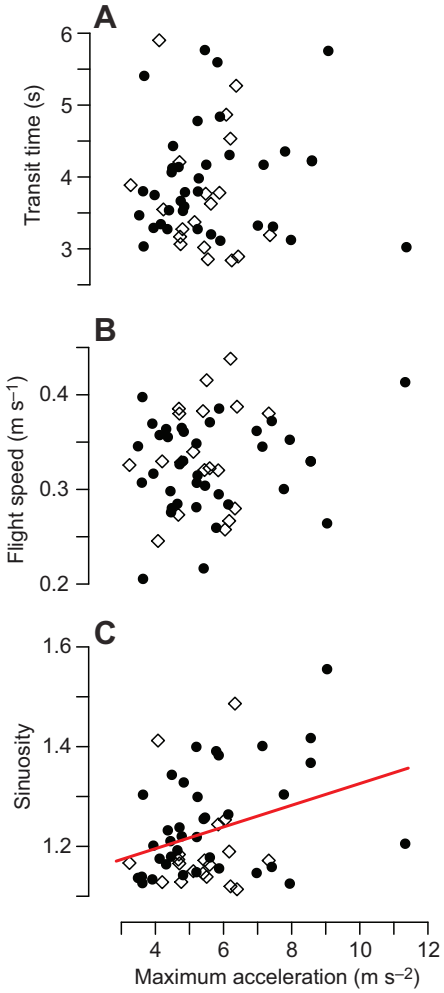

Fig. 5. Effect of maximum acceleration on flight performance across trials in the flight tunnels. (A) Transit time, (B) flight speed and (C) sinuosity data are shown versus maximum acceleration for the vertical flight tunnel (filled circles) and horizontal flight tunnel (open diamonds). Red lines show results of ordinary least squares regression for variables where maximum acceleration has a significant effect at the α=0.05 level.

Corrective maneuvers and flight performance in clutter

One important proximate factor in determining both path sinuosity and median flight speed was the number of corrective maneuvers performed by bees during flight trials. We found that performing more corrective maneuvers significantly increased path sinuosity and decreased median flight speed (Fig. 6B,C), and that the number of corrective maneuvers increased significantly with body size (Fig. 6A). These corrective maneuvers appear to be distinct from saccades or intermittent turns characteristic of flight in flies (Tammero and Dickinson, 2002) and bees (Boeddeker et al., 2010), as they were not distributed continuously throughout flights; corrective maneuvers were instead concentrated at times just before the bees passed obstacles (visible as traces that drop below the *x*-axis in Fig. 2A), and thus appear to be a form of collision avoidance behavior. The reason that corrective maneuvers affect path sinuosity seems clear, as such maneuvers necessarily increase the path length of flights. The relationship between corrective maneuvers and median speed is somewhat less clear, but is most likely driven by the reduction in velocity associated with the direction reversals that were performed as bees approached obstacles (Fig. 2).

Why do larger bees reverse direction to avoid obstacles more often than smaller bees? Potential explanations include allometric scaling of the visual system among bumblebees (see below), as well as the possibility that the extended body dimensions of larger bees increase the risk of collision. If collisions are more likely to occur in large bees as a result of their body dimensions and bees respond to impending collisions with corrective maneuvers (which appears to be true; Fig. 2A), then this could explain the greater number of corrective maneuvers in larger bees. This hypothesis raises intriguing questions about how individual-level flight characteristics are tuned in bees. For example, do large and small bees have innate differences in collision avoidance behavior, or are these differences learned? Future studies addressing the role of learning and other factors

The Journal of Experimental Biology (2015) 218, 2728-2737 doi:10.1242/jeb.121293

Table 1. Results from ordinary least squares and major axis regression of four flight metrics against body size

			OLS		MA	
Variable (y)	P	R^2	Slope	Intercept	Slope	Intercept
Transit time (s)	≪0.01	0.26	0.53	1.55	1.10	2.58
Max. acceleration (m s^{-2})	0.10	0.03	0.24	1.17	4.22	8.4
Sinuosity	≪0.01	0.30	0.24	0.52	0.28	0.59
Median flight speed (m s^{-1})	≪0.01	0.20	−0.38	−1.19	−0.72	−1.80

OLS, ordinary least squares; MA, major axis.
All equations are of the form $\log_{10}(y)$=intercept+slope×$\log_{10}$(body length), where body length is in m.

contributing to the flight path characteristics of individual bees flying through complex environments will be of particular interest in parsing these intriguing hypotheses.

Additional drivers of sinuosity and flight speed

Corrective maneuvers explain some, but not all, of the effect of body size on flight performance; the number of corrective maneuvers can account for approximately 67% of the variation in sinuosity and 45% of the variation in flight speed (see Materials and methods, 'Are corrective maneuvers sufficient to explain variation in speed and sinuosity?'). Some of the additional variation in path sinuosity with body size could result from simple geometry: larger bees have to leave more space between their body centroid and nearby obstacles to avoid collisions, and this necessarily results in longer, more sinuous flight paths. Assuming geometric similarity in flight paths, minimum path length through the obstacle course should be approximately 12% higher in a 24 mm bee versus a 12 mm one (assuming a clearance radius equal to half body length), perhaps helping to explain some of the residual variation in sinuosity.

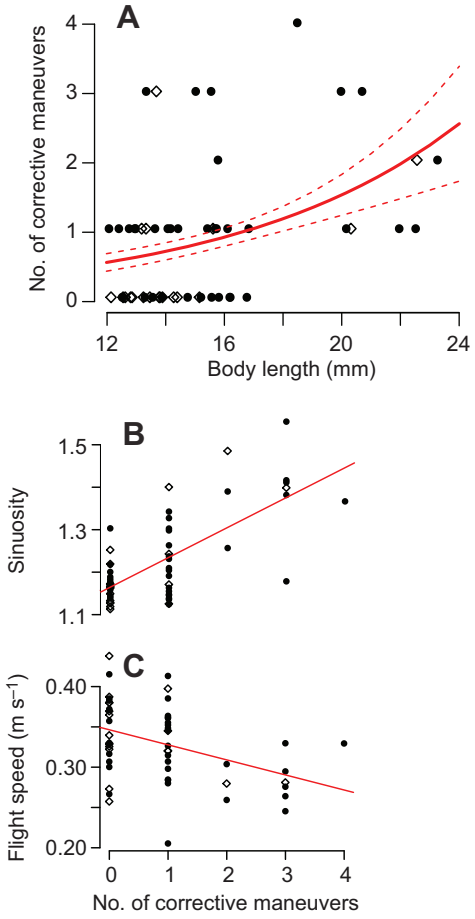

Fig. 6. Body length, sinuosity and flight speed versus number of corrective maneuvers. (A) Number of corrective maneuvers versus body length across all trials for the vertical flight tunnel (filled circles) and horizontal flight tunnel (open diamonds). Solid red line shows the predicted values ±1 s.d. (dashed lines) from a generalized model. (B) Sinuosity and (C) flight speed versus the number of corrective maneuvers across trials. Solid red lines represent the results of ordinary least squares regression for variables where the number of corrective maneuvers has a significant effect at the α=0.05 level.

The variation in flight speed across bees is somewhat less well explained by the number of course corrections, implying that other important factors contribute to the relationship between body size and flight speed. One known driver of free-flight speed in insects is cage size; in hawkmoths (*Manduca sexta*), smaller cages result in lower flight speeds, particularly near walls (Stevenson et al., 1995). If bumblebees react similarly to cages, and if the effects of cage size are relative to body length rather than being a function of absolute distance, then the same obstacle course may induce slower flight in larger bees than in smaller ones.

The mechanism that would drive such a body size-specific response to similar obstacle spacing is not clear, but it could be related to the processing of optic flow (i.e. the pattern of image motion across the eye), which many insects use to regulate flight speed. When enclosure size decreases, the rate of optic flow increases as a result of the increased proximity of enclosure surfaces and edges. Hawkmoths likely decrease flight speed in small enclosures in response to the increased optic flow rate near surfaces. Honeybees (Srinivasanet al., 1996) and bumblebees (Baird et al., 2010) similarly reduce flight speed in narrower tunnels in response to increased optic flow rate. The allometric scaling of the visual system in bumblebees could also contribute to this effect. Visual acuity (measured as the inverse of ommatidial acceptance angle) and the number of ommatidia per eye both increase with body size in bumblebees (Spaethe, 2003), and these factors could potentially affect the sensing of optic flow rate.

Regardless of the mechanisms involved, one of the ultimate reasons for reducing flight speed with body size in cluttered environments could be the scaling of material stresses (and the associated structural damage) during collisions with obstacles. In particular, material stress (τ) is defined as $\tau=\mathbf{F}/A$, where $\mathbf{F}$ is force and A is area. Assuming constant velocity and impact time, the force during a collision with an immovable object will be proportional to mass, and area will be proportional to surface area. As the ratio of volume (i.e. mass) to surface area increases with body size, this implies that material stresses (and thus potential damage) increase with body size. The scaling of material stress plays an important role in the allometry of body design and posture in mammals (Biewener, 1990), and may play an important role in the allometry of collisions during terrestrial locomotion in insects (Jayaram and Full, 2015). Thus, reducing flight velocity could be a strategy for reducing momentum and the potential damage that would result from

The Journal of Experimental Biology (2015) 218, 2728-2737 doi:10.1242/jeb.121293

collisions in larger bees. The need to mitigate damage resulting from collisions has clearly played an important role in shaping insect wing morphology (Foster and Cartar, 2011; Mountcastle and Combes, 2014), but few data exist to directly address the hypothesis that collision damage scales allometrically in insects.

Anisotropy of acceleration performance

Our finding that maximum accelerations are larger along the lateral axis is in accordance with previous findings that bumblebees flying through unsteady flow display the greatest accelerations in the lateral direction (Ravi et al., 2013). While in the previous study it was difficult to distinguish the effects of flow perturbations from voluntary flight maneuvers, the accelerations observed in the current study were clearly voluntary. Whether these results reflect a fundamental mechanical limitation on accelerations produced along the vertical and longitudinal axes, or whether there is an alternative explanation (such as behavioral disposition to lateral movements) remains unclear. Roll-based, lateral maneuvers are also dominant in honeybee flight (Boeddeker et al., 2010), so this may be a general feature of hymenopteran flight, or of insect flight more broadly; however, comparative data on movement along various axes during free flight in a wide range of insects is necessary to determine the generality of these results.

Conclusions

Our results show that maximum acceleration capacity is not the most important driver of flight performance in cluttered environments. Rather, flight speed and path length seem to be more critical in determining how quickly bees can negotiate complex environments. Both of these components may be strongly affected by learning, and one important limitation to the current study is that individual experience was not controlled, nor were individuals tracked over repeated trials to determine whether their performance changed with experience. While we do not believe that experience is likely to confound our results concerning body size, as the average size of bumblebee workers typically does not change over time (Couvillon et al., 2010) (so bees of different sizes should not differ systematically in age and experience level), this study cannot directly address the importance of learning for flight performance in cluttered environments. However, previous work clearly shows that on a larger spatial scale, bumblebees optimize flight routes (Lihoreau et al., 2012) and increase flight speed (Ohashi et al., 2008) with experience. Likewise, age may have important effects on flight performance (Vance et al., 2009), either through physiological changes or through the accumulation of morphological damage (Cartar, 1992). Future work addressing the role of behavioral context, learning and path optimization within individuals across time will be particularly important for understanding how flying insects negotiate complex natural environments.

Another limitation of not tracking individual bees is that single bees could be represented multiple times in the dataset, potentially resulting in pseudoreplication of the data. While we do not believe that pseudoreplication plays a significant role in our dataset, because we recorded trials from only a small fraction of the total foraging trips from the hive per day (~20 trials recorded per day out of several hundred foraging trips), our methodology cannot directly address the importance of this effect.

We also performed the current work with a single colony of *B. impatiens*, and social insects can display marked behavioral differences between colonies (LeBoeuf and Grozinger, 2014; Pinter-Wollman, 2012; Maebe et al., 2013). There has been no previous work to our knowledge exploring colony-level variation in flight performance, and our single-hive experimental design did not allow us to test for colony-level effects. Investigating colony-level differences in flight performance is an important future direction for studies of the biomechanics and behavioral responses of bees flying in complex environments.

Regardless of the mechanisms driving the effect of body size on flight performance, our results support the hypothesis that confined environments reduce flight speed compared with open environments, thereby increasing flight energy cost for bumblebees. This cost appears to be higher for larger bees; our wind tunnel tests demonstrate that larger individuals are capable of faster forward flight (and thus lower cost of transport, or energy required to move a given distance), but they are restricted to operating at flight speeds lower than those of small individuals when flying in clutter (Fig. 4D). This finding suggests an intriguing way in which the relationship between body size and flight speed may be affected by obstacle spacing in natural environments. At high spatial frequency (i.e. with small distances between obstacles), small bees can move through the environment more rapidly than large ones, while at very low spatial frequency (i.e. functionally open environments), large bees likely move faster. This implies that at some intermediate spatial frequency, there should be no effect of body size on flight performance. Future work investigating how the spatial frequency of obstacles affects the relationship between body size and flight performance, and exploring the variation in spatial frequencies found in natural environments would be particularly interesting.

The tradeoff we have demonstrated between flight performance in cluttered versus open environments also has important implications for the evolution of body size in insects, and in bumblebees in particular, as workers from the same hive can vary by up to an order of magnitude in size (Goulson, 2003). Large bumblebee workers outperform small workers in nearly every task measured to date (Cnaani and Hefetz, 1994; Goulson et al., 2002; Kapustjanskij et al., 2007; although see Couvillon and Dornhaus, 2010), but spatially complex environments may provide an important context where small body size is favored (Foster and Cartar, 2011). Future work investigating whether the differences in transit time observed here translate to differential resource acquisition rates in cluttered environments would be of particular interest in understanding the ecological implications of our findings.

MATERIALS AND METHODS

Maximum flight speed in a wind tunnel

A captive, mature colony of *B. impatiens* (BioBest) was given unlimited access to nectar and pollen in a foraging chamber. Individual foragers were removed from the chamber, weighed and introduced into the working section (90×45×45 cm) of a wind tunnel. Wind speed was set at 2 m s^{-1} until bees initiated upwind flight, then raised incrementally after 8 s of sustained flight at each speed until the bee was unable to maintain forward flight. Wind speed was then reduced until bees resumed flight. This procedure was repeated two more times to collect three total estimates of top flight speed, the highest of which was recorded as maximum flight speed.

An important limitation of this wind tunnel assay, which is inherent to most lab-based locomotory studies, is that lab-based assays of flight performance may not always be reflective of performance in natural environments (Combes et al., 2012; Riley et al., 1999). Our wind tunnel differs from natural environments in important ways. First, the arena through which insects fly is greatly reduced. Second, in our arena, bees receive little to no optic flow despite flying at high speeds. While this situation has a potential natural analog (i.e. a bee flying into a strong headwind with a high wind speed but low or zero ground speed; see Riley et al., 1999 for a discussion of bumblebee flight in crosswinds), it is nonetheless important to note that top flight speeds in a wind tunnel may not accurately reflect top

flight speeds in natural environments. While we do not believe this will change the overall direction of the allometry of top flight speed (as larger bees are more likely to be impaired by the size constraints of the tunnel than small bees), laboratory assays of flight performance often underestimate true flight capacity (Combes et al., 2012; Riley et al., 1999); thus, we consider it likely that bumblebees flying in open, natural environments are capable of faster top flight speeds than those reported here.

Flight performance in clutter

Two flight tunnels (13×13×100 cm) were connected at one end to a foraging chamber containing a single mature, captive colony of *B. impatiens* and at the other end to openings allowing access to the outdoor environment. The colony was provided with nectar but not pollen in the hive, motivating foragers to exit and enter the hive through the flight tunnels to gather pollen. Each flight tunnel was diamond-shaped in cross-section and contained four triangular obstacles; the obstacles blocked half the cross-sectional area of the tunnel and were evenly spaced 20 cm apart in alternating orientations (Fig. 1), forcing bees to maneuver around the obstacles. In the 'vertical' flight tunnel, alternating triangles blocked the upper and lower halves of the tunnel, forcing bees to maneuver up and down. In the 'horizontal' tunnel, triangles blocked the left and right sides of the tunnel, forcing bees to maneuver side-to-side (Fig. 1).

The bottom two surfaces of the flight tunnels were covered with a black and white textured floral pattern that provided strong optic flow, while the upper two surfaces of the tunnels were left open to allow for filming and digitization. Obstacles were covered in tan paper that allowed them to be distinguished from the background, but did not obstruct visualization and digitization. The hive and flight tunnels were located in a temperature-controlled room maintained at 22°C and were surrounded on three sides by windows that provided natural lighting. The clear tunnel walls allowed bees at least a partial view of objects within the naturalistic arena of the room where experiments were conducted. All trials were collected between 3 and 6 June 2013 between 10:00 h and 18:00 h, a period during which bumblebees typically forage. Any flight sequences where bees did not make clear progress through the flight tunnels or where they collided with the external walls of the tunnel were excluded from the analysis.

Three-dimensional flight paths were recorded at 125 frames s^{-1} using two calibrated and synchronized Photron SA3 video cameras positioned approximately 1.5 m lateral to and 0.5 m above the two tunnels, with an angle of approximately 60 deg between them. Body centroids were digitized using DLTdv5 (Hedrick, 2008) and position traces were filtered (10 Hz low-pass, fifth order Butterworth) in Matlab. Body length was measured from each video sequence by digitizing the position of the head and tip of the abdomen, and measuring the three-dimensional distance between these points. These measurements were performed in three frames from different segments of the same video, to account for any potential effects of posture, and the mean of these three measurements was used as an estimate of body length. Average pair-wise correlations between the three independent measurements of body length for each bee were high (mean r=0.92), indicating that this is a reliable estimate of body length. Body length and wet body mass were also found to be highly correlated in a random sample of 20 *B. impatiens* workers from a separate BioBest hive (Pearson correlation coefficient=0.95, supplementary material Fig. S3), as is common in many insects (Rogers et al., 1977).

To investigate characteristic velocity profiles of bees maneuvering around obstacles, we separated each trial into spatially discrete turning maneuvers, each spanning from 10 cm before to 10 cm after one of the four obstacles in the axial direction (Fig. 2). These maneuvers were composed of four different types: two types of lateral maneuvers (maneuvering either to the left or to the right of an obstacle) and two types of vertical maneuvers (maneuvering either over or under an obstacle). Because of qualitative similarity (see supplementary material Fig. S4), maneuvers to the right of an obstacle were reflected across the x–z plane and pooled with maneuvers to the left of an obstacle. Similarly, maneuvers over an obstacle were reflected across the x–y plane and combined with maneuvers under an obstacle. We also pooled maneuvers from different parts of the obstacle courses (i.e. the first versus the last obstacle encountered) because there were no clear qualitative differences between these (see supplementary material Fig. S5). Through this process, all maneuvers performed by bees traversing the two obstacle courses were condensed down to two basic types: a lateral maneuver or a vertical maneuver. Trends in axial, lateral and vertical velocity during these manuevers were characterized using local regression smoothing and spatial binning of instantaneous velocity values (Fig. 2).

Transit time was calculated as the total number of digitized frames divided by the frame rate, normalized by the proportion of the obstacle course traversed during the sequence (i.e. linear distance traveled along the long axis of the tunnel divided by total tunnel length). Path sinuosity was calculated as the total path length (i.e. the sum of instantaneous displacements along the entire flight trajectory) divided by linear displacement, or the three-dimensional distance between the start and end points of the flight path. Instantaneous flight speeds were calculated as instantaneous displacement divided by frame length (0.008 s), and median speed along the flight path was determined for each trial.

Instantaneous accelerations were calculated along three axes in a global frame of reference, with the axial axis parallel to the long axis of the flight tunnel, the lateral axis perpendicular to the tunnel axis in the horizontal plane, and the vertical axis oriented in the direction of gravity. Accelerations measured along these global axes are not necessarily correlated with accelerations produced in the bee's frame of reference, as the bee's longitudinal body axis can rotate (e.g. yaw) relative to the longitudinal axis of the flight tunnel. In our experiments, however, bumblebees appeared to maintain a forward-facing body orientation (in line with the longitudinal axis of the tunnel) nearly continuously throughout all flights; this is consistent with the largely roll-based, lateral maneuvering that bumblebees perform when flying towards a target in oncoming flow (Ravi et al., 2013), as well as with landmark-oriented flights in honeybees (Boeddeker and Hemmi, 2010). Under these conditions, global accelerations are highly correlated with accelerations in the bee's frame of reference, and thus we consider global accelerations to be reliable estimates of accelerations produced in the local body frame.

Instantaneous total acceleration was calculated at each time step from acceleration vectors in the three global axes by applying the Pythagorean theorem in three dimensions. The resulting total acceleration encompasses both tangential acceleration (i.e. change in speed along a linear trajectory) and radial acceleration (i.e. acceleration perpendicular to the flight trajectory associated with turning). We estimated maximum acceleration during each trial as the 95th percentile of instantaneous accelerations throughout the sequence. This metric provides a conservative estimate of maximum acceleration, which minimizes the effects of noise introduced by digitizing and differentiation; two less conservative estimates (98th percentile of accelerations and the average of the two highest acceleration peaks) yielded qualitatively similar results (supplementary material Fig. S2).

The number of corrective maneuvers performed was quantified by summing the number of sign changes in axial velocity, then dividing this number by two and rounding up to the nearest integer. If a bee flying forward comes to a stop in front of an obstacle, flies backward briefly, then continues flying forward past the obstacle, this counts as a single corrective maneuver. Sign changes in axial velocity can be caused by either voluntary corrective maneuvers or involuntary collisions with obstacles. In practice, however, apparent collisions were rare (accounting for less than 10% of sign changes in axial velocity), and often occurred as part of a voluntary deceleration (i.e. the bee had begun to decelerate and then lightly clipped the obstacle before completely decelerating). Because of their relative rarity and because video resolution made it nearly impossible to distinguish between near-collisions and maneuvers where the bees made physical contact with the obstacle, all sign changes of axial velocity were included in the count of corrective maneuvers.

Data analysis

All statistical analyses were performed in R (R Development Core Team, 2008) with α=0.05. To test for differences in lateral versus vertical acceleration between the two different flight tunnels, we performed a two-way ANOVA with acceleration direction and obstacle course orientation as explanatory factors, and maximum acceleration as a response variable; this was followed by *post hoc* t-tests (paired between acceleration axes, unpaired

between obstacle courses). To test for overall transit time differences between the two flight tunnels, we performed an unpaired *t*-test of normalized transit time versus obstacle orientation.

The relationships between log-transformed body size (preferable for allometric data; Mascaro et al., 2014) and flight metrics were analyzed with linear regression models, including obstacle orientation (vertical versus horizontal) and flight direction (exiting versus entering the hive) as covariates, using the lm( ) function in R. No significant effects of obstacle orientation or flight direction were found for any of the flight metrics, so these variables were removed. Final models (with all trials pooled) analyzed the relationship between flight metrics and body size using major axis regression (generally more appropriate for allometric data than ordinary least squares regression; Warton et al., 2006), using the lmodel2 package in R. Results from both ordinary least squares regression and major axis regression are reported in Table 1 and shown in Fig. 4.

Because accelerations are particularly sensitive to digitizing noise and the effects of filtering frequency, we performed a sensitivity analysis on the linear regression between log-transformed maximum acceleration and body length, comparing the slope and significance of this relationship as filtering frequency changes, and using three different metrics of maximum acceleration (peak acceleration, 98th percentile and 95th percentile). Although acceleration metrics and filter frequency strongly affected both the slope and significance of the relationship, the estimated slope between these variables was always positive (supplementary material Fig. S2).

We used ordinary least squares regression to test the effect of maximum acceleration on path sinuosity, median flight speed and transit time (Fig. 5), and the effect of the number of corrective maneuvers on path sinuosity (Fig. 6B) and median flight velocity (Fig. 6C). To test the effects of body size on the number of corrective maneuvers (Fig. 6A), we created a generalized linear model with a Poisson distribution (more appropriate for count data than simple linear regression) and log link using the glm( ) function in R (R Development Core Team, 2008).

It is important to note that the number of observations differed between the two flight arenas, with the vertical flight tunnel having nearly twice as many (N=37) trials as the horizontal flight tunnel (N=19). The horizontal flight tunnel also had relatively few trials with large bees (i.e. bees over 17 mm in length). To determine whether this affected our findings, we ran the same analyses on data from the vertical and horizontal flight tunnels separately (results not shown). Data from the vertical flight tunnel displayed the same relationships and qualitative patterns of significance as the pooled data in all analyses. Data from the horizontal flight tunnel showed the same relationships as the pooled data in all analyses, and the same levels of significance in most analyses, with two exceptions: the effect of body size on flight speed (Fig. 4D) was only marginally significant for the horizontal tunnel data alone (P=0.06) and the effect of maximum acceleration on path sinuosity (Fig. 5C) was not significant (P=0.42). The lack of statistical significance in these two relationships for the horizontal data alone may be due to the smaller number of data points for large bees in this flight tunnel, which would reduce our power to identify statistical trends.

Are corrective maneuvers sufficient to explain variation in speed and sinuosity?

One way to address this question is to combine the models of (a) effects of body size on the number of corrective maneuvers and (b) effects of corrective maneuvers on sinuosity and flight speed to predict the effect size of observed variation in sinuosity and flight speed. These estimates can then be compared with the observed variation in sinuosity and speed across body size. For example, our model predicts roughly 0.53 corrective maneuvers for a 12 mm bee on average and 2.53 corrective maneuvers for a 24 mm bee (Fig. 6A). In turn, our model of the effect of corrective maneuvers on sinuosity predicts a sinuosity of 1.20 for 0.53 corrective maneuvers and a sinuosity of 1.34 for 2.53 corrective maneuvers (Fig. 6B). In combination, these models thus predict that path sinuosity will change from 1.2 to 1.34, going from a 12 to a 24 mm bee (an effect size of 0.14). Our ordinary least squares model of the effect of body length on sinuosity, however, predicts a shift in path sinuosity from 1.16 to 1.37 over the same size range, with an effect size of 0.21 (Fig. 4C). From this, we conclude that the effect of body length on the number of corrective maneuvers can explain roughly 67% of the variance in sinuosity across body size. For median flight speed, we predict a shift from 0.336 m s^{-1} to 0.299 m s^{-1} (Fig. 6C) over the same range of body length. The actual shift over this range is from 0.355 m s^{-1} to 0.272 m s^{-1} (Fig. 6C), indicating that the effect of body size on corrective maneuvers can explain around 45% of the observed variation in flight speed across body size. It should also be noted that these estimates are based on ordinary least squares regression, which offers a more conservative prediction of the effect of body size than major axis regression.

Acknowledgements

The authors would like to thank Jude Russo and Teressa Alexander for assistance with data processing, and John Tuthill and Kaushik Jayaram for helpful discussions on optic flow and collision damage in insects, respectively.

Competing interests

The authors declare no competing or financial interests.

Author contributions

J.D.C., S.R., A.M.M. and S.A.C. designed the experiments. J.D.C. and S.R. performed the experimental trials. J.D.C. performed computational and statistical analyses. J.D.C., S.R., A.M.M. and S.A.C. wrote the manuscript.

Funding

This work was supported by National Science Foundation (NSF) grant CCF-0926158 and an NSF GRFP fellowship to J.D.C.

Supplementary material

Supplementary material available online at
http://jeb.biologists.org/lookup/suppl/doi:10.1242/jeb.121293/-/DC1

References

Aldridge, H. D. J. N. and Brigham, R. M. (1988). Load carrying and maneuverability in an insectivorous bat: a test of the 5% 'rule' of radio-telemetry. *J. Mamm.* **69**, 379-382.

Andersson, M. and Norberg, R. Å. (1981). Evolution of reversed sexual size dimorphism and role partitioning among predatory birds, with a size scaling of flight performance. *Biol. J. Linn. Soc.* **15**, 105-130.

Baird, E., Kornfeldt, T. and Dacke, M. (2010). Minimum viewing angle for visually guided ground speed control in bumblebees. *J. Exp. Biol.* **213**, 1625-1632.

Biewener, A. A. (1990). Biomechanics of mammalian terrestrial locomotion. *Science* **250**, 1097-1103.

Boeddeker, N. and Hemmi, J. M. (2010). Visual gaze control during peering flight manoeuvres in honeybees. *Proc. R. Soc. B Biol. Sci.* **277**, 1209-1217.

Boeddeker, N., Dittmar, L., Sturzl, W. and Egelhaaf, M. (2010). The fine structure of honeybee head and body yaw movements in a homing task. *Proc. R. Soc. B Biol. Sci.* **277**, 1899-1906.

Buchwald, R. and Dudley, R. (2010). Limits to vertical force and power production in bumblebees (Hymenoptera: *Bombus impatiens*). *J. Exp. Biol.* **213**, 426-432.

Cnaani, J. and Hefetz, A. (1994). The effect of workers size frequency distribution on colony development in *Bombus terrestris*. *Insect. Soc.* **41**, 301-307.

Cartar, R. V. (1992). Morphological senescence and longevity: an experiment relating wing wear and life span in foraging wild bumble bees. *J. Anim. Ecol.* **61**, 225-231.

Combes, S. A. and Dudley, R. (2009). Turbulence-driven instabilities limit insect flight performance. *Proc. Natl. Acad. Sci. USA* **106**, 9105-9108.

Combes, S. A., Rundle, D. E., Iwasaki, J. M. and Crall, J. D. (2012). Linking biomechanics and ecology through predator-prey interactions: flight performance of dragonflies and their prey. *J. Exp. Biol.* **215**, 903-913.

Couvillon, M. J., Jandt, J. M., Duong, N. and Dornhaus, A. (2010). Ontogeny of worker body size distribution in bumble bee (*Bombus impatiens*) colonies. *Ecol. Entomol.* **35**, 424-435.

Crompton, B., Thomason, J. C. and McLachlan, A. (2003). Mating in a viscous universe: the race is to the agile, not to the swift. *Proc. R. Soc. B Biol. Sci.* **270**, 1991-1995.

Dickinson, M. H., Farley, C. T., Full, R. J., Koehl, M. A. R., Kram, R. and Lehman, S. (2000). How animals move: an integrative view. *Science* **288**, 100-106.

Dillon, M. E. and Dudley, R. (2004). Allometry of maximum vertical force production during hovering flight of neotropical orchid bees (Apidae: Euglossini). *J. Exp. Biol.* **207**, 417-425.

Domenici, P. (2001). The scaling of locomotor performance in predator-prey encounters: from fish to killer whales. *Comp. Biochem. Physiol. A Mol. Integr. Physiol.* **131**, 169-182.

Dudley, R. (2002a). Mechanisms and implications of animal flight maneuverability. *Integr. Comp. Biol.* **42**, 135-140.

Dudley, R. (2002b). *The Biomechanics of Insect Flight*. Princeton: Princeton University Press.

Dudley, R. and Ellington, C. P. (1990). Mechanics of forward flight in bumblebees: II. Quasi-steady lift and power requirements. *J. Exp. Biol.* **148**, 53-88.
Ellington, C. P., Machin, K. E. and Casey, T. M. (1990). Oxygen consumption of bumblebees in forward flight. *Nature* **347**, 472-473.
Foster, D. J. and Cartar, R. V. (2011). What causes wing wear in foraging bumble bees? *J. Exp. Biol.* **214**, 1896-1901.
Goulson, D. (2003). *Bumblebees.* USA: Oxford University Press.
Goulson, D., Peat, J., Stout, J. C., Tucker, J., Darvill, B., Derwent, L. C. and Hughes, W. O. H. (2002). Can alloethism in workers of the bumblebee, *Bombus terrestris*, be explained in terms of foraging efficiency? *Anim. Behav.* **64**, 123-130.
Hadley, A. S. and Betts, M. G. (2009). Tropical deforestation alters hummingbird movement patterns. *Biol. Lett.* **5**, 207-210.
Hedrick, T. L. (2008). Software techniques for two- and three-dimensional kinematic measurements of biological and biomimetic systems. *Bioinspir. Biomim.* **3**, 034001.
Hedrick, T. L., Cheng, B. and Deng, X. (2009). Wingbeat time and the scaling of passive rotational damping in flapping flight. *Science* **324**, 252-255.
Heinrich, B. (2004). *Bumblebee Economics*. Harvard: Harvard University Press.
Jayaram, K. and Full, R. J. (2015). Body size limit predictions for mechanically mediated maneuvers. *Int. Comp. Biol.* **55**, E88.
Kapustjanskij, A., Streinzer, M., Paulus, H. F. and Spaethe, J. (2007). Bigger is better: implications of body size for flight ability under different light conditions and the evolution of alloethism in bumblebees. *Funct. Ecol.* **21**, 1130-1136.
Kern, R., Boeddeker, N., Dittmar, L. and Egelhaaf, M. (2012). Blowfly flight characteristics are shaped by environmental features and controlled by optic flow information. *J. Exp. Biol.* **215**, 2501-2514.
LeBoeuf, A. C. and Grozinger, C. M. (2014). Me and we: the interplay between individual and group behavioral variation in social collectives. *Curr. Opin. Insect Sci.* **5**, 16-24.
Lihoreau, M., Chittka, L., Le Comber, S. C. and Raine, N. E. (2012). Bees do not use nearest-neighbour rules for optimization of multi-location routes. *Biol. Lett.* **8**, 13-16.
Lin, H.-T., Ros, I. G. and Biewener, A. A. (2014). Through the eyes of a bird: modelling visually guided obstacle flight. *J. R. Soc. Interface* **11**, 20140239-20140239.
Maebe, K., Meeus, I. and Smagghe, G. (2013). Recruitment to forage of bumblebees in artificial low light is less impaired in light sensitive colonies, and not only determined by external morphological parameters. *J. Insect Physiol.* **59**, 913-918.
Marden, J. H. (1987). Maximum lift production during takeoff in flying animals. *J. Exp. Biol.* **130**, 235-258.
Mascaro, J., Litton, C. M. and Hughes, R. F. (2014). Is logarithmic transformation necessary in allometry? Ten, one-hundred, one-thousand-times yes. *Biol. J.* **111**, 230-233.
Morice, S., Pincebourde, S., Darboux, F., Kaiser, W. and Casas, J. (2013). Predator-Prey Pursuit-Evasion games in structurally complex environments. *Integr. Comp. Biol.* **53**, 767-779.
Mountcastle, A. M. and Combes, S. A. (2014). Biomechanical strategies for mitigating collision damage in insect wings: structural design versus embedded elastic materials. *J. Exp. Biol.* **217**, 1108-1115.
Norberg, U. M. and Rayner, J. M. (1987). Ecological morphology and flight in bats (Mammalia; Chiroptera): wing adaptations, flight performance, foraging strategy and echolocation. *Philos. Trans. R. Soc. Lond. B Biol. Sci.* **316**, 335-427.
Ohashi, K., Leslie, A. and Thomson, J. D. (2008). Trapline foraging by bumble bees: V. Effects of experience and priority on competitive performance. *Behav. Ecol.* **19**, 936-948.
Pinter-Wollman, N. (2012). Personality in social insects: how does worker personality determine colony personality. *Curr. Zool.* **58**, 579-587.
R Development Core Team (2008). *R: A Language and Environment for Statistical Computing*. R Foundation for Statistical Computing, Vienna, Austria. ISBN 3-900051-07-0, URL http://www.R-project.org.
Ravi, S., Crall, J. D., Fisher, A. and Combes, S. A. (2013). Rolling with the flow: bumblebees flying in unsteady wakes. *J. Exp. Biol.* **216**, 4299-4309.
Riley, J. R., Reynolds, D. R., Smith, A. D., Edwards, A. S., Osborne, J. L., Williams, I. H. and McCartney, H. A. (1999). Compensation for wind drift by bumble-bees. *Nature* **400**, 126.
Rogers, L. E., Buschbom, R. L. and Watson, C. R. (1977). Length-weight relationships of shrub-steppe invertebrates. *Ann. Entomol. Soc. Am.* **70**, 51-53.
Shepard, E. L. C., Wilson, R. P., Rees, W. G., Grundy, E., Lambertucci, S. A. and Vosper, S. B. (2013). Energy landscapes shape animal movement ecology. *Am. Nat.* **182**, 298-312.
Spaethe, J. (2003). Interindividual variation of eye optics and single object resolution in bumblebees. *J. Exp. Biol.* **206**, 3447-3453.
Srinivasan, M., Zhang, S. W., Lehrer, M. and Collett, T. (1996). Honeybee navigation en route to the goal: visual flight control and odometry. *J. Exp. Biol.* **199**, 237-244.
Stevenson, R., Corbo, K., Baca, L. and Le, Q. (1995). Cage size and flight speed of the tobacco hawkmoth *Manduca sexta*. *J. Exp. Biol.* **198**, 1665-1672.
Stockwell, E. F. (2001). Morphology and flight manoeuvrability in New World leaf-nosed bats (Chiroptera: Phyllostomidae). *J. Zool.* **254**, 505-514.
Swaddle, J. P. and Witter, M. S. (1998). Cluttered habitats reduce wing asymmetry and increase flight performance in European starlings. *Behav. Ecol. Sociobiol.* **42**, 281-287.
Tammero, L. F. and Dickinson, M. H. (2002). The influence of visual landscape on the free flight behavior of the fruit fly *Drosophila melanogaster*. *J. Exp. Biol.* **205**, 327-343.
Thomas, A. L. R. (1996). The flight of birds that have wings and a tail: variable geometry expands the envelope of flight performance. *J. Theor. Biol.* **183**, 237-245.
Thomas, A. L. R. and Balmford, A. (1995). How natural selection shapes birds' tails. *Am. Nat.* **146**, 848-868.
Vance, J. T., Williams, J. B., Elekonich, M. M. and Roberts, S. P. (2009). The effects of age and behavioral development on honey bee (Apis mellifera) flight performance. *J. Exp. Biol.* **212**, 2604-2611.
Vogel, S. (1994). *Life in Moving Fluids*. Princeton: Princeton University Press.
Warton, D. I., Wright, I. J., Falster, D. S. and Westoby, M. (2006). Bivariate line-fitting methods for allometry. *Biol. Rev.* **81**, 259.

Chapter 2: Foraging in an unsteady world: bumblebee flight performance in field-realistic turbulence

Reprinted from:
Crall, J. D., Chang J.J., Oppenheimer, R.L., S. A. (2017). Foraging in an unsteady world: bumblebee flight performance in field-realistic turbulence. *Interface Focus* 7(1): 20160086, DOI: 10.1098/rsfs.2016.0086

INTERFACE FOCUS

rsfs.royalsocietypublishing.org

Research

Cite this article: Crall JD, Chang JJ, Oppenheimer RL, Combes SA. 2017 Foraging in an unsteady world: bumblebee flight performance in field-realistic turbulence. *Interface Focus* **7**: 20160086.
http://dx.doi.org/10.1098/rsfs.2016.0086

One contribution of 19 to a theme issue 'Coevolving advances in animal flight and aerial robotics'.

Subject Areas:
biomechanics

Keywords:
insect flight, stability, bee, environmental complexity, wind, radio-frequency identification (RFID)

Author for correspondence:
J. D. Crall
e-mail: james.crall@gmail.com

Electronic supplementary material is available online at https://dx.doi.org/10.6084/m9.figshare.c.3575195.

THE ROYAL SOCIETY PUBLISHING

Foraging in an unsteady world: bumblebee flight performance in field-realistic turbulence

J. D. Crall[1], J. J. Chang[2], R. L. Oppenheimer[3] and S. A. Combes[4]

[1]Department of Organismic and Evolutionary Biology, Harvard University, Cambridge, MA, USA
[2]Department of Neuroscience, Columbia University, New York, NY, USA
[3]Department of Biological Sciences, University of New Hampshire, Durham, NH, USA
[4]Department of Neurobiology, Physiology, and Behavior, University of California, Davis, Davis, CA, USA

JDC, 0000-0002-8981-3782

Natural environments are characterized by variable wind that can pose significant challenges for flying animals and robots. However, our understanding of the flow conditions that animals experience outdoors and how these impact flight performance remains limited. Here, we combine laboratory and field experiments to characterize wind conditions encountered by foraging bumblebees in outdoor environments and test the effects of these conditions on flight. We used radio-frequency tags to track foraging activity of uniquely identified bumblebee (*Bombus impatiens*) workers, while simultaneously recording local wind flows. Despite being subjected to a wide range of speeds and turbulence intensities, we find that bees do not avoid foraging in windy conditions. We then examined the impacts of turbulence on bumblebee flight in a wind tunnel. Rolling instabilities increased in turbulence, but only at higher wind speeds. Bees displayed higher mean wingbeat frequency and stroke amplitude in these conditions, as well as increased asymmetry in stroke amplitude—suggesting that bees employ an array of active responses to enable flight in turbulence, which may increase the energetic cost of flight. Our results provide the first direct evidence that moderate, environmentally relevant turbulence affects insect flight performance, and suggest that flying insects use diverse mechanisms to cope with these instabilities.

1. Introduction

Natural environments are highly complex. In addition to structural and visual complexity [1,2], outdoor environments vary substantially over time, with abiotic conditions (e.g. wind [3], temperature [4] and light, among others) varying over timescales ranging from seconds to seasons. Such environmental complexity can pose significant challenges to flying animals that must move through natural habitats to forage for food [5], capture prey or escape from predators [6], and find mates [7], potentially restricting when and where they can fly, or increasing the energetic cost of flight. Variation in the cost of locomotion can impact key aspects of animal ecology by affecting movement at the landscape scale [8]. The challenges associated with manoeuvring through complex environments have likely played a key role in shaping the evolutionary and ecological pressures on flying animals [9,10]. Understanding how animals contend with the complexities of natural environments—whether this involves active or passive coping mechanisms, or avoidance of certain conditions—is thus key for understanding their evolution and ecology, as well as for providing guiding principles for the design of micro-aerial vehicles (MAVs) capable of traversing outdoor environments.

Wind variability represents one of the most important, and potentially most challenging, components of environmental complexity for flying animals and MAVs. Wind carries substantial kinetic energy [3], and varies locally over timescales that are typically much faster (i.e. sub-second scale) than other

abiotic conditions, such as temperature and light. Air flows in natural environments are highly variable across a range of spatio-temporal scales [3,11], and can affect the performance, energetics, and behaviour of flying animals [12–14]. Instabilities imposed by high-frequency variation in wind flow may also pose a significant control challenge for both flying insects and MAVs [15].

Environmental air flows can be characterized as a combination of mean flow, and fluctuations around this flow (often quantified as 'turbulence intensity', or standard deviation of flow speed divided by the mean) [3]. While we have a relatively strong understanding of how mean flows affect the locomotion and ecology of flying animals, we know comparatively little about how turbulence impacts animal flight performance [16]. Recently, a number of wind tunnel studies have helped elucidate the effects of variable, but structured flows such as von Kármán vortex trails that form behind cylinders, on flight in both hummingbirds [13,17] and insects [18–20]. While such flows may be locally dominant (e.g. immediately downstream of physical objects in the environment such as tree branches), aerial environments are more often characterized by turbulent flow consisting of a chaotic mix of eddies of many sizes and frequencies [3]. Previous work has shown that turbulence limits top flight speed and increases drag (and presumably associated energetic costs) in orchid bees [12]. A single previous indoor wind tunnel study has shown that hummingbirds display flight instabilities in freestream turbulence at a relatively high flow speed ($5\ m\ s^{-1}$), and that birds alter several aspects of their wing kinematics in response [18]. In addition, recent computational work [21] has suggested that turbulence may have only minimal effects on the mean aerodynamic properties of flying insects, despite leading to increased fluctuations of instantaneous aerodynamic forces. It thus remains unclear whether turbulence has a significant impact on insect flight performance at environmentally relevant levels.

A key limitation to our current understanding of this issue is the dearth of information available on turbulent flow conditions experienced by flying insects in nature. While wind flows in natural environments have been characterized extensively [3,11]—albeit often at timescales that are of little relevance for flying insects—to our knowledge no previous studies have simultaneously recorded local flow variability and the activity of flying animals, which would provide direct information about the wind environments actually experienced.

Here, we use a combination of field studies and wind tunnel tests to answer the questions: (i) what range of wind speeds and turbulence intensities do foraging bumblebees (*Bombus impatiens*) typically experience and (ii) how do environmentally relevant flow conditions affect body stability and wing kinematics?

2. Material and methods

2.1. Field study

Eighty-seven bumblebee workers (*B. impatiens*) were removed from a commercial colony (BioBest) located in an open field at the Harvard Forest in Petersham, MA, over the course of 2 days (15–16 August 2012). Each bee was cold-anaesthetized and outfitted with a unique radio-frequency identification (RFID) tag (1.4×8 mm, 32 mg, Freevision Technologies). Intertegular span (IT span, a common proxy for body size in bees [22,23]) was measured with calipers to the nearest 0.1 mm, and bees were returned to the colony. After a 5-day acclimation period, two custom RFID readers placed in series at the hive's only opening recorded all forager transits to and from the colony over a two-week period (21 August–4 September 2012; figure 1*b*). The two adjacent RFID readers allowed us to distinguish entrances and exits from the colony, from which we determined the timing and duration of foraging bouts undertaken by uniquely identified bees. Simultaneously, we recorded three-dimensional instantaneous wind speeds at 5 Hz using a sonic anemometer (CSAT3, Campbell-Scientific®), located approximately 3 m from the hive, and approximately 2 m off the ground (figure 1*a*). While such stationary recording does not provide direct data on the wind environment experienced by individual, mobile bees in flight, bumblebees typically forage over relatively short distances (approx. 275 m, [24]), and the colony was situated within a homogeneous, grassy landscape. The static measurements presented here are thus likely to be representative of average conditions experienced by these bees during local foraging flights.

We combined these two datasets to investigate the natural distribution of wind conditions experienced by bumblebee foragers, using the bees' foraging activity to sample the wind environment. For each foraging bout, we measured the mean wind speed and turbulence intensity (σ_{wind}/μ_{wind}, where σ is standard deviation, and μ is the mean of instantaneous wind speeds, respectively) for each 10-s interval over the duration of the foraging bout (figure 2*a*). These brief measurement intervals were intended to capture higher frequency wind fluctuations (which would be more likely to cause rotational instabilities of the body), rather than lower frequency changes in mean wind speed (which would be experienced as linear perturbations or changes in overall flow direction). Standard deviation of wind speed was calculated by averaging the standard deviations of instantaneous flow speed in each of the three directions (u, v and w) measured independently, and this was divided by mean flow speed in the primary wind direction. Mean wind speeds and turbulence intensities for all such 10-s time intervals were then pooled to determine the distribution of flows experienced by foraging bees.

To test whether bees were less likely to forage during periods of high wind speed or turbulence, we then calculated the mean wind speed and turbulence intensity for each foraging bout, and compared this to the mean wind speed and turbulence intensity during a simulated foraging bout of the same length and on the same day, but starting at a randomly sampled time between 6.00 and 17.00 (figure 2*b*,*c*), when the majority of foraging activity occurred (figure 1*c*).

2.2. Wind tunnel experiments

2.2.1. Study organisms and experimental design

Mature bumblebee (*B. impatiens*) colonies were acquired from BioBest® and maintained in a temperature-controlled laboratory environment from June to August 2014 at the Concord Field Station, Bedford, MA. Bees were given *ad libitum* access to artificial nectar (BioGluc®) and fresh pollen in a foraging chamber.

Prior to experimental trials, individual foragers (i.e. bees actively foraging outside the nest chamber) were removed from the colony, cold-anaesthetized and outfitted with a triangular marker (as in [25]), attached to the dorsal part of their thorax with cyanocrylate glue. After tag attachment, individual bees were isolated for at least 1 h to increase feeding motivation, then introduced to the downstream end of the working section ($0.9 \times 0.5 \times 0.5$ m) of a wind tunnel with low-speed, laminar flow (less than $0.5\ m\ s^{-1}$). On the upstream end of the wind tunnel, we placed an artificial flower (purple, approx. 2 cm diameter) with a pipette tip in the middle containing a few drops of artificial nectar, attached to a thin metal rod (figure 3*a*). Each bee was

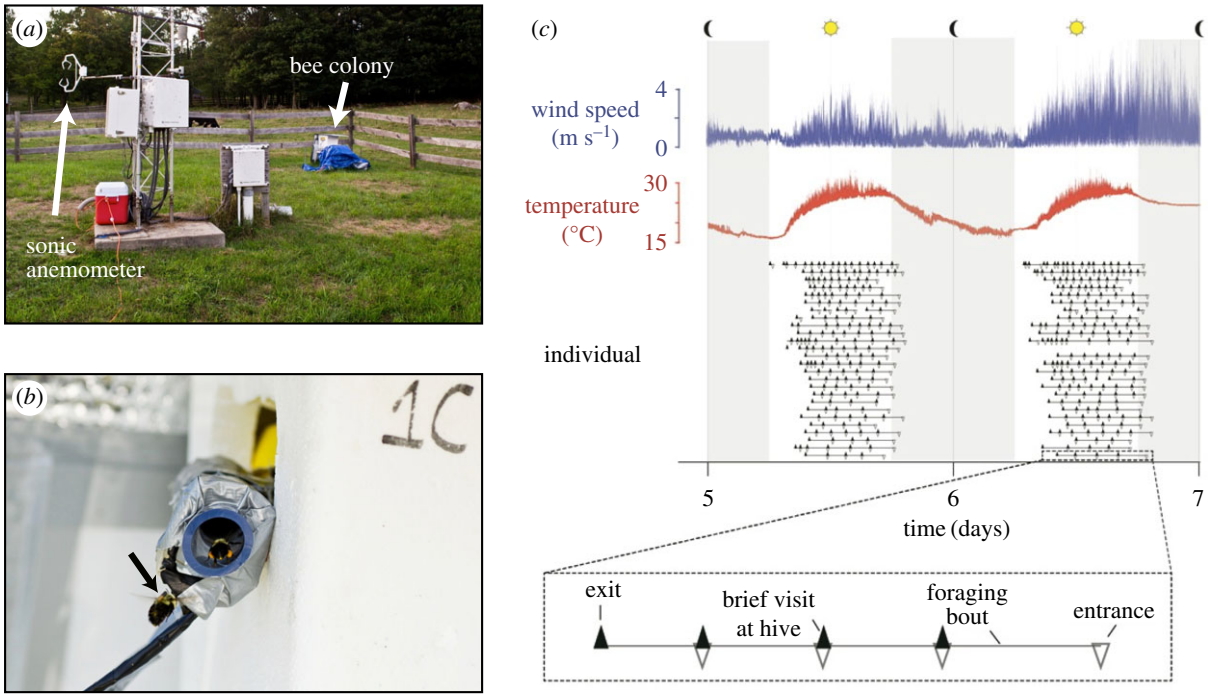

Figure 1. Simultaneous sampling of environmental wind and bumblebee foraging behaviour. (*a*) Field experimental set-up, showing location of the experimental bumblebee colony and adjacent sonic anemometer for recording wind speed and turbulence. (*b*) RFID-tagged bumblebee forager (black arrow) approaching the nest entrance. (*c*) Sample data collected over 2 days, showing environmental wind (blue, top), temperature (red, middle), and foraging behaviour of individual bumblebee workers (black, bottom). For each worker, nest exits and entrances are indicated by filled and open triangles, respectively, arranged along a single row.

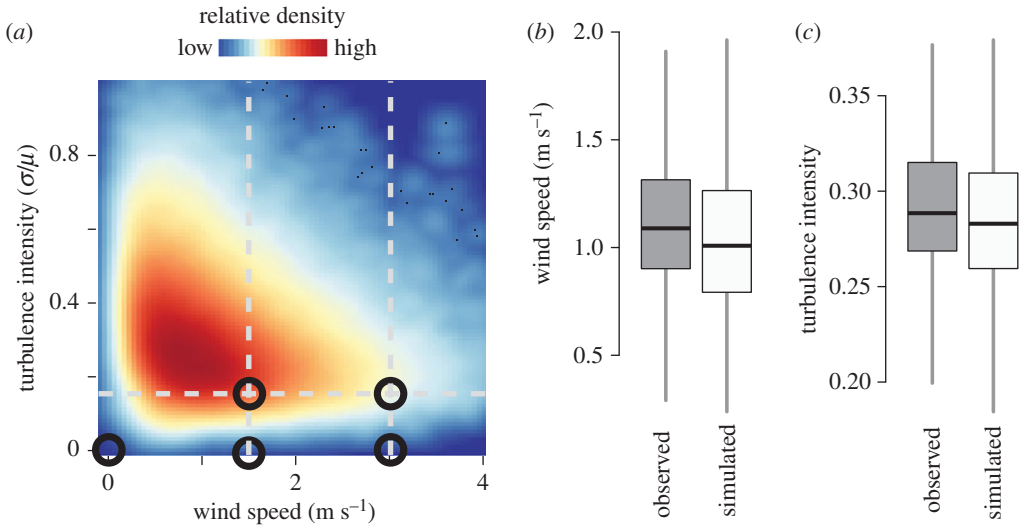

Figure 2. Foraging bumblebees experience highly variable wind environments. (*a*) Heat map of instantaneous wind speeds and turbulence intensities observed over 10-s intervals during all bumblebee foraging bouts. Dashed grey lines and open black circles show combinations of wind speeds and turbulence intensity used in subsequent wind tunnel experiments. (*b*,*c*) Mean wind speed (*b*) and turbulence intensity (*c*) of observed (grey) versus simulated (white) foraging bouts. Boxes show the median and inter-quartile range (IQR), and whiskers indicate data range (75th and 25th $\pm$ 1.5 $\times$ IQR, respectively).

allowed to explore the wind tunnel until it found the artificial flower and began feeding. After this, the purple artificial flower was removed, leaving only the pipette tip (to minimize flow disturbance), and the bee was again released from the downstream end of the wind tunnel. This procedure was repeated under one of five experimental flow conditions, presented in a randomized order: 0 m s^{-1} flow, 1.5 m s^{-1} laminar flow, 1.5 m s^{-1} turbulent flow, 3.0 m s^{-1} laminar flow and 3.0 m s^{-1} turbulent flow.

Turbulence was introduced into the working section of the wind tunnel via a grid located upstream of the working section (figure 3*a*). This grid introduced near-isotropic turbulence with a turbulence intensity of approximately 15% (compared to less than 2% in laminar flow [18]). The power spectrum of experimental turbulence displayed a $-5/3$ slope, characteristic of fully mixed turbulence (figure 3*b*, [26]). For a more detailed description of flow conditions and turbulence spectra, see [18].

2.2.2. Kinematic reconstruction

Flights were recorded within an interrogation volume of approximately 200 cm^3 just downstream of the artificial flower at 5000 frames per second using three Photron SA3 cameras, calibrated via direct linear transformation [27]. The three markers on the triangular tags of the bees' thorax (figure 3*c*) were tracked automatically using DLTdv5 [27] under manual supervision (electronic supplementary material, movie S1). For a subset of

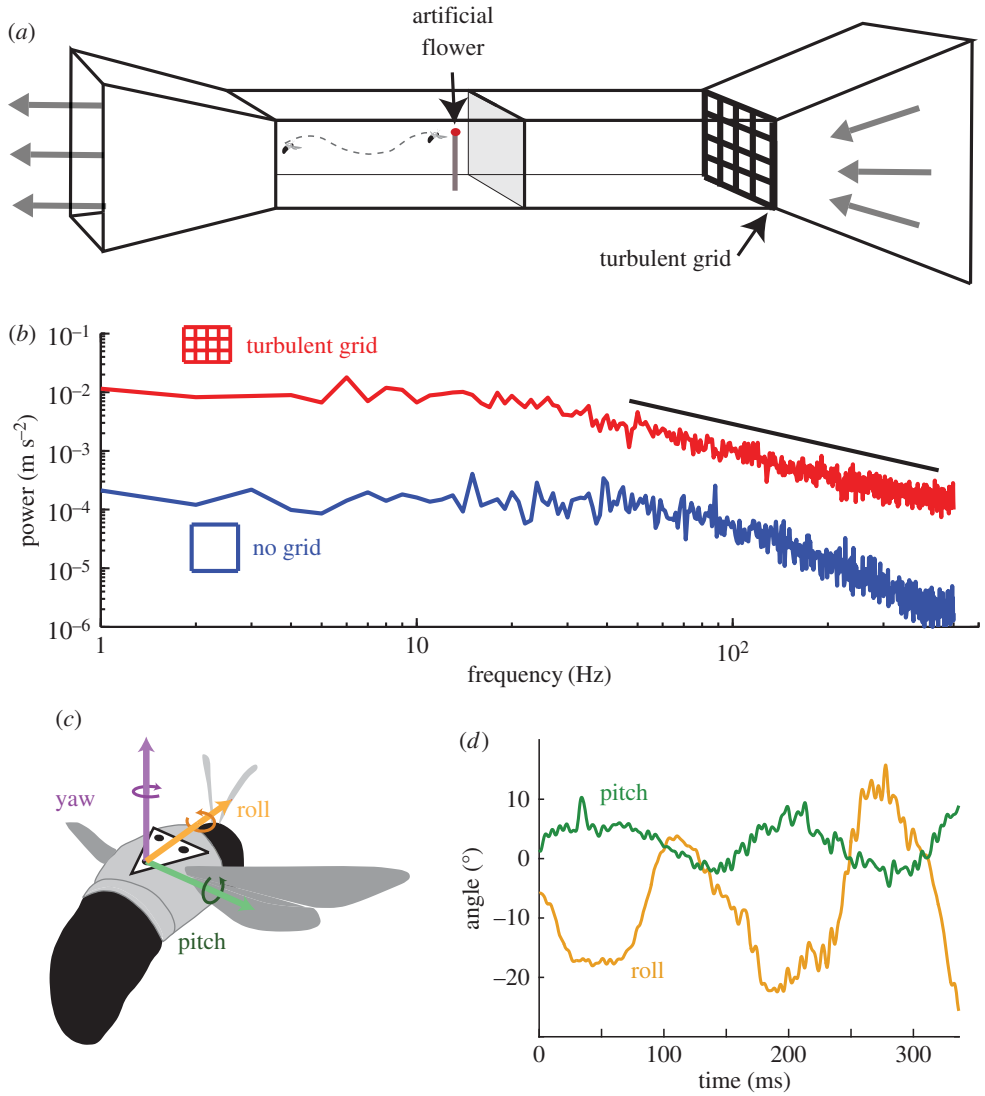

Figure 3. Wind tunnel experiments to test the effect of turbulent flow on bumblebee flight. (*a*) Schematic diagram of wind tunnel design. (*b*) Turbulent power spectra for laminar (blue) and turbulent (red) flow conditions in the wind tunnel. Black line indicates the expected −5/3 decay characteristic of freestream turbulence in natural environments. (*c*) Schematic drawing of a bumblebee showing the three axes of body angular orientation. (*d*) Sample trace of pitch and roll over a single trial with turbulent flow at 1.5 m s^{-2}.

bees, wingtip positions of both wings at each stroke reversal were manually digitized (electronic supplementary material, movie S1), and the positions of the wing bases were recorded at five evenly spaced frames throughout the video sequence. Three-dimensional kinematics of these points were then calculated via DLTdv5 [27]. To reduce digitization noise, three-dimensional coordinates were smoothed using a fifth-order Butterworth filter with a low-pass cut-off frequency of 1000 Hz, and the first and last 30 frames of each trial sequence were removed from subsequent analyses to reduce filtering artefacts.

Roll, pitch and yaw orientations of the body were calculated from the three triangular markers on the bee's thorax, following [25] (figure 3*c*,*d*). Standard deviations of body orientations were calculated after filtering the roll, pitch and yaw data using a fifth-order Butterworth filter with a high-pass frequency cut-off of 10 Hz, to remove low-frequency casting motions [25]. For each wing stroke digitized, amplitude was calculated separately for each wing, by rotating data into the body frame using the body's instantaneous roll, pitch and yaw orientations (x'–y'–z'), then calculating the minimum angle between the wingtip location at pronation, the wing base, and the wingtip location at supination. Asymmetry in left–right amplitude was calculated for each wing stroke, and the maximum value and variance of stroke asymmetry were calculated for each trial. Correlations between stroke-by-stroke amplitude asymmetry and body roll angle were assessed.

To estimate variation in the position of pronation and supination, we calculated the wing sweep angle at pronation and supination independently, with respect to the sagittal plane of the bee body, projected into the x'–y' plane. Wingbeat frequency was calculated manually by counting wing strokes in the camera view where the bee was visible for the longest time period.

2.2.3. Statistical models for effects of flow

To investigate the effects of flow speed and turbulence on body and wing kinematics, we constructed a series of linear mixed effects models using the 'lmer' function [28] in R. These models allowed us to test for effects of experimental conditions, while accounting for variation across individuals. First, we tested the effects of wind speed (independent of flow condition) on body and wing kinematics by building models with flow speed as a fixed effect and individual as a random effect, using only laminar flow trials. To test the effects of turbulence, we then constructed separate models for each of the non-zero flow speeds (1.5 and 3.0 m s^{-1}) with flow condition as a fixed effect and individual as a random effect. *P*-values for fixed effects (i.e. flow speed and condition)

were calculated in the 'lmerTest' package [29], using Satterthwaite approximations for denominator degrees of freedom.

3. Results

3.1. Field study

We recorded a total of 1934 foraging bouts from 33 unique bees over 14 days (figure 1*c*). Across all foraging bouts, the median wind speed was 1.00 m s^{-1}, and the median turbulence intensity was 0.28 (figure 2*a*). However, there was substantial variation in both wind metrics, with wind speed ranging from 0.22 to 3.06 m s^{-1} (1st and 99th percentile, respectively), and turbulence intensity ranging from 0.10 to 0.57 (1st and 99th percentile, respectively). Mean within-bout wind speeds and turbulence intensities during individual foraging bouts were not lower than that expected under random simulation (figure 2*b*,*c*; wind speed, one-sided paired *t*-test, d.f. = 1933, $t = 9.22$, $p > 0.99$; turbulence intensity, one-sided paired *t*-test, d.f. = 1933, $t = 8.72$, $p > 0.99$), supporting the hypothesis that bees do not adjust the timing of their foraging to avoid windy conditions.

3.2. Wind tunnel experiments

In the wind tunnel, we recorded a total of 96 flight trials from 21 unique bumblebee foragers, and analysed body and wing kinematics for a subset of 65 trials from 13 bees (figure 3*d*). Standard deviation of roll orientation increased significantly in turbulent flow when compared with laminar flow at 3.0 m s^{-1} (figure 4*a* and table 1), but not at 1.5 m s^{-1} (table 1). Standard deviation of roll in laminar flow was significantly higher at 3.0 m s^{-1} than in still air (figure 4*a* and table 1) but there was no significant difference between still air and 1.5 m s^{-1} laminar flow or between 1.5 and 3.0 m s^{-1} laminar flow (figure 4*a* and table 1). In a separate model including body mass and [flow condition × speed] as fixed effects, we found no effect of body mass (dry mass, range = 35.3–68.1 mg across experimental individuals) on standard deviation of roll position ($t = -0.885$, d.f. = 9.9, $p = 0.397$). Standard deviation of pitch orientation did not differ significantly with flow or speed (table 1).

Mean wingbeat frequency displayed a small but statistically significant increase of approximately 4.5 Hz in turbulence at 3.0 m s^{-1} compared to laminar flow (figure 4*b* and table 1), while there was no significant difference at 1.5 m s^{-1} (table 1). Wingbeat frequency was significantly lower in 1.5 m s^{-1} laminar flow than in either still air (figure 4*b* and table 1) or 3.0 m s^{-1} laminar flow (figure 4*b* and table 1).

Mean stroke amplitude showed a marginally significant increase of approximately 4° in turbulence at 3.0 m s^{-1} compared with laminar flow (figure 4*c* and table 1), while there was no significant difference at 1.5 m s^{-1} (table 1). Stroke amplitude was significantly lower in both 1.5 m s^{-1} laminar flow (figure 4*c* and table 1) and 3.0 m s^{-1} laminar flow (figure 4*c* and table 1) than in still air, but showed no difference between 1.5 and 3.0 m s^{-1} laminar flow (figure 4*c* and table 1).

Within-trial variance in stroke amplitude asymmetry showed a marginally significant increase in turbulence when compared with laminar flow at 3.0 m s^{-1} (figure 5*a* and table 1), but not at 1.5 m s^{-1} (figure 5*a* and table 1). Variance in stroke amplitude asymmetry was significantly higher in 1.5 m s^{-1} laminar flow than in either still air (figure 5*a* and table 1) or 3.0 m s^{-1} laminar flow (figure 5*a* and table 1), but there was no difference between 1.5 and 3.0 m s^{-1} laminar flow (figure 5*a* and table 1).

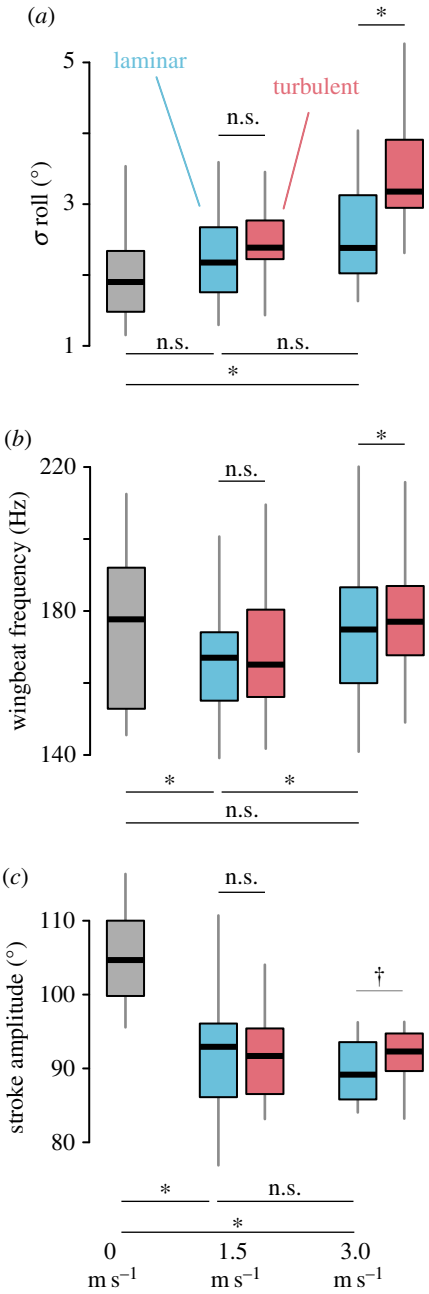

Figure 4. Body stability and mean wing kinematics across flow conditions. (*a*) Standard deviation of roll orientation, (*b*) mean wingbeat frequency and (*c*) mean stroke amplitude by speed and flow condition, with laminar trials in blue and turbulent trials in red. Bars above show comparisons between laminar and turbulent flow trials, at 1.5 and 3.0 m s^{-1}, and bars below show comparisons between laminar flow trials across speeds. Asterisks indicate significant differences between groups at the $\alpha = 0.05$ level, and daggers indicate marginal significance ($0.05 < p < 0.10$). Boxplots show the median and IQR, and whiskers depict the data range (75th and 25th ± 1.5 × IQR, respectively).

Maximum within-trial stroke amplitude asymmetry increased significantly in turbulence when compared with laminar flow at 3.0 m s^{-1} (figure 5*b* and table 1), but not at 1.5 m s^{-1} (figure 5*b* and table 1). Maximum stroke amplitude asymmetry showed no significant difference across flow speeds in laminar wind (figure 5*b* and table 1).

Roll orientation of the body and left–right stroke amplitude asymmetry were positively correlated across trials (figure 5*c*,*e*,

Table 1. Summary of linear mixed effects models examining the effects of wind speed and turbulence on body and wing kinematics in bumblebee (*Bombus impatiens*) foragers. Significant effects ($p < 0.05$) are highlighted in bold, while marginally significant effects ($0.05 < p < 0.10$) are highlighted in italics. See text for details of model specification.

variable	comparison (m s^{-1})	effect	d.f.	*t*	*p*-value
standard deviation of roll (high frequency, °)	1.5 (lam) versus 0	0.28	21.7	1.02	0.31
	3.0 (lam) versus 0	**0.57**	**21.7**	**2.1**	**0.048**
	3.0 (lam) versus 1.5 (tur)	0.29	22	1.01	0.33
	1.5 (tur) versus 1.5 (lam)	0.25	10.1	1.3	0.22
	3.0 (tur) versus 3.0 (lam)	**0.88**	**21**	**2.62**	**0.016**
standard deviation of pitch (high frequency, °)	1.5 (lam) versus 0	0.042	20.91	0.39	0.7
	3.0 (lam) versus 0	0.049	20.91	0.46	0.65
	3.0 (lam) versus 1.5 (tur)	6.8×10^{-3}	11	0.064	0.95
	1.5 (tur) versus 1.5 (lam)	0.12	10.99	1.11	0.292
	3.0 (tur) versus 3.0 (lam)	0.12	9.99	1.24	0.243
wingbeat frequency (Hz)	**1.5 (lam) versus 0**	**−7.91**	**33.4**	**−3.3**	**2.3×10^{-3}**
	3.0 (lam) versus 0	−1.42	33.3	−0.59	0.56
	3.0 (lam) versus 1.5 (tur)	**6.45**	**19.1**	**4.12**	**5.7×10^{-4}**
	1.5 (tur) versus 1.5 (lam)	1.31	20	0.78	0.44
	3.0 (tur) versus 3.0 (lam)	**4.52**	**1.62**	**2.79**	**0.012**
stroke amplitude (°)	**1.5 (lam) versus 0**	**−13.84**	**24.72**	**−6.24**	**1.65×10^{-6}**
	3.0 (lam) versus 0	**−15.66**	**23.22**	**−6.93**	**4.41×10^{-7}**
	3.0 (lam) versus 1.5 (tur)	−1.84	13.08	−0.82	0.43
	1.5 (tur) versus 1.5 (lam)	0.165	12.38	0.099	0.92
	3.0 (tur) versus 3.0 (lam)	*3.98*	*12.64*	*2.13*	*0.054*
variance in L-R amplitude asymmetry (°)	**1.5 (lam) versus 0**	**30.87**	**31**	**2.23**	**0.033**
	3.0 (lam) versus 0	20.96	31	1.48	0.15
	3.0 (lam) versus 1.5 (tur)	−9.91	21	−0.62	0.54
	1.5 (tur) versus 1.5 (lam)	−11.43	15.09	−0.76	0.46
	3.0 (tur) versus 3.0 (lam)	*25.37*	*23*	*1.96*	*0.062*
maximum L-R amplitude asymmetry (°)	1.5 (lam) versus 0	2.46	24.3	0.98	0.34
	3.0 (lam) versus 0	−1.43	22.56	−0.56	0.58
	3.0 (lam) versus 1.5 (tur)	−4.38	24	−1.61	0.12
	1.5 (tur) versus 1.5 (lam)	−0.67	24	−0.28	0.78
	3.0 (tur) versus 3.0 (lam)	**7.15**	**12.75**	**3.15**	**7.8×10^{-3}**

one-sample *t*-test, d.f. = 58, $t = 9.28$, $p = 4.5 \times 10^{-13}$) and experimental flow conditions (electronic supplementary material, figure S1). Within-trial variance in the angle of supination was significantly higher than within-trial variance in the angle of pronation (figure 5*d*,*f*, paired *t*-test, d.f. = 58, $t = -8.00$, $p = 6.13 \times 10^{-11}$).

4. Discussion

The results of our field study clearly demonstrate that turbulence is a common challenge for insects flying in natural environments (figures 1 and 2). Wind speed and turbulence intensity vary substantially in the environments where bees forage (figures 1 and 2) and bees do not avoid foraging during periods of higher flow speeds or turbulence intensities (figure 2*b*,*c*). This indicates that bees are subjected to substantial turbulence and variable wind speeds during their daily foraging activities. It is important to note that the measurements of environmental flow presented here were collected at a single location in space over a relatively short time window, and so likely do not represent the full range of flow conditions that foraging bees experience. Our data show that bees do not alter their foraging patterns within the range of flow speeds and turbulence intensities measured, but the question of whether their foraging activity is curtailed by more severe wind conditions remains unanswered.

We were able to reproduce some aspects of environmentally realistic turbulence in our wind tunnel, although the turbulence intensities generated were on the lower end of what bees experience in outdoor environments (figure 2*a*). The wind tunnel experiments revealed that both body stability and wing kinematics were affected by turbulent flow, but only at the higher end of environmentally relevant speeds (i.e. 3.0 m s^{-1}, figures 2 and 4). While previous work has demonstrated that the flight performance of orchid bees and hummingbirds is

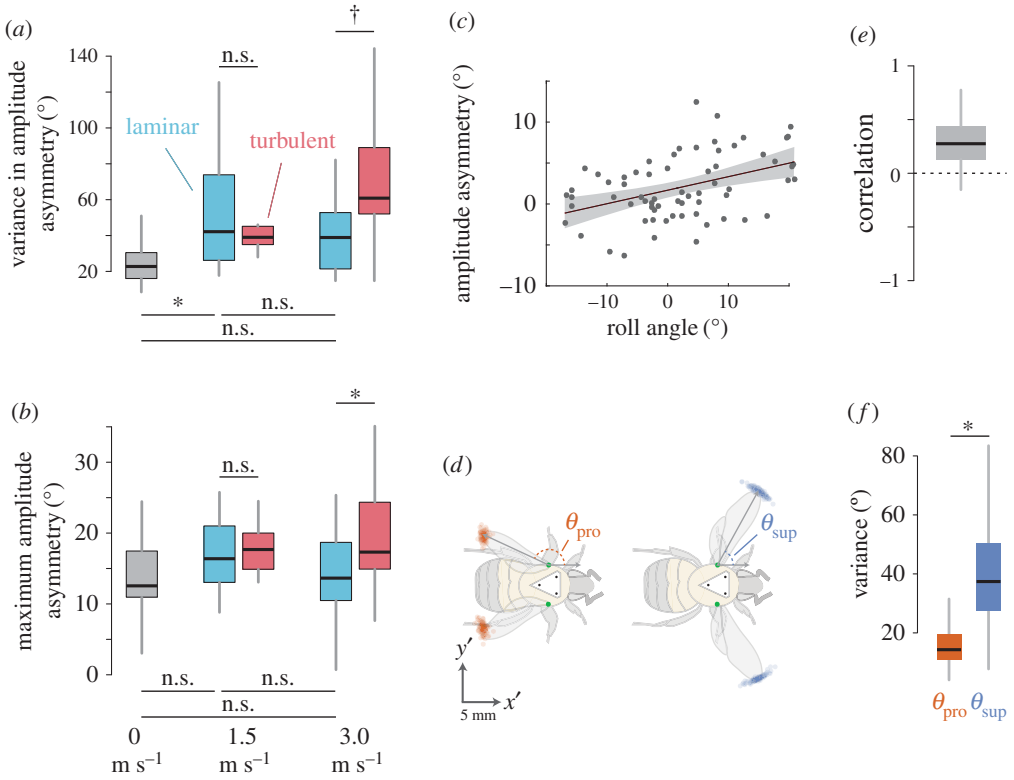

Figure 5. Variability in wing kinematics during flight in turbulence. (*a*) Within-trial variance in left–right amplitude asymmetry and (*b*) maximum left–right amplitude asymmetry, with laminar trials in blue and turbulent trials in red. Bars above show comparisons between laminar and turbulent flow trials, at 1.5 and 3.0 m s^{-1}, and bars below show comparisons between laminar flow trials across speeds. (*c*,*e*) Correlations between absolute roll angle of the body and asymmetry in stroke amplitude between the left and right wings, shown (*c*) for each stroke during one trial and (*e*) stroke-averaged correlations across all trials. (*d*) Locations of wingtips at pronation (orange) and supination (blue) during a single trial, rotated into the body frame. (*f*) Variance of pronation angle (orange) and supination angle (blue) across trials. Boxplots show the median and IQR, while whiskers depict the data range (75th and 25th $\pm$ 1.5 $\times$ IQR, respectively). Asterisks indicate significant differences between groups at the $\alpha = 0.05$ level, and daggers indicate marginal significance ($0.05 < p < 0.10$).

affected by turbulence at higher wind speeds (approx. 4 m s^{-1} and above, [12,18]), our results provide the first direct evidence that turbulence affects animal flight performance at lower, environmentally relevant wind speeds and turbulence intensities (figures 2 and 4). Further work is needed to generate wind tunnel flows that mimic what bees most commonly experience in the environment—low mean speeds but high turbulence intensities (e.g. speeds approx. 1 m s^{-1} and turbulence intensities of 0.25–0.30; figure 2*a*), so that the effects of these common flow conditions on flight performance can be assessed.

Bumblebees in our study responded to the increased body instability introduced by turbulence at higher flow speeds with a variety of active changes in wing kinematics. Bees displayed a small but statistically significant increase in wingbeat frequency in turbulence (figure 4*b*), consistent with results from hawkmoths flying in von Kármán vortex flows [19] and hummingbirds flying in turbulence [18]. This increase in wingbeat frequency may increase the energetic cost of flight due to an associated increase in the inertial power requirements for accelerating and decelerating the wings [30]. However, this increase in wingbeat frequency may represent an important strategy for increasing control authority, by reducing the time between wing strokes and thus decreasing the delay in updating control input to wing kinematics, a key factor in insect flight control [31]. Recent physical modelling studies also suggest that wings flapping more rapidly experience more consistent flow fields that are driven by kinematic forcing, and less subject to the random fluctuations of external, turbulent flows [32]. Bumblebees in our study also displayed a trend towards increased mean stroke amplitude in turbulent flow at higher speeds (figure 4*c*), suggesting a potential demand for higher aerodynamic power output during flight in turbulence [33–35].

In addition to shifts in mean wing kinematics, we found that bumblebees flying in turbulence displayed more variable and extreme wing kinematics (figure 5), suggesting that they respond actively to at least some of the high-frequency body instabilities induced by turbulent flow [21]. The significant correlation between roll angle of the body and left–right asymmetry in wing stroke amplitude (figure 5*c*) is consistent with the hypothesis that bees employ stroke amplitude asymmetry to help control body orientation during flight [36]. Asymmetric stroke amplitude could lead to both asymmetric lift generation and asymmetric stroke-averaged drag between the wing pairs, thus generating a net torque on the body [37].

Interestingly, bees appear to primarily adjust the angle of supination, rather than pronation, when modulating stroke amplitude (figure 5*d*,*f*). This could represent a strategy of simplifying control by reducing the number of free kinematics parameters. However, such simplification may also create coupling between kinematic parameters (in this case, between stroke amplitude and mean stroke position, potentially inducing pitching moments on the body [9]). Strategies for simplifying control mechanisms while avoiding disadvantageous coupling of kinematic parameters represent a potentially fruitful area of future research for both biological studies and bio-robotic applications. While in the current study we examined only the wingtip kinematics at stroke reversals, bumblebees may use a variety of other kinematic strategies to control body attitude

in addition to asymmetric stroke amplitude. Future work investigating time-varying wing kinematics in turbulence could be highly informative for revealing the full suite of kinematic control mechanisms available to insects flying in variable wind flows [36].

Overall, our results suggest that even relatively low levels of environmental turbulence, typical of those encountered on a daily basis by insects flying through natural aerial environments, can impact flight stability. We found that bumblebees respond to the instabilities resulting from turbulence with both static (e.g. altered mean values) and dynamic (stroke by stroke) changes in wing kinematics.

However, this study of one animal species in a single wind environment by necessity represents only a small fraction of variation in natural wind environments. Mean wind speeds and turbulence intensities vary substantially within habitats (e.g. higher turbulence and wind speed in forest canopies than in understories [11]), as well as across habitats [3]. In addition, while we focused here on exploring the effects of relatively small-scale, higher frequency turbulence (with an integral length scale—the size of the largest eddy—in our wind tunnel of approx. 4 cm [18]), wind flows in natural environments are characterized by integral length scales that typically range up to metre or kilometre scales. Our wind tunnel experiment recreated a naturalistic turbulence spectrum at higher frequencies [18], but was missing low-frequency components of turbulence, which are characteristic of natural environments but challenging to recreate in all but the largest laboratory wind tunnels. Future work linking flight behaviour to environmental flow characteristics, particularly studies exploring the effects of eddy size and more extreme wind conditions on insect flight, will be helpful in understanding the role of turbulence in the behaviour and ecology of flying insects.

Our results most probably represent only a subset of the strategies for coping with turbulence among animal fliers. Indeed, our findings suggest that bumblebees may use a set of mechanisms for increasing stability in turbulence that are distinct even from closely related orchid bees [38], suggesting the possibility of a wide range of turbulence-mitigation strategies among biological fliers. Exploring such strategies is of particular interest given recent advances in biologically inspired flying robots [39]. While there is growing demand and interest in small, autonomous flying robots for use in urban, agricultural and natural environments, navigating such complex physical environments remains a significant challenge for MAVs [40,41].

Future work exploring a broader range of animal species that must cope with environmental turbulence in diverse natural environments is of crucial importance for understanding the ecology and evolution of flight in animals. Such work may also reveal diverse flight stability mechanisms among flying animals applicable to the promising, but challenging development of autonomous robots operating at the scale of flying animals. In addition to these biological studies inspiring robotic design, the recent development of insect-scale, flapping-wing robots [39] provides an unprecedented opportunity for experimental exploration of basic questions regarding the control and stability of flying animals that are difficult or impossible to explore in real animals, or by using established modelling approaches such as dynamic scaling [42]. Future work that takes advantage of these synergies has the potential to shed light on how flying animals cope with the wide range of complex, natural environments they encounter, and reveal principles that could aid in the design of robust, bioinspired flying robots capable of meeting these same challenges.

Data accessibility. Associated data and custom scripts are deposited on zenodo.org.

Competing interests. We declare we have no competing interests.

Funding. This research was supported by an NSF Graduate Research Fellowship to J.D.C., a Robert K. Enders Field Biology Award of Swarthmore College to J.J.C., and NSF grant no. CCF-0926158 and IOS-1253677 to S.A.C.

Acknowledgements. We would like to thank Elizabeth Crone, Mark VanScoy, and Callin Switzer for their help in field experiments, as well as Sridhar Ravi for helpful discussions of turbulence data.

References

1. Schwegmann A, Lindemann JP, Egelhaaf M. 2014 Depth information in natural environments derived from optic flow by insect motion detection system: a model analysis. *Front. Comput. Neurosci.* **8**, 994. (doi:10.3389/fncom.2014.00083)
2. Hunter MD. 2002 Landscape structure, habitat fragmentation, and the ecology of insects. *Agric. For. Entomol.* **4**, 159–166. (doi:10.1046/j.1461-9563.2002.00152.x)
3. Stull RB. 1988 *An introduction to boundary layer meteorology*. New York, NY: Springer Science & Business Media.
4. Kingsolver JG, Higgins JK, Augustine KE. 2015 Fluctuating temperatures and ectotherm growth: distinguishing non-linear and time-dependent effects. *J. Exp. Biol.* **218**, 2218–2225. (doi:10.1242/jeb.120733)
5. Crall JD, Ravi S, Mountcastle AM, Combes SA. 2015 Bumblebee flight performance in cluttered environments: effects of obstacle orientation, body size and acceleration. *J. Exp. Biol.* **218**, 2728–2737. (doi:10.1242/jeb.121293)
6. Morice S, Pincebourde S, Darboux F, Kaiser W, Casas J. 2013 Predator–prey pursuit–evasion games in structurally complex environments. *Integr. Comp. Biol.* **53**, 767–779. (doi:10.1093/icb/ict061)
7. Dickinson MH, Farley CT, Full RJ, Koehl MA, Kram R, Lehman S. 2000 How animals move: an integrative view. *Science* **288**, 100–106. (doi:10.1126/science.288.5463.100)
8. Shepard ELC, Wilson RP, Rees WG, Grundy E, Lambertucci SA, Vosper SB. 2013 Energy landscapes shape animal movement ecology. *Am. Nat.* **182**, 298–312. (doi:10.1086/671257)
9. Dudley R. 2002 *The biomechanics of insect flight*. Princeton, NJ: Princeton University Press.
10. Norberg UM, Rayner JMV. 1987 Ecological morphology and flight in bats (Mammalia; Chiroptera): wing adaptations, flight performance, foraging strategy and echolocation. *Phil. Trans. R. Soc. Lond. B* **316**, 335–427. (doi:10.1098/rstb.1987.0030)
11. Kruijt B, Malhi Y, Lloyd J, Norbre AD, Miranda AC, Pereira MGP, Culf A, Grace J. 2000 Turbulence statistics above and within two Amazon rain forest canopies. *Boundary-Layer Meteorol.* **94**, 297–331. (doi:10.1023/A:1002401829007)
12. Combes SA, Dudley R. 2009 Turbulence-driven instabilities limit insect flight performance. *Proc. Natl Acad. Sci. USA* **106**, 9105–9108. (doi:10.1073/pnas.0902186106)
13. Ortega-Jimenez VM, Sapir N, Wolf M, Variano EA, Dudley R. 2014 Into turbulent air: size-dependent effects of von Karman vortex streets on hummingbird flight kinematics and energetics. *Proc. R. Soc. B* **281**, 20140180. (doi:10.1098/rspb.2014.0180)
14. Chang JJ, Crall JD, Combes SA. 2016 Wind alters landing dynamics in bumblebees. *J. Exp. Biol.* **219**, 2819–2822. (doi:10.1242/jeb.137976)

15. Fuller SB, Straw AD, Peek MY, Murray RM, Dickinson MH. 2014 Flying *Drosophila* stabilize their vision-based velocity controller by sensing wind with their antennae. *Proc. Natl Acad. Sci. USA* **111**, E1182–E1191. (doi:10.1073/pnas.1323529111)
16. Shepard ELC, Ross AN, Portugal SJ. 2016 Moving in a moving medium: new perspectives on flight. *Phil. Trans. R. Soc. B* **371**, 20150382. (doi:10.1098/rstb.2015.0382)
17. Ortega-Jimenez VM, Badger M, Wang H, Dudley R. 2016 Into rude air: hummingbird flight performance in variable aerial environments. *Phil. Trans. R. Soc. B* **371**, 20150387. (doi:10.1098/rstb.2015.0387)
18. Ravi S, Crall JD, McNeilly L, Gagliardi SF, Biewener AA, Combes SA. 2015 Hummingbird flight stability and control in freestream turbulent winds. *J. Exp. Biol.* **218**, 1444–1452. (doi:10.1242/jeb.114553)
19. Ortega-Jimenez VM, Greeter JSM, Mittal R, Hedrick TL. 2013 Hawkmoth flight stability in turbulent vortex streets. *J. Exp. Biol.* **216**, 4567–4579. (doi:10.1242/jeb.089672)
20. Ortega-Jimenez VM, Mittal R, Hedrick TL. 2014 Hawkmoth flight performance in tornado-like whirlwind vortices. *Bioinspir. Biomim.* **9**, 025003. (doi:10.1088/1748-3182/9/2/025003)
21. Engels T, Kolomenskiy D, Schneider K, Lehmann FO. 2016 Bumblebee flight in heavy turbulence. *Phys. Rev. Lett.* **116**, 028103. (doi:10.1103/PhysRevLett.116.028103)
22. Greenleaf SS, Williams NM, Winfree R, Kremen C. 2007 Bee foraging ranges and their relationship to body size. *Oecologia* **153**, 589–596. (doi:10.1007/s00442-007-0752-9)
23. Winfree R, Griswold T, Kremen C. 2007 Effect of human disturbance on bee communities in a forested ecosystem. *Conserv. Biol.* **21**, 213–223. (doi:10.1111/j.1523-1739.2006.00574.x)
24. Osborne JL, Clark SJ, Morris RJ, Williams IH, Riley JR, Smith AD, Reynolds DR, Edwards AS. 1999 A landscape-scale study of bumble bee foraging range and constancy, using harmonic radar. *J. Appl. Ecol.* **36**, 519–533. (doi:10.1046/j.1365-2664.1999.00428.x)
25. Ravi S, Crall JD, Fisher A, Combes SA. 2013 Rolling with the flow: bumblebees flying in unsteady wakes. *J. Exp. Biol.* **216**, 4299–4309. (doi:10.1242/jeb.090845)
26. Pope SB. 2000 *Turbulent flows*. Cambridge, UK: Cambridge University Press.
27. Hedrick TL. 2008 Software techniques for two- and three-dimensional kinematic measurements of biological and biomimetic systems. *Bioinspir. Biomim.* **3**, 034001. (doi:10.1088/1748-3182/3/3/034001)
28. Bates D, Mächler M, Bolker B, & Walker S. 2015 Fitting linear mixed-effects models using lme4. *J. Stat. Softw.* **67**, 1–48. (doi:10.18637/jss.v067.i01)
29. Kuznetsova A, Brockhoff PB, Christensen HB. 2014 *lmerTest: tests for random and fixed effects for linear mixed effect models* (*lmer objects of lme4 package*), *v. 2.0–25*. See https://cran.r-project.org/web/packages/lmerTest/index.html.
30. Dudley R, Ellington CP. 1990 Mechanics of forward flight in bumblebees: II. Quasi-steady lift and power requirements. *J. Exp. Biol.* **148**, 53–88.
31. Ristroph L, Ristroph G, Morozova S, Bergou AJ, Chang S, Guckenheimer J, Wang ZJ, Cohen I. 2013 Active and passive stabilization of body pitch in insect flight. *J. R Soc. Interface* **10**, 20130237. (doi:10.1098/rsif.2013.0237)
32. Fisher A, Ravi S, Watkins S, Watmuff J, Wang C, Liu H, Petersen P. 2016 The gust-mitigating potential of flapping wings. *Bioinspir. Biomim.* **11**, 046010. (doi:10.1088/1748-3190/11/4/046010)
33. Dillon ME, Dudley R. 2014 Surpassing Mt. Everest: extreme flight performance of alpine bumble-bees. *Biol. Lett.* **10**, 20130922. (doi:10.1098/rsbl.2013.0922)
34. Altshuler DL, Dickson WB, Vance JT, Roberts SP, Dickinson MH. 2005 Short-amplitude high-frequency wing strokes determine the aerodynamics of honeybee flight. *Proc. Natl. Acad. Sci. USA* **102**, 18 213–18 218. (doi:10.1073/pnas.0506590102)
35. Dudley R. 1995 Extraordinary flight performance of orchid bees (Apidae: Euglossini) hovering in heliox (80% He/20% O_2). *J. Exp. Biol.* **198**, 1065–1070.
36. Vance JT, Faruque I, Humbert JS. 2013 Kinematic strategies for mitigating gust perturbations in insects. *Bioinspir. Biomim.* **8**, 016004. (doi:10.1088/1748-3182/8/1/016004)
37. Hedrick TL, Cheng B, Deng X. 2009 Wingbeat time and the scaling of passive rotational damping in flapping flight. *Science* **324**, 252–255. (doi:10.1126/science.1168431)
38. Romiguier J, Cameron SA, Woodard SH, Fischman BJ, Keller L, Praz CJ. 2015 Phylogenomics controlling for base compositional bias reveals a single origin of eusociality in corbiculate bees. *Mol. Biol. Evol.* **33**, 670–678. (doi:10.1093/molbev/msv258)
39. Ma KY, Chirarattananon P, Fuller SB, Wood RJ. 2013 Controlled flight of a biologically inspired, insect-scale robot. *Science* **340**, 603–607. (doi:10.1126/science.1231806)
40. Floreano D, Wood RJ. 2015 Science, technology and the future of small autonomous drones. *Nature* **521**, 460–466. (doi:10.1038/nature14542)
41. Watkins S, Mohamed A, Fisher A, Clothier R, Carrese R, Fletcher DF. 2015 Towards autonomous MAV soaring in cities: CFD simulation, EFD measurement and flight trials. *Int. J. Micro Air Veh.* **7**, 441–448. (doi:10.1260/1756-8293.7.4.441)
42. Dickinson MH, Lehmann FO, Sane SP. 1999 Wing rotation and the aerodynamic basis of insect flight. *Science* **284**, 1954–1960. (doi:10.1126/science.284.5422.1954)

Chapter 3: Wind alters landing dynamics in bees

Reprinted from:
Chang, J. J., Crall, J. D., & Combes, S. A. (2016). Wind alters landing dynamics in bumblebees. *The Journal of Experimental Biology*, *219*(Pt 18), 2819–2822. http://doi.org/10.1242/jeb.137976

© 2016. Published by The Company of Biologists Ltd | Journal of Experimental Biology (2016) 219, 2819-2822 doi:10.1242/jeb.137976

SHORT COMMUNICATION

Wind alters landing dynamics in bumblebees

Jeremy J. Chang[1,2,*], James D. Crall[2,*,‡] and Stacey A. Combes[3]

ABSTRACT

Landing is an important but understudied behavior that flying animals must perform constantly. In still air, insects decelerate smoothly prior to landing by employing the relatively simple strategy of maintaining a constant rate of image expansion during their approach. However, it is unclear whether insects employ this strategy when faced with challenging flight environments. Here, we tested the effects of wind on bumblebees (*Bombus impatiens*) landing on flowers. We find that bees' approach paths to flowers shift from multidirectional in still air to unidirectional in wind, regardless of flower orientation. In addition, bees landing in a 3.5 m s^{-1} headwind do not decelerate smoothly, but rather maintain a high flight speed until contact, resulting in higher peak decelerations upon impact. These findings suggest that wind has a strong influence on insect landing behavior and performance, with important implications for the design of micro aerial vehicles and the ecomechanics of insect flight.

KEY WORDS: Insect flight, Animal flight, Pollinator, Bee, Physiological ecology, Optic flow, Collision avoidance

INTRODUCTION

Landing is a challenging behavior that flying animals must perform tens to hundreds of times each day while moving through natural environments, but it has received substantially less attention than other flight behaviors. Previous studies in honey bees (*Apis mellifera*) and fruit flies (*Drosophila melanogaster*) have demonstrated that the visual system plays an important role in controlling approach speed to landing surfaces (Evangelista et al., 2010; Srinivasan et al., 2000), as well as triggering key landing behaviors (van Breugel and Dickinson, 2012). In particular, recent work has shown that insects regulate flight speed during landing by the relatively simple strategy of maintaining a constant rate of image expansion (Baird et al., 2013), causing flight speed to decrease smoothly to zero as the landing target draws closer.

Although this landing strategy has the potential to work in nearly all situations, it is unknown whether flying insects can or do employ this strategy in the more challenging flight conditions characteristic of natural environments. One ubiquitous environmental challenge is wind: in natural environments, wind flows are highly variable and impact bees' flight stability (Combes and Dudley, 2009; Ravi et al., 2013).

Wind could also affect insects' landing patterns – or locomotory behaviors that precede landing – including the direction from which insects approach a landing target, and changes in body attitude and velocity. Wind increases drag forces on the body and wings of flying insects, and this may make fine control of body attitude and flight speed more challenging. Wind could also restrict the range of angles from which an insect can approach a target, as flying cross-wind is likely to be more challenging than flying upwind.

In this study, we investigated the effects of wind on bumblebees (*Bombus impatiens*) landing on flowers, to test the hypotheses that (a) approach angles are restricted in the presence of wind, and (b) bees employ the same smooth deceleration strategy when landing on flowers, regardless of external wind conditions.

MATERIALS AND METHODS

Specimen preparation

Oxeye daisies (*Leucanthemum vulgare*) were collected at the Concord Field Station in Bedford, MA, USA, and trimmed to 31 cm, reflecting the average height in the field (31.3±5.60 cm; N=23). Bumblebees (*Bombus impatiens* Cresson 1863) were acquired from Biobest Laboratories and maintained between June and August 2015 with *ad libitum* access to pollen and nectar.

Prior to each experiment, similarly sized bees (intertegular span, 4.63±0.43 mm; mass, 0.165±0.038 g; N=28) were isolated, cold-anesthetized, and outfitted with a BEEtag (Crall et al., 2015) tracking marker (3×4 mm) attached to the dorsal side of the scutum with cyanoacrylate adhesive (Fig. 1A). Marked bees were starved for ∼2 h before trials to increase feeding motivation.

Test conditions

Flight trials were conducted in a 6 m-long wind tunnel with a test section of 0.9×0.5×0.5 m. Grid patterns were fixed to the side panels of the working section to provide optic flow signals. For each trial, a fresh flower was placed in the upstream end of the test chamber with the stem elevated to form a ∼50 deg angle with the floor of the working section.

A small drop of nectar (Biogluc) was placed on the flower before each trial. A single bee was released downstream from the flower, allowed to fly until it landed on the flower (Fig. 1A), and then re-captured after ∼5 s of feeding and placed back at the initial release point.

Each bee was tested in four different experimental conditions: trials were conducted either with or without wind (3.5 m s^{-1}), and with the flower stem oriented either parallel or perpendicular to the long axis of the wind tunnel (i.e. the direction of flow when wind was present). Because the flexible stems allowed flowers to reorient in wind (Fig. S1), we ran two additional conditions with the flower stem immobilized while oriented either perpendicular or parallel to flow, to test for confounding effects of floral reorientation on bee approach angles (Fig. S2). Experimental conditions were presented in randomized order. Following the final trial, we immediately froze bees at −20°C, weighed them and measured their intertegular span.

[1]Department of Biology, Swarthmore College, Swarthmore, PA 19081, USA. [2]Department of Organismic and Evolutionary Biology, Harvard University, Concord Field Station, Bedford, MA 01730, USA. [3]Department of Neurobiology, Physiology and Behavior, University of California, Davis, CA 95616, USA.
*These authors contributed equally to this work

‡Author for correspondence (james.crall@gmail.com)

J.D.C., 0000-0002-8981-3782

Received 25 January 2016; Accepted 10 July 2016

Journal of Experimental Biology (2016) 219, 2819-2822 doi:10.1242/jeb.137976

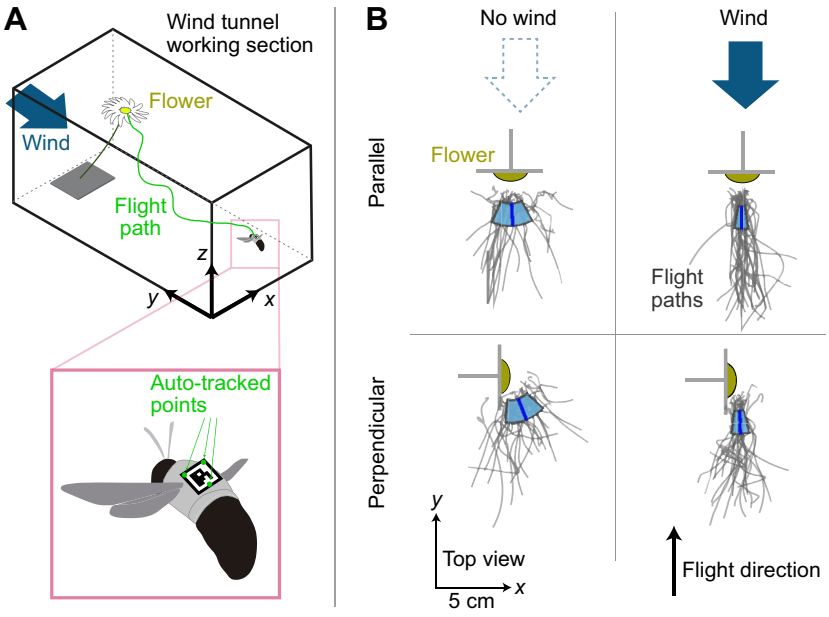

Fig. 1. Wind restricts approach angles of bumblebees landing on flowers. (A) Schematic illustration of the wind tunnel working section and BEEtag markers used to digitize body trajectories and orientations. (B) Flight traces (gray lines) of bees approaching flowers in still air (left, *N*=31 parallel, *N*=27 perpendicular) or 3.5 m s^{-1} laminar flow (right, *N*=29 parallel, *N*=25 perpendicular), with flowers oriented either parallel (top, *N*=31 in still air, *N*=27 in wind) or perpendicular (bottom, *N*=29 in still air, *N*=25 in wind) to the long axis of the wind tunnel. Thick blue lines and light blue shaded regions show the mean and standard deviation, respectively, of landing angles across bees for each trial condition.

High-speed videography and analysis

Flight trials were filmed within a cubic interrogation volume with two Photron SA3 high-speed cameras recording at 1000 Hz. The volume was calibrated via DLT (Hedrick, 2008).

BEEtag was used to track bees' body kinematics (Crall et al., 2015). The BEEtag software was modified to extract the coordinates of three points on the tag (Fig. 1A), which were converted to three-dimensional coordinates using DLTdv5 (Hedrick, 2008). Digitization noise was removed from position data with a low-pass, 5th order Butterworth filter with a cutoff frequency of 100 Hz. Instantaneous velocities and accelerations were calculated through numerical differentiation, and instantaneous roll and pitch angles were calculated following Ravi et al. (2013).

We defined two spatial regions: a 'landing' region, spanning 1.5–3 cm from the flower (roughly 1–2 bumblebee body lengths, capturing the period of flight just prior to contact with the flower), and an 'approach' region, spanning 5–7 cm from the flower (the distance range when bees first entered the interrogation volume). The angle from which bees approached and landed on flowers (the 'landing angle') was calculated by averaging position data within the landing region, converted to spherical coordinates centered on the flower. We calculated average flight speed and roll and pitch angles within each of these spatial regions, and defined the maximum deceleration associated with collision/landing as the most negative instantaneous change in speed during the last 100 ms of each trial. Throughout this paper, 'flight speed' refers to ground speed (i.e. speed in the global coordinate system), rather than air speed (i.e. speed including the 3.5 m s^{-1} air flow in trials with wind).

Statistics

All statistical analyses were performed in R. For linear mixed effects (LME) models, initial models were run with wind, orientation and wind×orientation as fixed effects and individual as a random effect using the 'lme' function in R. Non-significant effects were removed from the final model. For results on approach and landing speed, orientation and interaction (wind×orientation) effects were not significant, and data were pooled for still air and wind trials.

RESULTS AND DISCUSSION

We tracked 112 flights paths of 28 different bees across the four primary experimental conditions: with a flexible flower positioned parallel to the long axis of the wind tunnel in still air (*N*=31) or in the presence of a 3.5 m s^{-1} wind (*N*=27), and with the flower positioned perpendicular to the tunnel axis in still air (*N*=29) or in a 3.5 m s^{-1} wind (*N*=25).

Effects of wind on floral approach angle

In still air, the landing angle changed significantly with flower orientation; bees approaching a perpendicularly oriented flower shifted their flight path to align more closely with the face of the flower (Fig. 1B; LME, d.f.=32, t=−3.33, P=0.002). In the presence of wind, landing angles did not differ significantly with flower orientation (Fig. 1B; LME, d.f.=27, t=−1.00, P=0.33); rather, bees flew directly upwind to land on the flower, regardless of its orientation. While this could theoretically be caused by floral reorientation in the presence of wind (Fig. S1), this does not appear to be the case here: we saw no difference in landing angle when flowers were immobilized with wire to prevent reorientation (Fig. S2). Landing angles were also more restricted (i.e. had lower variance) in wind compared with still air, regardless of how the flower was oriented (Fig. 1B; parallel: F-test, F=0.109, d.f.=26, P≪0.01; perpendicular: F-test, F=0.236, d.f.=28, P≪0.01). Yaw angles were also more restricted in all wind trials, with bees approaching the flowers with their bodies oriented more directly upstream than in still air, independent of flower orientation (data not shown).

The observation that landing angles are restricted in the presence of wind is consistent with the intuitive (but to our knowledge untested) hypothesis that cross-wind flight and landing is more challenging than flying with the body axis oriented directly upwind, as the former would require substantial side-slip and/or continuous readjustment of body yaw and roll. It is also possible that olfaction plays a role in restricting landing angles, as scents emitted from the flowers could be carried downstream, exposing bees to olfactory cues. However, given that bees are known to rely strongly on visual cues when in close proximity to a floral stimulus (Srinivasan et al.,

Journal of Experimental Biology (2016) 219, 2819-2822 doi:10.1242/jeb.137976

2000; Vladusich et al., 2005; Lunau, 1992), we believe that olfaction plays only a minor role (if any) in our results.

The restriction of bumblebee landing angles in wind observed here may have important consequences for the ecomechanics of pollination. Floral orientation is highly variable in nature, and past studies have shown that some orientations (e.g. horizontal or downward-facing flowers) promote unidirectional approach paths, allowing for more consistent contact with the flower's reproductive organs, as compared with other orientations (e.g. upward-facing flowers) that allow pollinators to approach from many directions (Fenster et al., 2009). Wind, already known to have important direct effects on flower reorientation (Etnier and Vogel, 2000), might add another dimension of complexity to the interaction between flowers and their pollinators.

Effects of wind on landing speed and body orientation

Wind also had a significant effect on bee flight speed prior to landing. During the approach phase (5–7 cm from the flower), there was no difference in the mean speed of bees flying in wind versus still air (Fig. 2A–C; LME, d.f.=71, t=0.075, P=0.94). However, bees in still air reduced their ground speed significantly between approach and landing (Fig. 2A,D; mean change in speed, landing−approach= −0.171 m s^{-1}, paired t-test: t=−14.26, d.f.=54, P≪0.001), whereas bees flying in a 3.5 m s^{-1} headwind showed no significant change in ground speed (Fig. 2B,D; mean change=−0.004 m s^{-1}, t-test: t=−0.265, d.f.=54, P=0.79). Peak deceleration upon landing was also significantly higher in wind than in still air (Fig. 2E,F; LME, d.f.=72, t=−6.78, P≪0.01).

Diverse taxa of flying insects use visual cues to decelerate smoothly (and thus reduce impact forces) when landing (Baird et al., 2013; Srinivasan et al., 2000; van Breugel and Dickinson, 2012), and the relatively simple control strategy of maintaining a constant rate of image expansion has been proposed as potentially universal, allowing smooth landing on a surface of any orientation (Baird et al., 2013). Our results confirm that bumblebees flying in still air follow a pattern of smooth deceleration consistent with that shown for honeybees [Fig. 2; albeit on a somewhat different spatial scale (Baird et al., 2013), consistent with recent work in bumblebees (Reber et al., 2016)].

Bumblebees landing on flowers in wind, however, do not follow this pattern; they do not reduce their speed smoothly – in fact, they do not reduce their speed at all prior to landing (Fig. 2D). As a result, they experience higher peak decelerations (and thus impact forces) upon landing (Fig. 2E).

Why do bumblebees landing in wind display such apparently anomalous behavior? There are at least two possible explanations. First, this pattern could result from an active shift in control strategy. Roll instability (quantified here as standard deviation of roll) was higher in wind (Fig. 3A; LME, d.f.=71, t=7.55, P≪0.01), and this increased instability could make it challenging for bees to maintain fine control over their speed. In other words, they may abandon a smooth deceleration strategy in favor of a reliable (but physically damaging) collision-based landing strategy.

Alternatively, the patterns we observed could be the result of reduced airflow in the immediate wake of the flower, which may cause bees' ground speed to rise suddenly, even if they are attempting to regulate speed using the same visual cues as in still air. Any object in flow creates a downstream region of reduced flow speed as a result of drag. An insect approaching an object such as a flower from downstream would experience this area of reduced flow as a sudden reduction in headwind, which (in the absence of any change in flight kinematics) would actually increase the ground speed of the insect. To effectively reduce ground speed when moving through this region of low flow, the insect would have to rapidly alter its wing and/or body kinematics to reduce its air speed far beyond what is normally required for smooth landing, to compensate for the sudden difference in environmental wind speed.

Our results lend tentative support to the latter hypothesis. Mean pitch angle was lower (i.e. more pitched forward) for bees flying in wind versus still air (Fig. 3B; LME, d.f.=71, t=−20.62, P≪0.01), consistent with the role of pitch in determining thrust angle and forward flight speed in bees (Dudley and Ellington, 1990). Bees flying in wind changed their pitch angle significantly between the approach and landing phases, pitching up by approximately 5 deg prior to landing (Fig. 3C; mean change, landing–approach=4.89 deg, t-test: t=6.41, d.f.=54, P≪0.001). This was significantly greater than the change in pitch seen during flight in still air (Fig. 3C; LME, d.f.=70, t=4.31, P<0.001), which was not

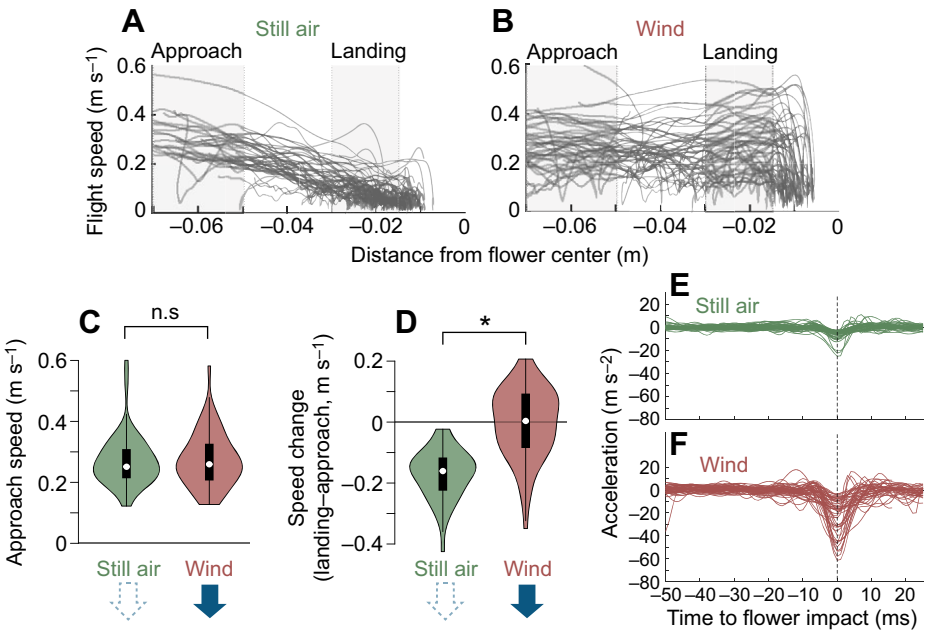

Fig. 2. Wind affects landing speed and impact decelerations. (A,B) Flight speed versus distance from the flower center in (A) still air and (B) 3.5 m s^{-1} wind. Each gray line represents data from a single trial, with trials pooled from parallel and perpendicular flower orientations. (C) Mean speed during the approach phase (5–7 cm from the flower) in still air versus wind. (D) Speed change between approach and landing phases (1.5–3 cm from flower) in still air versus wind. (E,F) Acceleration versus time to flower impact in (E) still air and (F) wind. Asterisk indicates significant difference at the α=0.05 level. Distributions in C and D are shown as violin plots, which depict the estimated kernel density plot (curved line), in addition to median (white-filled marker), interquartile range (thick black line) and 95th percentile range (thin black line). N=60 for still air trials, N=52 for wind trials.

Journal of Experimental Biology (2016) 219, 2819-2822 doi:10.1242/jeb.137976

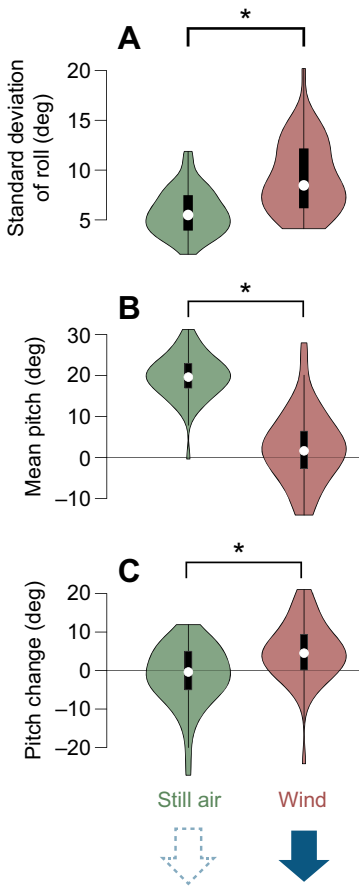

Fig. 3. Wind affects body orientations during approach and landing. (A) Standard deviation of roll angle in still air versus 3.5 m s^{-1} wind over the entire flight sequence. (B) Mean pitch angle in still air versus 3.5 m s^{-1} wind over the entire flight sequence. (C) Change in pitch angle between approach and landing phases in still air versus 3.5 m s^{-1} wind. Distributions are shown as violin plots, which depict the estimated kernel density plot (curved line), in addition to median (white-filled marker), interquartile range (thick black line) and 95th percentile range (thin black line). Asterisks indicate a significant difference between groups at the α=0.05 level. *N*=60 for still air trials, *N*=52 for wind trials.

significantly different from zero (Fig. 3C; mean change=−1.32 deg, *t*-test: *t*=−1.14, d.f.=44, *P*=0.26). This result suggests that bees may actually be attempting to reduce their flight speed in preparation for landing, but because of the sudden reduction in wind behind the flower, their ground speed remains constant.

Regardless of the specific mechanism, our results indicate that insects either do not choose to or are unable to perform controlled, low-impact landings in the presence of strong wind. Thus, high-impact landings are likely to occur regularly for insects flying in challenging, natural environments. This suggests the need for robust morphological designs capable of absorbing repeated impact forces while avoiding catastrophic damage, such as the buckling joints present in some insect wings (Mountcastle and Combes, 2014). Future work investigating the design of the landing apparatus in insects will be informative for understanding the evolutionary ecology of insect flight, as well as providing potential design principles for biomimetic, robotic applications.

Acknowledgements
The authors thank Callin Switzer for assistance with statistics.

Competing interests
The authors declare no competing or financial interests.

Author contributions
Specimen preparation and data collection were performed by J.J.C.; J.D.C. performed statistical analysis. All authors contributed equally to the conception and design of the experiments, and interpretation of results being published. J.J.C. and J.D.C. contributed equally to the writing of the paper.

Funding
This research was supported by the Robert K. Enders Field Biology Award of Swarthmore College to J.J.C., a National Science Foundation Graduate Research Fellowship to J.D.C., and National Science Foundation grants CCF-0926158 and IOS-1253677 to S.A.C.

Data availability
Kinematic data and example tracking scripts are available at zenodo.org (http://www.zenodo.org/record/60234#.V7Mv4pMrKt8).

Supplementary information
Supplementary information available online at
http://jeb.biologists.org/lookup/doi/10.1242/jeb.137976.supplemental

References

Baird, E., Boeddeker, N., Ibbotson, M. R. and Srinivasan, M. V. (2013). A universal strategy for visually guided landing. *Proc. Natl. Acad. Sci. USA* **110**, 18686-18691.
Combes, S. A. and Dudley, R. (2009). Turbulence-driven instabilities limit insect flight performance. *Proc. Natl. Acad. Sci. USA* **106**, 9105-9108.
Crall, J. D., Gravish, N., Mountcastle, A. M. and Combes, S. A. (2015). BEEtag: a low-cost, image-based tracking system for the study of animal behavior and locomotion. *PLoS ONE* **10**, e0136487.
Dudley, R. and Ellington, C. P. (1990). Mechanics of forward flight in bumblebees: I. Kinematics and morphology. *J. Exp. Biol.* **148**, 19-52.
Etnier, S. A. and Vogel, S. (2000). Reorientation of daffodil (*Narcissus: Amaryllidaceae*) flowers in wind: drag reduction and torsional flexibility. *Am. J. Bot.* **87**, 29.
Evangelista, C., Kraft, P., Dacke, M., Reinhard, J. and Srinivasan, M. V. (2010). The moment before touchdown: landing manoeuvres of the honeybee *Apis mellifera*. *J. Exp. Biol.* **213**, 262-270.
Fenster, C. B., Armbruster, W. S. and Dudash, M. R. (2009). Specialization of flowers: is floral orientation an overlooked first step? *New Phytol.* **183**, 502-506.
Hedrick, T. L. (2008). Software techniques for two- and three-dimensional kinematic measurements of biological and biomimetic systems. *Bioinspir. Biomim.* **3**, 034001.
Lunau, K. (1992). Innate recognition of flowers by bumble bees: orientation of antennae to visual stamen signals. *Can. J. Zool.* **70**, 2139-2144.
Mountcastle, A. M. and Combes, S. A. (2014). Biomechanical strategies for mitigating collision damage in insect wings: structural design versus embedded elastic materials. *J. Exp. Biol.* **217**, 1108-1115.
Ravi, S., Crall, J. D., Fisher, A. and Combes, S. A. (2013). Rolling with the flow: bumblebees flying in unsteady wakes. *J. Exp. Biol.* **216**, 4299-4309.
Reber, T., Baird, E. and Dacke, M. (2016). The final moments of landing in bumblebees, Bombus terrestris. *J. Comp. Physiol. A* **202**, 277-285.
Srinivasan, M. V., Zhang, S. W., Chahl, J. S., Barth, E. and Venkatesh, S. (2000). How honeybees make grazing landings on flat surfaces. *Biol. Cybern.* **83**, 171-183.
van Breugel, F. and Dickinson, M. H. (2012). The visual control of landing and obstacle avoidance in the fruit fly *Drosophila melanogaster*. *J. Exp. Bio.* **215**, 1783-1798.
Vladusich, T., Hemmi, J. M., Srinivasan, M. V. and Zeil, J. (2005). Interactions of visual odometry and landmark guidance during food search in honeybees. *J. Exp. Biol.* **208**, 4123-4135.

Chapter 4: BEEtag: A low-cost, image-tracked tracking system for the study of animal behavior and locomotion

Reprinted from:
Crall, J. D., Gravish, N., Mountcastle, A. M., & Combes, S. A. (2015). BEEtag: A Low-Cost, Image-Based Tracking System for the Study of Animal Behavior and Locomotion. *PLoS ONE*, *10*(9), e0136487–13.
http://doi.org/10.1371/journal.pone.0136487

PLOS | ONE

RESEARCH ARTICLE

BEEtag: A Low-Cost, Image-Based Tracking System for the Study of Animal Behavior and Locomotion

James D. Crall[1]*, Nick Gravish[1,2], Andrew M. Mountcastle[1], Stacey A. Combes[1]

1 Concord Field Station, Organismic and Evolutionary Biology, Harvard University, Bedford, Massachusetts, United States of America, **2** School of Engineering and Applied Sciences, Harvard University, Cambridge, Massachusetts, United States of America

* james.crall@gmail.com

Citation: Crall JD, Gravish N, Mountcastle AM, Combes SA (2015) BEEtag: A Low-Cost, Image-Based Tracking System for the Study of Animal Behavior and Locomotion. PLoS ONE 10(9): e0136487. doi:10.1371/journal.pone.0136487

Editor: Giorgio F Gilestro, Imperial College London, UNITED KINGDOM

Received: May 12, 2015

Accepted: August 4, 2015

Published: September 2, 2015

Data Availability Statement: All relevant data are within the paper and its Supporting Information files.

Funding: This work was funded by an NSF GRFP fellowship to James Crall and an NSF CAREER grant to Stacey Combes (IOS-1253677). Nick Gravish would like to acknowledge funding from the James S. McDonnell foundation.

Competing Interests: The authors have declared that no competing interests exist.

Abstract

A fundamental challenge common to studies of animal movement, behavior, and ecology is the collection of high-quality datasets on spatial positions of animals as they change through space and time. Recent innovations in tracking technology have allowed researchers to collect large and highly accurate datasets on animal spatiotemporal position while vastly decreasing the time and cost of collecting such data. One technique that is of particular relevance to the study of behavioral ecology involves tracking visual tags that can be uniquely identified in separate images or movie frames. These tags can be located within images that are visually complex, making them particularly well suited for longitudinal studies of animal behavior and movement in naturalistic environments. While several software packages have been developed that use computer vision to identify visual tags, these software packages are either (a) not optimized for identification of single tags, which is generally of the most interest for biologists, or (b) suffer from licensing issues, and therefore their use in the study of animal behavior has been limited. Here, we present BEEtag, an open-source, image-based tracking system in Matlab that allows for unique identification of individual animals or anatomical markers. The primary advantages of this system are that it (a) independently identifies animals or marked points in each frame of a video, limiting error propagation, (b) performs well in images with complex backgrounds, and (c) is low-cost. To validate the use of this tracking system in animal behavior, we mark and track individual bumblebees (*Bombus impatiens*) and recover individual patterns of space use and activity within the nest. Finally, we discuss the advantages and limitations of this software package and its application to the study of animal movement, behavior, and ecology.

Introduction

A fundamental challenge facing diverse fields of research is the accurate reconstruction of spatial position information over time. In biology, for example, fields such as biomechanics,

animal behavior, and ecology all depend heavily on reconstructing accurate spatiotemporal data on either anatomical components (e.g. different joints) of animals or their entire bodies. Traditionally, such tracking has been done primarily through human observation or manual tracking of positional information. Studies of animal locomotion, for example, have often involved manual (although frequently computer-aided) tracking of anatomical features to reconstruct accurate movement kinematics [1,2]. On the other hand, studies of animal behavior and ecology have often involved marking animals with uniquely identifiable tags combined with manual observation [3].

While such data sets have been indispensable for advancing their respective fields, manual collection of these data is time-intensive, laborious, and poorly-suited to generating large datasets, particularly those that involve tracking either multiple individuals or body parts simultaneously. In recent decades, advances in tracking technology have allowed researchers to collect large, highly accurate datasets in a fraction of the time taken by manual methods. For example, semi-automated marker tracking [4] or visual hull reconstruction [5] have allowed for the collection of highly accurate spatiotemporal datasets on animal locomotion. In ethology, automated tracking techniques have allowed for the collection of vast, highly-accurate behavioral datasets [6–8], which can be used, for example, in detailed quantitative analysis of animal behavior [9,10].

A fundamental limit of many of the tracking methods described above, however, is the need for a controlled, laboratory environment for high-quality tracking results, which for certain research questions can present a significant limitation. Partially for this reason, radio-frequency identification (RFID) technology, which does not require a controlled visual environment for identification, has become particularly popular among behavioral ecologists for tracking and identifying individuals in both vertebrate (see [11] for an excellent review of the use of this technology in birds) and invertebrate [12,13] animals. While robust to limitations of the visual environment, however, the spatial information provided by RFID is limited, since spatial position is only recorded when an animal is near an RFID reader, and the technology is therefore of limited utility for addressing certain experimental questions.

Increasingly, automated image-based tracking has been used to explore basic questions in behavior and ecology [8]. However, each tracking method has distinct strengths and limitations. One limitation that faces many image-based individual tracking methods is error propagation: since tracking is often based on using information from previous frames in a movie (e.g. spatial proximity of an animal from one frame to the next [4,14,15]), errors can be introduced when the paths of two animals cross. Such errors are generally irreversible and propagate through time, thus making it difficult or impossible to track individuals over long time periods. While computational advances can reduce [14] or nearly eliminate [7] this problem, these techniques still rely on controlled, homogenous visual environments for accurate tracking.

One method for avoiding such errors and allowing for long-term tracking of uniquely identified points or individuals in complex visual environments is to use markers that can be uniquely identified by computer-vision in each picture or frame. Image-based recognition of such markers has been widely used in commercial (e.g. barcodes and Quick-Response, or QR codes) as well as in augmented reality (ARTag, [16]) and camera-calibration (CALTag, [17]) applications. While such marker-systems have previously been used for high-throughput behavioral studies in ants [10], previous software packages are either not optimized for recognizing isolated tags (as desired for most applications in animal movement), or suffer from licensing issues, making access to these techniques limited. Here, we present and characterize BEEtag (**BE**havioral **E**cology tag), a new open-source software package in Matlab for tracking uniquely identifiable visual markers. First, we provide a basic description of the software and characterize its performance. Next, we validate the tracking system by marking and tracking

individual bumblebees (*Bombus impatiens*) within a nest. Finally, we consider the potential extensions, future applications, and limitations of this tracking technique.

Tag Design and Tracking Software

Tag design

We use a tag design that is inspired by similar markers for visual tracking such as ARtag [16] and CALTag [17]. Our tags consist of a 25 bit (5x5) code matrix of black and white pixels that is unique to each tag surrounded by (1) a white pixel border and (2) a black pixel border (Fig 1). The 25-bit matrix consists of a 15-bit identity code, and a 10-bit error check. The 15-bit identity is the binary representation of a number between 1 and 32767, left-padded with zeros and reoriented into a 5x3 pixel matrix (Fig 1A). A unique 10-bit error check is then generated for each code. The first 3 bits of this error code are parity checks (1 (white) for odd and 0 (black) for even) of each of the three columns of the 5x3 code matrix. The next two bits are generated by checking the parity of the first 3 and last 2 columns of the 5x3 code matrix, respectively. This 5-bit error check is then repeated and reversed to give a complete 10-bit error check (Fig 1). This simple binary image matrix can then be scaled to any size where it can be visualized by a camera, for example small tags for use with bumblebees (*Bombus impatiens*, Fig 1B, see below) or moderately larger tags for bigger invertebrates such as cockroaches (*Blaberus discoidalis*, Fig 1C, tags roughly 8 mm per side).

Generating a usable set of BEEtags

While a 15 bit encoding theoretically allows for 32,768 different possible code combinations, not all of these can be safely distinguished in practice when the orientation of the tag is unknown (as is the case in most tracking applications). We therefore restrict codes to be used in tracking based on two additional criteria. First, a tag must be valid in only one orientation (i.e. the 10-bit error check matches the 15-bit code in only one of the four possible tag orientations, Fig 1D). Second, any tag must have a Hamming distance of at least 3 (i.e. 3 bits are different) between itself and any valid tag (and its associated alternative orientations). These restrictions, which reduce the number of false positive tag identifications from an image, result in a set of 7,515 viable tags out of the 32,767 possibilities (Fig 1D). Since many users will not require the use of over 7,000 unique codes, we have also generated a set of 110 unique tags with a Hamming distance of at least 7, available with the BEEtag software package as "robustCodeList.mat."

Identifying BEEtags from an image or video frame

Using this technique, each tag can be uniquely identified in a still image or movie frame without prior knowledge of its position. The raw input for tracking is an image, in color or grayscale format. If tracking tags in a movie, each frame is extracted and analyzed as a separate image. If the frame or still image is in color, it is first converted to grayscale before further processing.

From the grayscale image, the first step is to threshold into a black and white image (Fig 2). In brief, this thresholding step works by converting the matrix of continuous pixel intensity values of an image (i.e. a grayscale image) into a binary matrix using a specified threshold value. This results in a binary (i.e. black and white) image, where zeros are represented by black and ones are represented by white. After converting to a binary image, the software finds all unique regions of white in the image and checks to see which are rectangular, and all of these regions are considered possible tags (Fig 1C). To verify which regions are true tags and identify

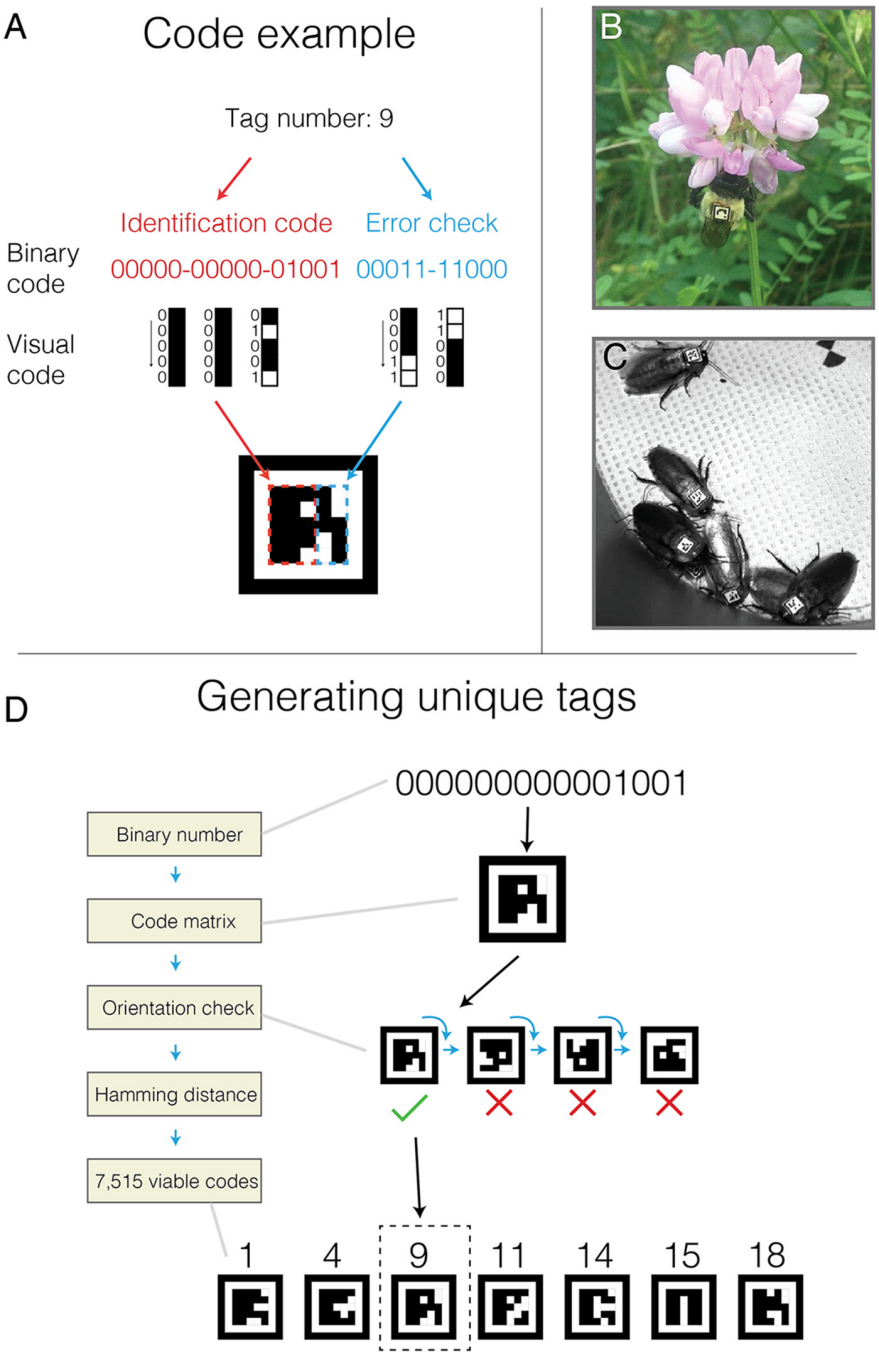

Fig 1. BEEtag code tructure and generation. (A) Basic tag design (see text for details). (B) A bumblebee worker (*Bombus impatiens*) outfitted with a BEEtag and encountered opportunistically in the natural environment. (C) Cockroaches (*Blaberus discoidalis*) outfitted with BEEtags. (D). Schematic representation of the process for generating a list of unique, usable BEEtags.

doi:10.1371/journal.pone.0136487.g001

them, the software then reads pixel values from within each white rectangle, converts them from black and white values to binary numbers, and references them against the list of viable tags described above. Finally, the position, identity, and orientation of all these tags are recorded and returned to the user as a Matlab structure array.

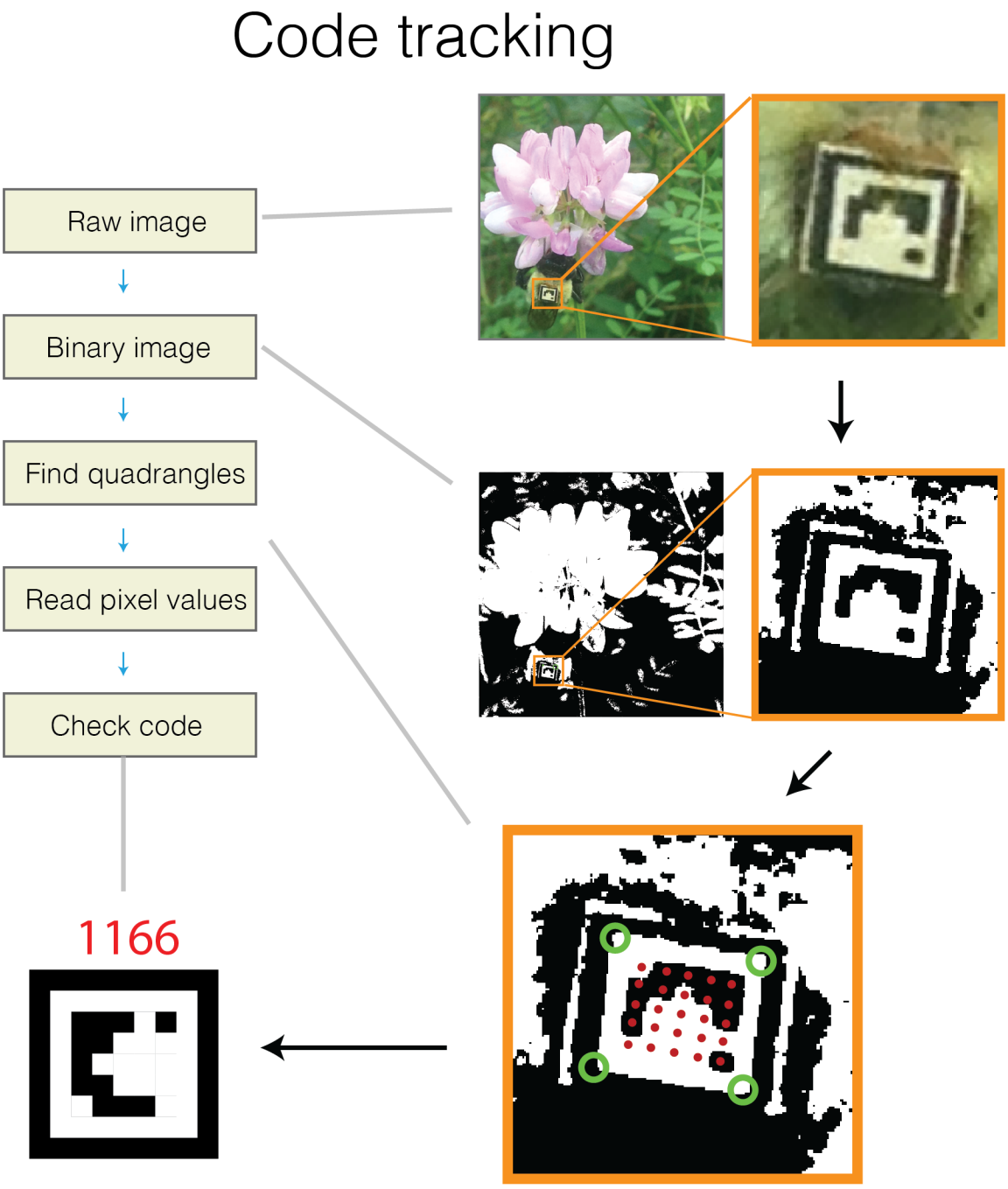

Fig 2. Schematic representation of the algorithm for identify unique BEEtags from an image. Green circles show identified corners of the white quadrangle, and red dots show points where separate pixel values were measured. See text for details.

doi:10.1371/journal.pone.0136487.g002

Software performance

To test the basic performance of the BEEtag software, we took a video of 12 printed tags with the built-in camera of an iPhone 5 from a constantly moving perspective (Fig 2A, S1 Movie, S1 Dataset). We identified codes in each frame while independently varying image resolution,

noise level, and black-white threshold levels to examine the effects of these parameters on tracking performance.

In general, tracking performance is strongly affected by all three of these parameters. Resolution was artificially modified using the "imresize" function in Matlab to a range of image resolutions. The average area (in pixels) of the 12 tags in the image was then calculated and the square root of this value taken to estimate the functional resolution of each tag, expressed as the mean length of each tag side (measured as the distance between 2 adjacent corners of the white rectangle containing the tag, Fig 3B). The portion of tags correctly tracked across 255 frames from this sample video dropped dramatically below a resolution of around 25 pixels per tag edge (Fig 3B).

We explored the extent to which noise impairs tracking performance (Fig 3C) by introducing Gaussian noise to each of 100 frames from the sample video using the "imnoise" function in Matlab. This function allowed us to apply Gaussian noise with varying levels of intensity (normalized to an image intensity of 0 to 1) to a full resolution image (i.e. around 38 pixels per tag edge). As expected, increased noise progressively impaired tracking performance, until values of around 0.05 (i.e. variance of 5% of the intensity range) when very few tags were successfully tracked (Fig 2C). Noise impairs tracking by both reducing the efficiency of quadrant tracking and increasing noise within the tag itself. In real applications, noise (i.e. "graininess")

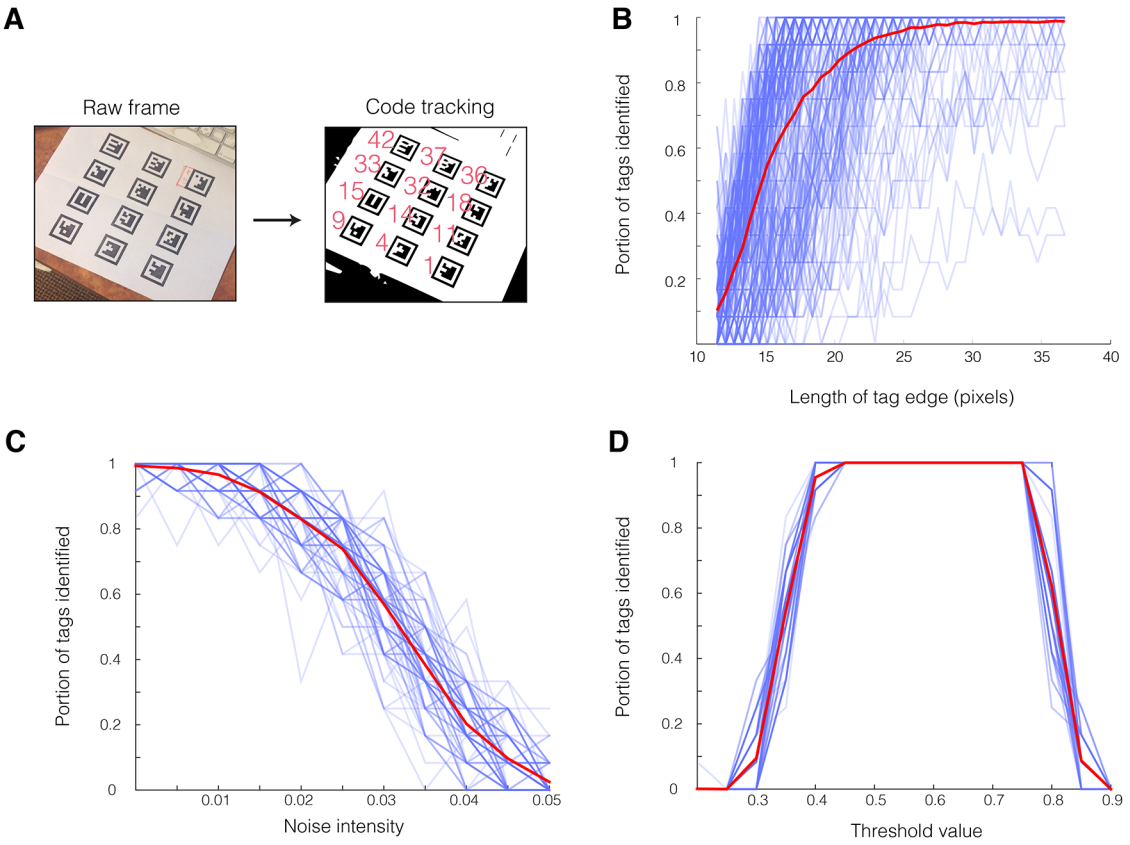

Fig 3. BEEtag tracking performance. Performance of the BEEtag tracking system in a sample video (A) in response to variation in resolution (B), gaussian noise (C), and binary threshold value (D). See text for details. Transparent blue lines show data from a single video frame (N = 277 in B and N = 100 in C-D), and thickened red lines show the mean across all frames.

doi:10.1371/journal.pone.0136487.g003

appears in images as a result of unwanted electronic signal, and can depend heavily on the sensor, camera, and recording settings used. For example, digital image noise increases significantly at higher ISO (or light sensitivity of the camera's sensor) values. In general, however, the noise values reported here are very high (the "0" noise value here represents the direct output of the camera, including digital noise), demonstrating that this tracking system is relatively robust to moderate noise levels. Nevertheless, noise remains an important consideration when designing an image-recording setup.

Finally, black-white thresholding values significantly affected tracking performance (Fig 3D). In parallel to the noise test, we tested the impact of threshold value on tracking performance across 100 frames of the same sample video described above, varying the threshold value over a range from 0.2 to 0.9, corresponding to a normalized intensity value. Tracking performance was optimal at intermediate threshold values, but significantly deteriorated at both low and high threshold values (Fig 3D). Since lighting conditions will vary substantially among real tracking applications, ideal threshold values will vary accordingly (see Experimental Validation below), and therefore finding an optimal tracking threshold will be an important step in each specific application of BEEtag. The BEEtag package also includes an option to use bradley adaptive thresholding to adjust for uneven lighting within images (see the "threshMode" option in the software package).

Overall, the rate of false positives for tag identification (i.e. the number of tags that are incorrectly identified, rather than not being identified) was low. Among 11,166 codes identified across the combination of 100 images and 15 resolution values described in the resolution test above, 5 were not values actually contained within the image, giving a false positive rate of ~0.04% (i.e. 99.96% of codes returned were correctly identified).

User interface

The BEEtag package consists of a small library of functions available in the supplementary material of this paper (S1 Code Supplement). Additionally, a continuously updated repository of the code is available at https://github.com/jamescrall/BEEtag. After installation (i.e. downloading all relevant functions and adding these to the Matlab search path), users interface with the software package primarily through the "locateCodes" function. This function takes a grayscale or color (rgb) image and returns the locations and relevant information (identity, orientation, etc.) of any BEEtag tags located in the image as a Matlab structure array. Users have the option of manually specifying the threshold value for binary image conversion, size limits for tags in pixels, and other visualization options.

Computational efficiency

An important consideration for any computational technique is computational efficiency. The computation time required for tracking BEEtags within single images or frames varies substantially between specific applications, and is heavily dependent on resolution, software parameter settings, and image complexity. In our tracking applications, we have found the time to process a single image to range from less than 100 ms for a relatively low resolution (i.e. ~600 x 400 pixels), simple image to over 30 seconds for a high resolution, complex image (i.e. a 6016 x 4000 image such as those described below), as processed on a Lenovo ThinkCentre desktop with an i7 processor and 4GB of RAM. For most applications, this range of computation times means that real-time image processing at frames rates of over 1 Hz may not be possible.

Experimental Validation: Spatial Behavior Patterns in a Bumblebee Colony

Study species and tag attachment

To validate the BEEtag tracking system, we outfitted individual bumblebees (*Bombus impatiens*) with unique BEEtags to track spatial movement of multiple individuals simultaneously within the nest. A single colony (Biobest) was maintained indoors but with access to the natural environment through a plastic tube, which allowed the bees to enter and exit the nest at will to forage for nectar and pollen. The colony was initially placed on July 9th, 2014 and given seven days to acclimate and begin normal foraging activity. On July 16th, we outfitted roughly 100 workers with unique BEEtags. All BEEtags used were printed on a single 8.5 x 11"sheet of waterproof, tear-resistant paper on a high-resolution (1200 dpi) laserjet printer at Staples. Each tag was cut out from the sheet by hand, measured roughly 2.1mm x 2.1 mm, and weighed around 1.83 mg. All bees except the queen were removed from the nest at the same time using a vacuum aspirator (Bioquip Products) and maintained for 30–60 min at 4°C to reduce activity level. Bees were then individually cold-anaesthetized at -20°C and outfitted with a unique tag attached with cyanoacrylate gel glue. After tagging, all bees were then returned to the nest and allowed to acclimate for 24 hours before data collection, which occurred on July 17th, 2014

Imaging setup and data collection

To capture images of sufficiently high resolution to track individual tags over the entire nest area (roughly 21.5 x 15.0 cm), we used an entry-level DSLR camera (Nikon D3200), operating at the maximum resolution of 6016 x 4000 pixels per image. The nest box was outfitted with a clear plexiglass top prior to data collection and illuminated by three red lights, to which bees have poor sensitivity [18]. The camera was placed ~ 1 m above the nest top and triggered automatically with a mechanical lever driven by an Arduino microcontroller. On July 17th, pictures were taken every 5 seconds between 12:00 pm and 12:30 pm, for a total of 372 photos. 20 of these photos were analyzed with 30 different threshold values to find the optimal threshold for tracking BEEtags (Fig 4M), which was then used to track the position of individual tags in each of the 372 frames (S1 Dataset).

Results and tracking performance

Overall, 3516 locations of 74 different tags were returned at the optimal threshold. In the absence of a feasible system for verification against human tracking, false positive rate can be estimated using the known range of valid tags in the pictures. Identified tags outside of this known range are clearly false positives. Of 3516 identified tags in 372 frames, one tag (identified once) fell out of this range and was thus a clear false positive. Since this estimate does not register false positives falling within the range of known tags, however, this number of false positives was then scaled proportionally to the number of tags falling outside the valid range, resulting in an overall correct identification rate of 99.97%, or a false positive rate of 0.03%.

Data from across 30 threshold values described above were used to estimate the number of recoverable tags in each frame (i.e. the total number of tags identified across all threshold values) estimated at a given threshold value. The optimal tracking threshold returned an average of around 90% of the recoverable tags in each frame (Fig 4M). Since the resolution of these tags (~33 pixels per edge) was above the obvious size threshold for optimal tracking (Fig 3B), untracked tags most likely result from heterogeneous lighting environment. In applications where it is important to track each tag in each frame, this tracking rate could be pushed closer

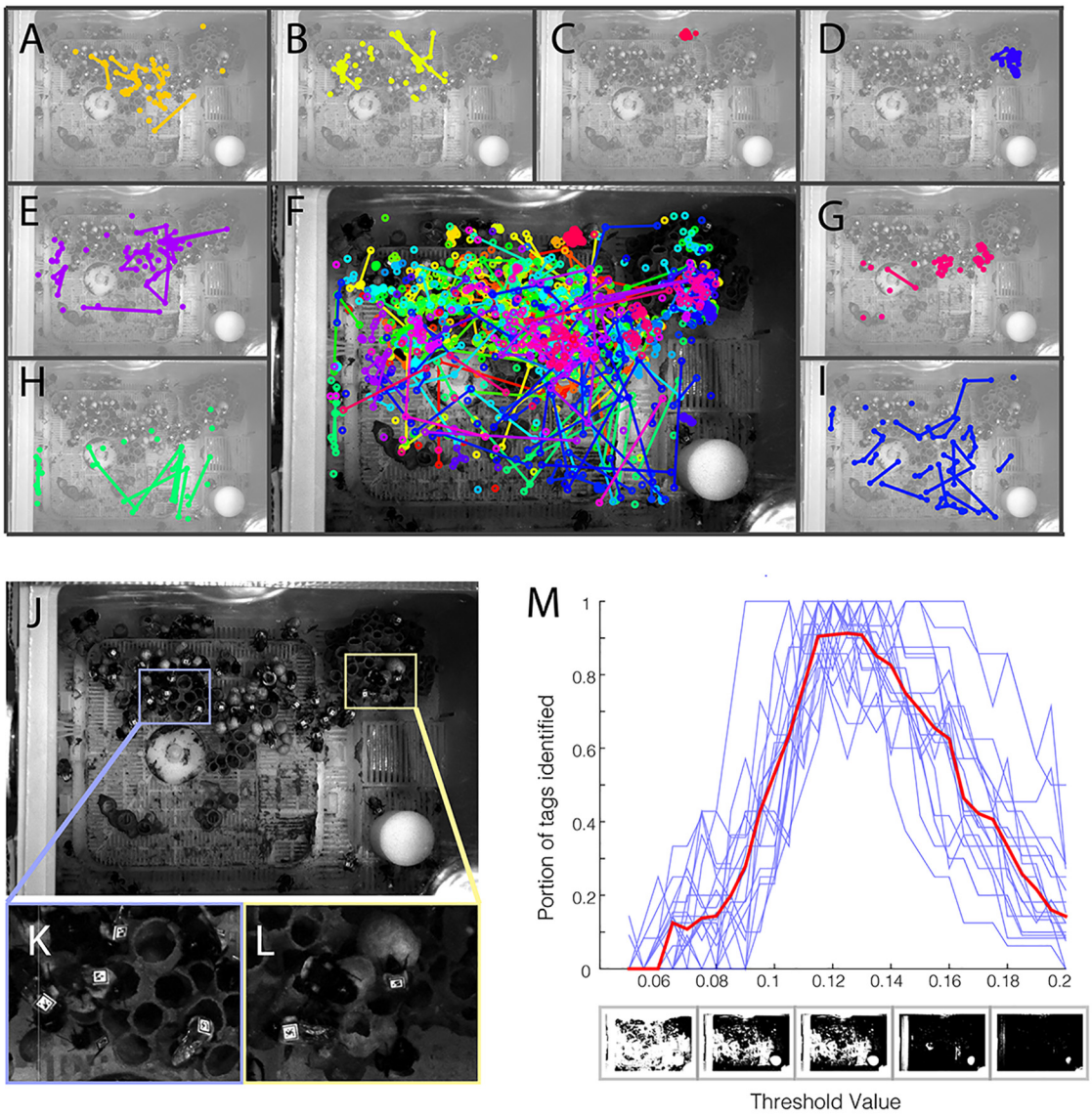

Fig 4. Validation of the BEEtag system in bumblebees (*Bombus impatiens*). (A-E, G-I) Spatial position over time for 8 individual bees, and (F) for all identified bees at the same time. Colors show the tracks of individual bees, and lines connect points where bees were identified in subsequent frames. (J) A sample raw image and (K-L) inlays demonstrating the complex background in the bumblebee nest. (M) Portion of tags identified vs. threshold value for individual pictures (blue lines) and averaged across all pictures (red line).

doi:10.1371/journal.pone.0136487.g004

to 100% by either (a) improving lighting homogeneity or (b) tracking each frame at multiple thresholds (at the cost of increased computation time).

These locations allow for the tracking of individual-level spatial behavior in the nest (see Fig 4F) and reveal individual variations in both activity and spatial preferences. For example, some bees remain in a relatively restricted portion of the nest (e.g. Fig 4C and 4D) while others roamed widely within the nest space (e.g. Fig 4I). Spatially, some bees restricted movement largely to the honey pots and developing brood (e.g. Fig 4B), while others tended to remain off the pots (e.g. Fig 4H) or showed mixed spatial behavior (e.g. Fig 4A, 4E and 4G).

Discussion

Here, we have presented a new open-source software package—BEEtag—for tracking unique visual markers and demonstrated its utility for studies of animal behavior. This package builds directly off previous work aimed at tracking individually identifiable markers [16,17] and extends previous efforts by providing a simple interface in Matlab that is intended to improve ease of use for researchers in behavioral ecology and other branches of the life sciences.

Tracking systems that utilize uniquely identifiable markers such as BEEtag (or ARTag and CALTag) have some fundamental advantages over other techniques. One primary advantage is that tags are identified independently in each photo or frame, so errors don't propagate across frames. For example, in most automated tracking systems (e.g. [4,14,15], with notable exceptions such as [7]), individual tracking depends on information from previous frames, and therefore when an individual is either (a) not tracked or (b) incorrectly tracked in one or a few frames (i.e. because the individual is occluded from view or interacts with another individual), tracking fails [7]. While acceptable for short-term data-collection, longer-term longitudinal data sets (as are often particularly relevant for behavioral ecology) are difficult or impossible to collect with such techniques.

Another important advantage of this tracking system is that it does not require a homogenous background, as do many optical tracking systems [7,14,15]. While it is possible in a controlled laboratory setting to create a homogenous background for automated detection of image regions associated with an animal's body, this is difficult or impossible in most naturalistic contexts [8]. BEEtags, on the other hand, are robust to complexity in the background image (see Fig 1B and Fig 4J–4L [although not necessarily lighting heterogeneity, Fig 4M, see discussion above]). For example, the sample image used in Fig 2 of a bumblebee worker with a BEEtag was taken opportunistically with an iPhone 5 against a natural background when the bee was encountered foraging outside of the nest, and emphasizes the robustness of this tracking system in natural environments.

Another important advantage of the BEEtag system is its cost. The examples included here used either an iPhone 5, or a commercially available Nikon DSLR camera (currently available for ~$500 USD), and tags were printed on waterproof, tear-resistant paper at a cost of $0.87 USD for 600 tags (approximately 0.145 cents each). This system thus makes the collection of high-quality, high-throughput behavioral datasets possible at an extremely low cost compared to alternative systems.

Like all other tracking systems, however, BEEtag has limitations that make it better suited to certain applications than others. First, the system requires the application of a tag. Handling [19] and tag application [20] can significantly affect stress levels [21] and behavior in animals [22]. While BEEtags are lightweight (depending on size and printing material), the potential biomechanical and behavioral effects of both tag attachment [23] and handling need to be carefully considered for each study organism and specific application.

Another important factor when considering the use of BEEtag for specific applications is computational intensity. As discussed above, computational time varies substantially depending on image resolution, complexity, and tracking settings, but is generally slower than necessary for real-time image processing applications. While it is still possible to use BEEtag on large, high frame-rate videos, such videos will generally need to be captured and analyzed at different times. For example, the tracking example presented above represents a small portion of a larger dataset consisting of over 80,000 images (data not shown). These images were captured over the course of several weeks and analyzed separately using a parallel supercomputer.

Since BEEtag depends on visual information, performance also can be substantially affected by (a) uneven lighting (see above and Fig 4M), (b) animal posture, and (c) tag cleanliness.

While issues of uneven lighting can be computationally overcome by either identifying codes at multiple threshold values, applying an appropriate high-pass spatial filter to images, or using adaptive thresholding (a user-specified option in BEEtag), the other limitations are more fundamental and mean that BEEtag tracking performance will be impaired in situations where tags are not visible (i.e. when animals are piled on top of each other) or cannot be kept clean (potentially an important consideration for freely behaving animals in natural environments).

Another important limitation when considering the utility of BEEtag for specific applications are the challenges of data storage and processing, which can be significant for any image processing techniques when compared to alternative tracking techniques such as RFID [12]. While performing processing in real time can minimize data storage problems, this is not possible in all applications. In particular, large images such as those used in the validation experiment described above (Fig 4) can be computationally intensive, and therefore impractical for real-time processing.

Alternative application and future directions

While we have focused here on using BEEtags for tracking the overall spatial position of individuals, the utility of this tracking system is not limited to ethology or behavioral ecology. One such potential direction that seems particularly promising is use in the field of animal locomotion. Focus in the study of animal locomotion has increasingly shifted from steady-state locomotion in laboratory environments to dynamic movement in complex, naturalistic environments [24–26], where tracking is particularly challenging [8]. Since having tags obscured for some or many frames is not highly problematic for BEEtag, we suggest that this tagging system could be of particular utility for tracking the kinematics of animal locomotion through cluttered environments, where they are likely to be temporarily obscured. Additionally, in applications where multiple rigid points are tracked in order to, for example, reconstruct three-dimensional body rotations [27], these points could be automatically extracted from a properly oriented BEEtag, thereby negating the need for manual or semi-automated digitizing [4].

The BEEtag package will be maintained regularly on the GitHub site, which allows for user contributions, and it is our hope that as use of this software increases, users will contribute improvements, modifications, and extensions that will enhance both performance and ease of use to the current implementation of BEEtag, as well as extending this technology to new applications.

Supporting Information

S1 Code Supplement. BEEtag tracking software. Functions and dependencies associated with the BEEtag tracking software for Matlab.
(ZIP)

S1 Dataset. Data from BEEtag tracking examples.
(MAT)

S1 Movie. BEEtag tracking example. Visualization of tracking results of 12 unique BEEtags in a movie taken with an iPhone 5. Inlay shows binary thresholded image used for code identification.
(MOV)

Acknowledgments

We are grateful to Benjamin de Bivort, Dominic Akandwanaho, Sawyer Hescock, and Andre Souffrant for help in debugging tracking software and placement of BEEtags on cockroaches.

This work was funded by an NSF GRFP fellowship to James Crall and an NSF CAREER grant to Stacey Combes (IOS-1253677). Nick Gravish would like to acknowledge funding from the James S. McDonnell foundation.

Author Contributions

Conceived and designed the experiments: JDC NG AMM SAC. Performed the experiments: JDC NG AMM. Analyzed the data: JDC. Contributed reagents/materials/analysis tools: JDC NG AMM SAC. Wrote the paper: JDC NG AMM SAC.

References

1. Wakeling JM, Ellington CP. Dragonfly flight. I. Gliding flight and steady-state aerodynamic forces. J Exp Biol. 1997; 200: 543–556. PMID: 9318238
2. Dudley R, Ellington CP. Mechanics of forward flight in bumblebees: I. Kinematics and morphology. Journal of Experimental Biology 1990; 148: 19–52.
3. Seeley TD, Camazine S, Sneyd J. Collective decision-making in honey bees: how colonies choose among nectar sources. Behav Ecol Sociobiol 1991; 28: 277–290.
4. Hedrick TL. Software techniques for two- and three-dimensional kinematic measurements of biological and biomimetic systems. Bioinspir Biomim. 2008; 3: 034001. doi: 10.1088/1748-3182/3/3/034001 PMID: 18591738
5. Ristroph L, Berman GJ, Bergou AJ, Wang ZJ, Cohen I. Automated hull reconstruction motion tracking (HRMT) applied to sideways maneuvers of free-flying insects. J Exp Biol. 2009; 212: 1324–1335. doi: 10.1242/jeb.025502 PMID: 19376953
6. Kain J, Stokes C, Gaudry Q, Song X, Foley J, Wilson R, et al. Leg-tracking and automated behavioural classification in Drosophila. Nat Comms. 2013; 4: 1910. doi: 10.1038/ncomms2908
7. Pérez-Escudero A, Vicente-Page J, Hinz RC, Arganda S, de Polavieja GG. idTracker: tracking individuals in a group by automatic identification of unmarked animals. Nat Meth. 2014; 11: 743–748. doi: 10.1038/nmeth.2994
8. Dell AI, Bender JA, Branson K, Couzin ID, de Polavieja GG, Noldus LPJJ, et al. Automated image-based tracking and its application in ecology. Trends in Ecology & Evolution 2014; 29: 417–428. doi: 10.1016/j.tree.2014.05.004
9. Berman GJ, Choi DM, Bialek W, Shaevitz JW. Mapping the stereotyped behaviour of freely moving fruit flies. Journal of The Royal Society Interface. 2014; 11: 20140672–20140672.
10. Mersch DP, Crespi A, Keller L. Tracking individuals shows spatial fidelity is a key regulator of ant social organization. Science 2013; 340: 1090–1093. PMID: 23599264
11. Bonter DN, Bridge ES. Applications of radio frequency identification (RFID) in ornithological research: a review. Journal of Field Ornithology. 2011; 82: 1–10.
12. Henry M, Beguin M, Requier F, Rollin O, Odoux JF, Aupinel P, et al. A Common Pesticide Decreases Foraging Success and Survival in Honey Bees. Science. 2012; 336: 348–350. doi: 10.1126/science.1215039 PMID: 22461498
13. Stelzer RJ, Chittka L. Bumblebee foraging rhythms under the midnight sun measured with radiofrequency identification. BMC Biol 2010; 8: 93. doi: 10.1186/1741-7007-8-93 PMID: 20587015
14. Branson K, Robie AA, Bender J, Pietro Perona, Dickinson MH. High-throughput ethomics in large groups of Drosophila. Nat Meth 2009; 6: 451–457. doi: 10.1038/nmeth.1328
15. de Chaumont F, Coura RD- S, Serreau P, Cressant A, Chabout J, Granon S, et al. Computerized video analysis of social interactions in mice. Nat Meth. 2012; 9: 410–417. doi: 10.1038/nmeth.1924
16. Fiala M. ARTag, a fiducial marker system using digital techniques. IEEE; 2005; 2: 590–596.
17. Atcheson B, Heide F, Heidrich W. CALTag: High Precision Fiducial Markers for Camera Calibration. Citeseer; 2010; 10: 41–48.
18. Briscoe AD, Chittka L. The evolution of color vision in insects. Annu Rev Entomol. Annual Reviews 4139 El Camino Way, PO Box 10139, Palo Alto, CA 94303–0139, USA; 2001; 46: 471–510. PMID: 11112177
19. Pankiw T, Page RE. Effect of pheromones, hormones, and handling on sucrose response thresholds of honey bees (Apis mellifera L.). J Comp Physiol A. 2003; 189: 675–684.
20. Dennis RL, Newberry RC, Cheng HW, Estevez I. Appearance Matters: Artificial Marking Alters Aggression and Stress. Poultry Science. 2008; 87: 1939–1946. doi: 10.3382/ps.2007-00311 PMID: 18809854

21. Sockman KW, Schwabl H. Plasma Corticosterone in Nestling American Kestrels: Effects of Age, Handling Stress, Yolk Androgens, and Body Condition. General and Comparative Endocrinology. 2001; 122: 205–212. doi: 10.1006/gcen.2001.7626 PMID: 11316426

22. Ropert-Coudert Y, Wilson RP. Trends and perspectives in animal-attached remote sensing. Frontiers in Ecology and the Environment. Eco Soc America; 2005; 3: 437–444.

23. Aldridge H, Brigham RM. Load carrying and maneuverability in an insectivorous bat: a test of the 5%"rule" of radio-telemetry. Journal of Mammalogy 1988;: 379–382.

24. Dickinson MH, Farley CT, Full RJ, Koehl M, Kram R, Lehman S. How animals move: an integrative view. Science. American Association for the Advancement of Science; 2000; 288: 100–106.

25. Combes SA, Rundle DE, Iwasaki JM, Crall JD. Linking biomechanics and ecology through predator-prey interactions: flight performance of dragonflies and their prey. Journal of Experimental Biology. 2012; 215: 903–913. doi: 10.1242/jeb.059394 PMID: 22357584

26. Daley MA, Biewener AA. Running over rough terrain reveals limb control for intrinsic stability. Proc Natl Acad Sci USA. 2006; 103: 15681–15686. doi: 10.1073/pnas.0601473103 PMID: 17032779

27. Ravi S, Crall J, Fisher A, Combes S. Rolling with the flow: Bumblebees flying in unsteady wakes. J Exp Biol. 2013; 216: 4299–4309. doi: 10.1242/jeb.090845 PMID: 24031057

Chapter 5: Behavioral idiosyncrasy structures task allocation and collective resilience in bee colonies

Title:

Behavioral idiosyncrasy structures task allocation and social resilience in bumblebee colonies

Authors:

James D Crall, Sarah Kocher, Robert L Oppenheimer, Nick Gravish, Andrew M. Mountcastle, Naomi E Pierce, Stacey A Combes

Abstract

Social insects live in colonies where many individuals cooperate to perform collective work. While behavioral specialization among workers (i.e. “division of labor”) is widely considered the key innovation of the ecologically-dominant social insects, the extent and function of behavioral idiosyncrasy across social insect colonies remains poorly, particularly in species with less advanced social organization. Here, we use an automated tracking system to continuously monitor nest behavior and foraging activity of uniquely identified workers from entire bumblebee (*Bombus impatiens*) colonies foraging in a natural environment. Despite weak task specialization (with nearly all workers performing multiple tasks each day), we nonetheless find widespread behavioral idiosyncrasy; workers show strong and stable inter-individual variation in spatial occupancy, activity level, and time devoted to different tasks. We also find a skewed distribution of foraging activity among individuals that is consistent across colonies and actively regulated in response to disturbance. Finally, we find that individual idiosyncrasies of space-use predict task switching in response to simulated predation, suggesting that spatial occupancy plays a key role in structuring information flow within colonies and their collective responses to disturbance. Our results highlight the importance of behavioral idiosyncrasy for structuring diverse aspects of task allocation, colony resilience, and information flow within social insect colonies, even in species that lack an organized division of labor.

Introduction

Social insects (i.e. ants, bees, wasps, and termites) are among the most ecologically dominant animals on the planet (Hölldobler & Wilson, 2009). Within social insect colonies, many individuals must cooperate to perform a variety of crucial collective tasks, including foraging for food and other resources, caring for developing young, maintaining and cleaning the nest, and defending the nest from predators and social parasites (Wilson, 1971). Division of labor is widely considered the key adaptation of social insects, allowing for increased colony efficiency by having either morphologically specialized workers with increased efficiency at their task, or by reducing the costs of task switching (Oster & Wilson, 1978; Wilson, 1968).

The importance of division of labor in social insects has come under increasing scrutiny, however, arising from several critical empirical observations. First, discrete, morphologically distinct worker castes are relatively rare in social insects, and the majority of species are instead characterized by monomorphic workers (Gordon, 2015; Oster & Wilson, 1978). (It is important to note that we focus here on differentiation of worker castes, as opposed to reproductive castes, i.e. morphological differences between reproductive and non-reproductive colony members.) Even in species where discrete castes are present (either morphological castes, or temporal castes, as found in honeybees and ants) and individual behavioral specialization is clear, workers are capable of switching tasks when colony demands change (Gordon, 1989; Tenczar, Lutz, Rao, Goldenfeld, & Robinson, 2014), suggesting a degree of flexibility inconsistent with strong, intrinsic differences between workers (Gordon, 2015). Recent work has even suggested abandoning use of the term “division of labor” altogether, in a call to shift emphasis from intrinsic variation between individuals in behavior toward an understanding of how interaction patterns generate task allocation in social insects (Gordon, 2015).

While the importance of division of labor *per se* in insect colonies has come under question, there is simultaneously growing appreciation and interest in the widespread role of individual behavioral variation in nearly all animal taxa (Wolf & Weissing, 2012). Animals show significant variation between individuals in nearly all behaviors

studied to date, from variation along the bold-shy behavioral spectrum (Sih, Bell, & Johnson, 2004), leadership (Kurvers et al., 2009), and even locomotor handed-ness in fruit flies (Buchanan, Kain, & de Bivort, 2015). There is increasing recognition of the parallels between behavioral syndromes in behavioral ecology and division of labor in social insects (Jandt et al., 2013; Jeanson & Weidenmüller, 2014) and growing interest in understanding both the proximate and ultimate origins of individual behavioral variability and its role in collective behavior of animal groups (Bengston, 2014; Jandt et al., 2013; Jeanson & Weidenmüller, 2014; LeBoeuf & Grozinger, 2014).

The role of individual variation remains a central question social insect behavior, with increasing focus on modeling the effects of inter-individual differences on collective behavior and dynamics of colonies (Beshers & Fewell, 2001; Bonabeau, Theraulaz, & Deneubourg, 1996). Response threshold models in particular have become the dominant paradigm for modeling patterns of task allocation within colonies based on individual variation among workers (Beshers & Fewell, 2001). In brief, these models assume workers vary in the stimulus level required to induce them to perform a task. Low-threshold individuals will perform a collective task at a lower level of stimulus, in turn reducing the collective stimulus and preventing the task stimulus from reaching a level high enough to induce high-threshold individuals to perform the task. However, in the absence of low-response threshold individuals in the colony, or if task demand is greatly increased, high-threshold individuals will perform the task. Response threshold models are thus attractive in part because they provide an elegantly simple explanation for how workers may both be specialized in behavior, but also flexible in response to disturbance (Bonabeau et al., 1996), consistent with empirical observation (Gordon, 1989). There is empirical support for response thresholds in a number of contexts, including bumblebee fanning behavior(Weidenmüller, 2004), foraging(Robinson & Page, 1989) and undertaking (Robinson & Page, 1988) in honeybees.

Despite their theoretical prominence, response threshold models have important limitations. For example, a key simplifying assumption of response threshold models is individuals are evenly mixed and have equal access to stimulus levels within the colony. Within social insect nests, however, there is now clear evidence that the distribution of

individuals is spatially heterogeneous (Jandt & Dornhaus, 2009; Mersch, Crespi, & Keller, 2013; Pinter-Wollman, 2015; Pinter-Wollman, Wollman, Guetz, Holmes, & Gordon, 2011). Information cues, as well as workers, are heterogeneously distributed in space and time within nests (Boer & Duchateau, 2006; Dornhaus, 2005; Mersch et al., 2013; Pinter-Wollman et al., 2011; Richardson & Gorochowski, 2015). While some models explicitly account for space-use within nests (e.g. foraging-for-work models (Tofts, 1993; Tofts & Franks, 1992)), these have most often treated spatial distributions as a consequence, rather than a cause, of task performance (although see (Pinter-Wollman, 2015; Richardson, Christensen, Franks, Jensen, & Sendova-Franks, 2011)). Despite growing interest in the spatial organization of work (and workers) in social insect colonies (Mersch et al., 2013; Quevillon, Hanks, Bansal, & Hughes, 2015; Richardson & Gorochowski, 2015), the functional role of spatial fidelity in division of labor and task allocation in social insect colonies remains largely unknown.

Thus, despite decades of research on the importance of behavioral castes, individual specialization, and division of labor in social insects, there remains substantial debate on the origins, extent, and importance of individual variation in social insect colonies. In part, this reflects the empirical challenge of investigating individual variation in collectively behaving insect groups, leaving basic questions unanswered about the distribution and consistency of behavioral among individual workers, particularly in species that live in smaller colonies and lack discrete behavioral castes. Automated behavioral tracking techniques are rapidly reshaping this field, however, allowing investigators to study behavior repertoires of large groups of individuals (Henry et al., 2012; Mersch et al., 2013) simultaneously, and in increasingly complex, naturalistic environments (Berdahl, Torney, Ioannou, Faria, & Couzin, 2013; Tenczar et al., 2014).

Here, we use an automated, image-based tracking system (BEEtag, (Crall, Gravish, Mountcastle, & Combes, 2015) to investigate the extent and function of individual behavioral variation among workers in the small (100-200 workers) and simple (lacking discrete castes) colonies of bumblebees (*Bombus impatiens*), foraging in natural environments. We use a combination of passive observation and experimental manipula-

tions to explore the structure of behavioral idiosyncrasy, the distribution of individual behaviors across entire colonies, and the role of this individual variation in structuring collective responses to colony perturbations.

Results

We recorded 1.21 million nest behavior sequences and 26,511 foraging transits from 1,717 unique bees across 19 colonies of *Bombus impatiens*, foraging freely in the outdoor environment in Bedford, MA between July and October 2015. For each colony, spatial locations of uniquely-identified workers within the nest were recorded in brief intervals (5 seconds, Video S1), while foraging transits into and out of the nest were recorded with motion-activated camera (Fig 1A, Video S2).

We combined activity and location information of individual workers with spatial-mapping of key nest components (i.e. developing eggs, larvae and pupae, wax pots for food storage, etc, Video S3) to evaluate the behavioral state of individual workers within the nest an average of 140 times daily (or approximately once every ten minutes, Fig 1B), 24 hours a day for up to two weeks. Foraging activity was monitored by a separate camera continuously recording bees transiting between the nest chamber and the outdoor foraging environment (Fig 1A, Video S2). Time spent foraging for each bee was estimated by combining information on foraging transits and presence within the colony. For each timestep, individual bees were thus categorized as performing one of four major task categories: (1) foraging, (2) brood care, (3) manipulating food and waxpots, (4) patrolling/cleaning, or (5) inactive.

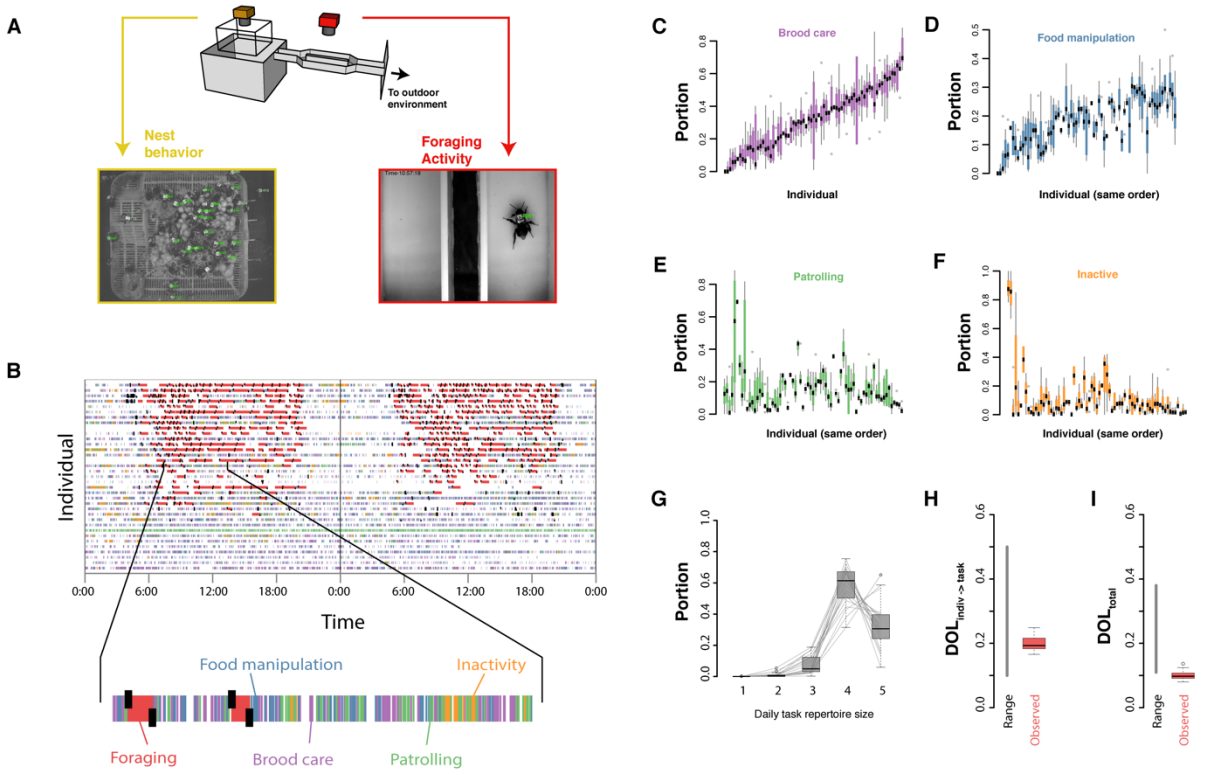

Figure 1. **Automated behavioral tracking in bumblebee colonies.** (A) Schematic diagram (above) and sample images from within nest (left, orange) and the foraging tunnel (right, red), showing tracked individual BEEtags in green. (B) Representative traces of individual behaviors over two days from a single colony ("c4"). (C-F) Portion of time spent engaged in different nest behaviors by individual workers, across all days from the same representative colony ("c4"). (G) Portion of bees exhibiting different daily task repertoire sizes, normalized by colony. Boxplots show variation across colonies (gray lines). (H-I) Individual specialization (DOLindiv-> task, H) and total division of labor (DOLtotal, I) calculated following (Gorelick et al., 2004). Thick gray lines show the range of published values for social insects, and red boxplots show the observed range for bumblebees. Boxplots in (G-I) show the median and inter-quartile range (IQR), while whiskers depict the data range (75^{th} and 25^{th} +/- 1.5*IQR, respectively)

Individual bees switched frequently between tasks (Fig 1B), with the vast majority (93%) of workers performing at least 4 (out of 5) different major tasks on a given day, and nearly all (99.4%) of bees performing at least 3 different tasks (Fig 1G). Consistent with this (and previous work, see (Jandt, Huang, & Dornhaus, 2009)), we found weak patterns of division of labor within bumblebee colonies: Individual specialization (Fig 1H, $DOL_{individuals\ ->\ tasks}$, mean = 0.20, sd = 0.02) and total division of labor (Fig 1I, DOL_{total},mean = 0.10, sd = 0.014]) were all on the low end of published values for social insects (Fig 1H-I, (Dornhaus, Holley, & Franks, 2009; Jandt et al., 2009; Jeanson, Kukuk,

& Fewell, 2005), and similar to values from previous work in bumblebees (Jandt et al., 2009)

Despite high levels of task flexibility and weak division of labor across colonies, however, individual workers nonetheless showed strongly idiosyncratic patterns of behavior. Despite performing multiple tasks each day, individual workers spent a highly repeatable portion of their time engaged in different tasks (Fig 1C-F, one-way ANOVA; portion of time in broodcare, df = 949, F = 3.75, $p < 10^{-16}$; portion of time manipulating food, df = 949, F = 3.25, $p < 10^{-16}$; portion of time inactive, df = 949, F = 4.52, $p < 10^{-16}$; portion of time patrolling, df = 949, F = 4.8, $p < 10^{-16}$). In addition to performing tasks with repeatable probabilities across days, individual workers also showed variable patterns of spatial occupancy, which were significantly repeatable within individuals across days (Fig 2A-C, $p < 10^{-39}$ for all colonies, two sample t-test)).

To (a) reduce the dimensionality of nest behavior and (b) explore the correlation structure between metrics of nest behavior, we performed a principle components analysis (PCA) on nest behavior among worker bees across individuals and experimental days (Fig S1). We found that the first two principle components explain a combined 51% of the observed variation in nest behavior (Fig 2E). The first principal component of nest behavior (PC1, Fig 2E) was correlated primarily with aspects of spatial occupancy, including a negative correlation with distance from the nest center (Fig S1), as well as being positively correlated with portion of time spent in either brood care or manipulating food stores (Fig S1) and positive correlations with brood and waxpot interactions rates, and social interaction strength, but had a weak correlation to metrics of activity level (Fig S1). In contrast, the second principle component of nest behavior (PC2 2, Fig 2E) was correlated with several metrics of activity level (average moving velocity, portion of time active, daily activity scope, etc). In addition to correlation with activity metrics, higher principal component 2 scores are also associated with rate of interaction with waxpots, as well as a negative correlation with the portion of time on the nest architecture that was spent on brood, rather than waxpots. Individual bees showed strong and significant repeatability for both principal components of nest behavior across (Fig 2D, PC1, one-

way ANOVA, df = 949, F = 5.57, $p < 10^{-16}$; PC2, one-way ANOVA, df = 949, F = 2.65, $p < 10^{-16}$).

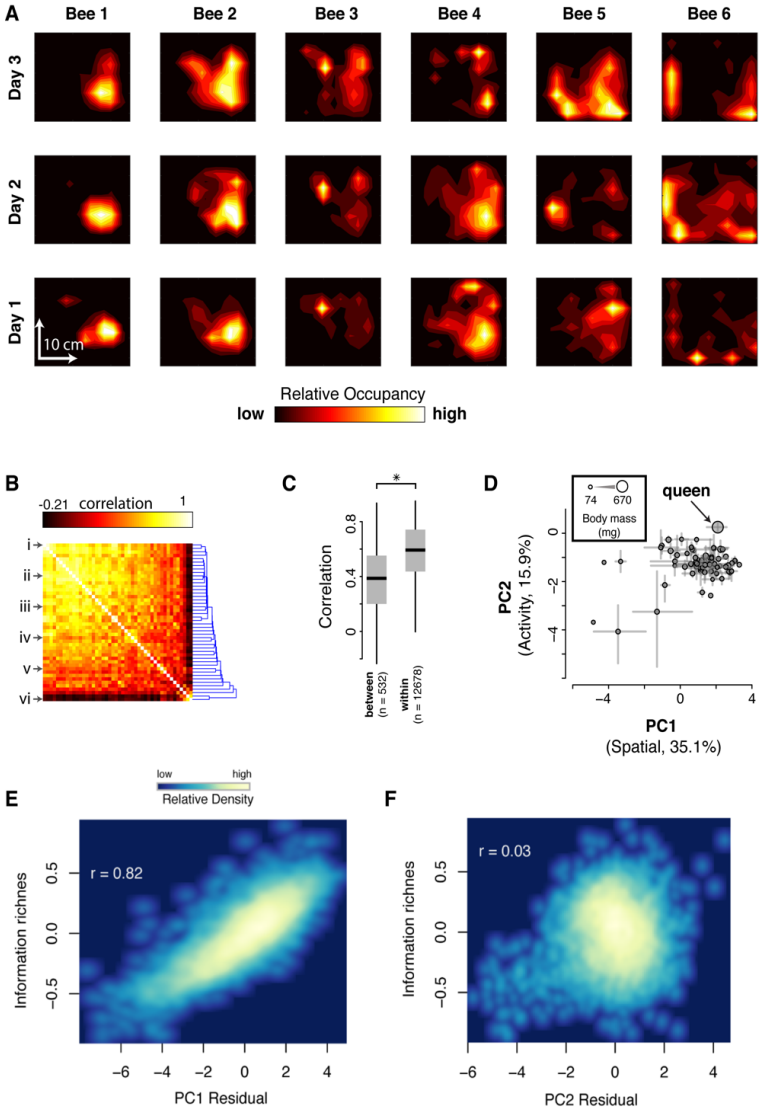

Figure 2. **Workers show idiosyncratic patterns of spatial fidelity and activity within the nest.** (A) Representative spatial occupancy patterns within the nest of six bumblebee workers over three days from a single colony ("c4"). Color indicates relatively occupancy, smoothed by kernel density estimation. (B) Correlation matrix of spatial occupancy pattern between workers for a single day from a single colony ("c4"), with dendrogram (in blue) showing linkage distance between bees. Color indicates correlation strength. (C) Correlation of spatial occupancy within and between individuals across days from a single colony ("c4"). Boxplots in show the median and inter-quartile range (IQR), while whiskers depict the data range (75^{th} and 25^{th} +/- 1.5*IQR, respectively) (D) Variation in principle components scores of individual workers across days from a single representative colony ("c4"). (E-F) Correlation between residual PC1 (E) and PC2 (F) scores and Information Richness. See Methods for details of Information Richness calculations.

To assess the relationship between components of nest behavior and information flow, we calculated overall information richness (which incorporates interaction strength with nestmates, as well as interaction rates with key sources of nest information, such as waxpots and brood) for each bee on each day. We found a strong correlation between PC1 and Information Richness but a very weak correlation between PC2 and Information Richness (Fig 2E-F).

All colonies showed a strong skew in the distribution of foraging activity among workers, with the majority of foraging performed by a relatively small number of bees (Fig 3A). We quantified the statistical inequality in foraging activity using the Gini coefficient (Fig 3B-C), and found a strong skew in foraging behavior across all colonies (0.71 +/- 0.09). Observed Gini coefficients were higher (i.e. more unequal) than simulated permutations of foraging activity treating (a) all bees in the colony as a single group ($df = 13$, $t = -18.8$, $p < 10^{-10}$, paired t-test), or (b) workers as belonging to one of two equivalent groups, foragers or non-foragers ($df = 13$, $t = -6.3$, $p = 2.8 \times 10^{-5}$, paired t-test), providing evidence for significant inequality among foragers, as well as between foragers and non-foragers.

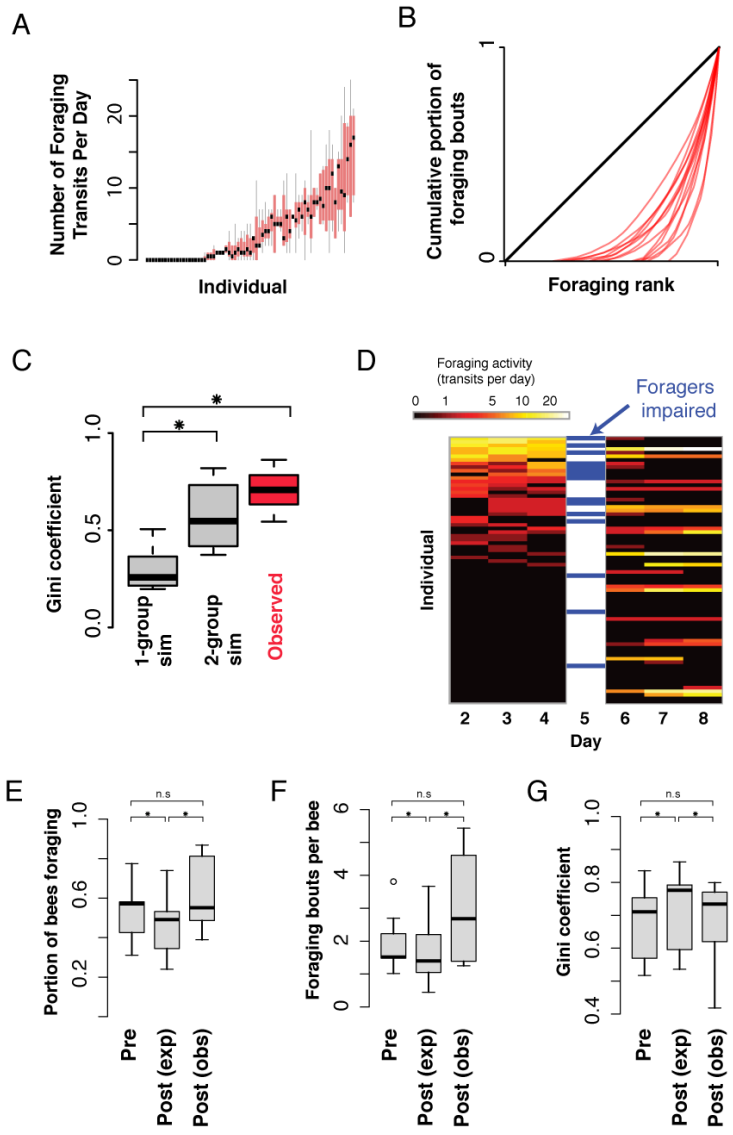

Figure 3. **Foraging activity is regulated at the colony level**. (A) Number of foraging transits per day by bi individual, for a single representative colony ("c4"). (B) Lorenz curves showing inequality in foraging activity across all experimental colonies (C) Observed Gini coefficients across experimental colonies (red) vs. simulations randomly distributing observed foraging activity across all bees within colonies (1-group, grey) and simulations randomly distributing observed foraging activity across foragers and non-foragers (2-group, grey). (D) Foraging activity of individual bees from a single representative colony for the three days before and after a simulated predation event, where 13 bees were foraging-impaired (via wing clipping). Boxplots (red) show the median and inter-quartile range (IQR), while whiskers depict the data range (75^{th} and 25^{th} +/- 1.5*IQR, respectively)

To investigate the regulation of foraging activity at the colony-level, we simulated predation by impairing (via wing clipping) or removing foragers from nine separate colo-

nies (Fig 3D) and tracking patterns of foraging activity in the 3 days before and after experimental manipulation (Fig 3D). We found qualitatively similar and statistically indistinguishable patterns between forager impairment and removal, so results from these manipulations were pooled. We found that both overall foraging activity at the colony level, as well as the portion of bees foraging, were significantly higher than expected based on forager loss (Fig 3, paired Wilcoxon tests, Post(expected) v Post (observed), bouts per bee, $v = 5$, $p = 0.039$; Portion of bees foraging, $v = 1$, $p = 0.0078$), and were not significantly different than pre-manipulation foraging levels (Fig 3, paired Wilcoxon tests, Post (observed) v. Pre, Bouts per bee, $v = 8$, $p = 0.098$; Portion of bees foraging, $v = 7$, $p = 0.074$). This same pattern held true for the inequality of foraging activity, with observed Gini coefficients significantly lower than expected after manipulation (Fig 3, paired Wilcoxon tests, Post (expected) v Post (observed), $v = 45$, $p = 0.039$) and showed no significant difference from pre-manipulation levels (Fig 3, paired Wilcoxon tests, Post (observed) v Pre, $v = 27$, $p = 0.65$).

Finally, we used this experimental manipulation to examine the relationship between idiosyncrasy of nest behavior and foraging activity. First, we used data from undisturbed colonies to examine the correlation between components of nest behavior and foraging activity. Consistent with previous work, we found strong evidence that foraging activity was body-size dependent ($df = 2771$, $z = 11.66$, $p < 10^{-16}$). After accounting for the effects of body size, however, we found that more central spatial behavior (i.e. higher PC1 scores) and lower activity scores (i.e lower PC2 scores) were both significantly correlated with foraging activity (Fig 4 A-B, PC1, $z = 2.63$, $p = 0.0086$; PC2, $z = 3.91$, $p = 9.13 \times 10^{-5}$).

To examine whether variation in nest behavior predicts task switching in response to disturbance, we then tested the relationships between nest behavior the day before simulated predation and the probability of switching to foraging the day after manipulation, among previously non-foraging bees. Body size did not affect whether workers initiated foraging after disturbance ($df = 158$, $z = 2.12$, $p = 0.068$). However, spatial

occupancy patterns (PC1) significantly predicted task switching in response to disturbance (Fig 4, df = 158, z = 3.04, p = 0.0024). In contrast, activity level (PC2) had no effect on the probability of initiating foraging (Fig 4, df = 158, z = 1.03, p = 0.30).

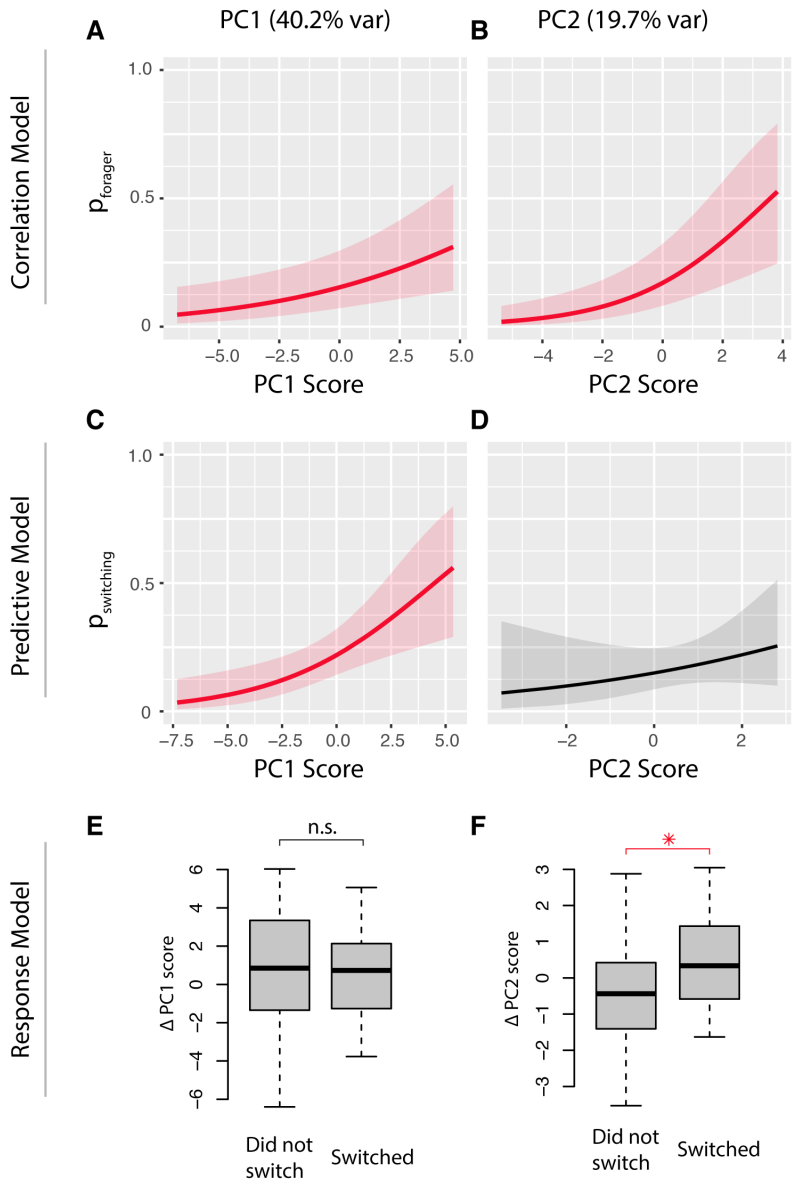

Figure 4. **Spatial fidelity within nests predicts task switching in response to colony disturbance.** (A-B) Correlation models: Probability of foraging relative to PC1 (A) and PC2 (B) scores in undisturbed colonies. (C-D) Predictive models: Probability of initiating foraging activity after simulated predation among previously non-foraging bees, relative to PC1 score (C) and PC2 score (D). (E-F) Response models: Change in PC1 (E) and PC2 (F) scores the day after disturbance among previously non-foraging bees that either initiated foraging after disturbance ("switched") or did not begin foraging ("Did not switch"). In A-D, thick lines show estimated effect, and shaded regions show 95% confidence intervals, with significant effects in red, and non-significant effects shown in grey. Effects plots in (A-D) and significance in (E-F) are based on generalized linear mixed effects models (see Methods for details).

Finally, we tested whether switching to foraging affected components of nest behavior the day after the disturbance occurred, again among bees that were not foraging before disturbance. We found that switching to foraging activity had no effect on spatial components of behavior (Fig 4E, Change in PC1, $z = 1.25$, $p = 0.21$), but did significantly affect activity patterns (Fig 4F, Change in PC2, $z = 2.82$, $p = 0.006$).

DISCUSSION

Understanding the role of individual behavior on collective behavior in social insects is of substantial theoretical importance (Beshers & Fewell, 2001; Bonabeau et al., 1996; Fewell, 2003; Tofts & Franks, 1992), but empirical data on the extent and patterns of individual behavioral variation in social insects, and particularly their distributions across entire colonies, are limited. Here, we demonstrate a technique for providing a comprehensive accounting of behavioral variation within and between entire colonies of social insects, and our results yield key insights relevant for understanding the role of behavioral idiosyncrasy in collective behavior of social insects.

Previous work investigating behavioral variation and specialization within bumblebee colonies has focused largely on alloethism (or behavioral variation associated with body size). Consistent with previous work, we find that body size has significant effects on worker behavior in bumblebees. However, we also find strong evidence that bumblebee workers display pervasive behavioral idiosyncrasy in task performance, spatial fidelity, and activity level, even after accounting for the effects of body size (Figs 1-2). This residual behavioral variation appears to play a key role in determining patterns of task switching in response to disturbance (Fig 4).

Interestingly, bumblebees display significant individual variation in behavior, while lacking strong division of labor or task specialization *per se*; Nearly all workers observed performed several different colony tasks each day (Fig 1), and displayed low specialization of individual workers to tasks ($DOL_{indiv \rightarrow tasks}$, Fig 1H) and total division of labor (DOL_{total}, Fig 1I).

We also found that both the overall level, as well as the distribution, of foraging are regulated at the colony level in bumblebees, and that bees respond to increased foraging demand (via simulated predation, an important natural pressure facing wild colonies) rapidly (within a day, Figs 3-4). In response to simulated predation and forager impairment, colonies increased foraging activity and decreased inequality (i.e. Gini coefficients) relative to predicted effects (and indistinguishable from levels before disturbance), suggesting that bumblebee colonies are capable of actively regulating both the degree and distribution of foraging activity at the colony level. Compensation for lost foraging activity came from previously foraging individuals increasing activity, as well as activation of previously non-foraging workers (Fig 3).

Our results support a key role for idiosyncrasy of spatial occupancy patterns within bumblebee colonies. Previous work investigating spatial sorting and fidelity in ants (Mersch et al., 2013) and honeybee (Baracchi & Cini, 2014) have found strong, discrete associations between space-use and task performance, with workers most predominantly interacting with other workers of a similar age and behavioral caste (i.e. nurses, foragers, cleaners). We see a fundamentally different pattern of spatial sorting in bumblebee colonies; while individual workers show repeatable patterns of spatial fidelity (Jandt & Dornhaus, 2009), they frequently switch tasks within the course of a single day, and patterns of spatial overlap and interaction with other bees are continuously, rather than discretely, distributed (Fig 2A-B). While previous work has documented spatial fidelity of workers (Jandt & Dornhaus, 2009) associated with task performance (Mersch et al., 2013; Sendova-Franks & Franks, 1995), it remains unclear to what extent spatial heterogeneity is a cause, rather than a consequence, of individual variation in task performance (Mersch et al., 2013; Sendova-Franks & Franks, 1994; Tofts, 1993; Tofts & Franks, 1992).

Our results here are consistent with a causal role of spatial idiosyncrasy in patterns of task switching and collective response to disturbance in social insect colonies (Fig 4E-F). In addition to having a significant relationship with foraging activity in undisturbed colonies (Fig 4A), spatial fidelity predicts which worker initiate foraging when colony-level demand for foraging is increased through predation. Specifically, workers that

were not foraging before the artificial disturbance, but had spatial occupancy patterns more closely resembling foragers (i.e. higher PC1 scores) were more likely to initiate foraging the day after disturbance (Fig 4C).

This pattern suggest that spatial occupancy plays a key role in patterning information flow within insect nests (Pinter-Wollman, 2015; Richardson & Gorochowski, 2015). Spatial occupancy patterns in our study were strongly correlates with overall Information Richness (Fig 2E-F). While there are potentially multiple sources of key information within bumblebee nests (i.e. social information (Renner & Nieh, 2008), signals from developing brood (Boer & Duchateau, 2006), and information stored in food pots (Dornhaus, 2005)), we find that these three information sources are strongly associated (Fig S3); Bees with strong access to social information also had high rates of interaction with brood and storage pots (Fig 2). Spatial occupancy also appears robust to changes in foraging activity; bees that initiated foraging in response to disturbance showed no significant shift in PC1 after disturbance, compared to workers that did not switch to foraging (Fig 4E), again consistent with spatial idiosyncrasy as a cause, rather than a consequence, of task performance.

In contrast to spatial fidelity, activity levels (represented here by PC2 scores), may be in part a consequence, rather than a cause, of foraging activity. In undisturbed colonies, bees with higher PC2 scores (i.e. spent more time inactive, moved slower when they were moving, etc.) were more likely to forage (Fig 4B). While PC2 score was not a significant predictor of which bees initiated foraging activity after disturbance (Fig 4D), PC2 scores shifted in response to initiation of foraging. This suggests that unlike spatial fidelity patterns, activity level is driven in part by foraging (as has been shown for the regulation of circadian rhythm in honeybees (Bloch & Robinson, 2001)), potentially reflecting the physiological demands of this behavior (Heinrich, 1975; 2004).

Overall, our results highlight the importance of idiosyncrasy across several dimensions of behavior in bumblebee colonies, and suggest important sources of individual variation (such as space use) beyond response thresholds that play an important, functional role in collective dynamics of social insect colonies. Within the framework of response threshold models, the probability of performing a given task is a product of

both the individual's response threshold, but also the stimulus level for that task *perceived* by the individual worker (rather than the absolute, colony-wide stimulus level per se). While response threshold models typically assume that these stimuli are evenly distributed within colonies (Beshers & Fewell, 2001), local cues and signals relevant for collective behavior are distributed heterogeneously within nests (Dornhaus, 2005; Pinter-Wollman et al., 2011), and our results lend empirical support to the importance of this spatial heterogeneity of information in structuring task allocation within colonies. This highlights the importance of investigating not only intrinsic individual differences in task preferences (for example in the form of variable response thresholds), but also the idiosyncratic perceptual worlds inhabited by distinct individuals and the factors that drive this variation.

While either spatial fidelity or variation in response threshold are potentially sufficient to explain observed patterns of task allocation independently, these mechanisms are not exclusive, and spatial fidelity could either mitigate or exacerbate inter-individual variance from response thresholds. The interaction between these two two factors is an important direction for future study, made increasingly feasible by high-throughput automated tracking techniques.

Most broadly, our results here highlight the ubiquity and importance of individual behavioral heterogeneity within social insect colonies, even in relatively simple insect societies where tasks are flexibly allocated and division of labor is weak (Gordon, 2015). While emphasis in the field of social insect ecology has been placed (understandably) on the importance of task allocation, behavior varies along many dimensions simultaneously. Automated tracking techniques large, multidimensional behavioral datasets they generate provide a rich description of behavior across many individual and contexts, and may help elucidate the organismal traits underlying patterns of task performance and collective behavior in social insects.

Materials and Methods

Animal care and tag attachment

We obtained 19 bumblebee (*Bombus impatiens*) colonies from BioBest between Juy 13th and October 7th, 2015. Before beginning behavioral experiments, all bees (including the queen) were removed from the colony and cold-anaesthetized at 4° C for 1-2 hours following (Crall et al., 2015). During this time, all brood (i.e. developing eggs, larvae, and pupae) and nest structure was removed intact from the original colony shipping container and transferred to a custom-designed nest chamber (see "Tracking Arena" below). Each bee was outfitted with a unique BEEtag printed on water-resistant paper, attached with cyanoacrylate glue to the mesoscutum. After recording the unique identification number and body mass of each bee (to the nearest 0.1 mg), bees were then returned to nest chamber containing their relocated nest structure and moved to one of three identical tracking arenas (Fig 1A).

Tracking arena

After tagging, colonies were transferred to one of three identical tracking arenas (Figure 1a, 0.20 x 0.19 x 0.13 m) located at the (Concord Field Station, Bedford, MA, 01730). The walls and floor of the nest chamber were constructed from black, extruded acrylic (6.3 mm thick). The walls and floor both had 1.6 mm-wide perforations running along their length at 1-inch intervals to allow for air circulation but prevent bees from escaping. The top of the nest box was constructed from clear, laser-cut extruded acrylic (3.1 mm thick) to allow for imaging. A monochrome digital camera (DMK 24UJ003, USB 3.0, Imaging Source, 3856 x 2764 pixels) with a wide-angle lens (Fujinon, 2.8-8 mm) was mounted on aluminum construction rails (25 mm, Thorlabs®) above the clear top of the nest box. The nest was illuminated with two 6-inch square arrays of red LEDs (Knema Lighting®), which provides minimal disturbance to nest behavior since bees have very poor sensitivity to red light (Skorupski & Chittka, 2010). The nest box, camera, and lighting array were covered with black cloth to exclude ambient light.

Each nest chamber was located in a temperature-controlled indoor environment, with direct access to the outdoors via a custom-designed foraging tunnel (Figure 1a), accessed through a 0.5 inch hole in one hole of the nest chamber. The foraging tunnel was split in the middle into two parallel tunnels (Figure 1a), each with a 1-way transit

valve to separate entrances and exits to the hive, as well as allowing the possibility of letting bees only into and not out of, the nest to forage. Before and after this parallel section, the foraging tunnel joined into a single passage. The foraging tunnel was constructed from laser-cut extruded acrylic (3.1 mm thick), opaque-white on the floor and sides of the tunnel, and clear on the top to allow for imaging. A digital camera (Point-Grey Chameleon3) was mounted above the parallel middle sections of the foraging tunnel. This region of the foraging tunnel was monitored using a single red LED array identical to those above the nest chamber on 16:8 hours light:dark cycle.

Colony deployment and experimental treatments

Each colony was deployed in the same location for 14-21 days. Automated tracking of nest and foraging behavior was initiated within 24 hours of colony deployment, typically before noon the next day (see "Image acquisition and processing" below). After tagging, each colony was supplied with a small amount of nectar (BioGluc) and fresh pollen (Koppert). After this initial food supply, no additional food was supplied and colonies were forced to forage in the outdoor environments for both nectar and pollen. All colonies initiated foraging within 24 hours.

After establishment, nest and foraging data were recorded continuously, except on days when experimental manipulations were introduced, which varied across colonies. Nine colonies were subjected to experimental manipulations not reported here, and data after experimental manipulations began are excluded from all analyses.

All remaining colonies were subjected to one of two manipulations intended to simulate the effects of forager-predation on colony behavior. In the first (forager removal), a researcher stationed at the colony entrance captured up to 15 active foragers from the colony (although less in some colonies) with a hand net and permanently removed these bees from the colony, providing a direct simulation of predation on foragers. Alternatively, in some colonies, foragers were captured in the same manner, but instead had their wings clipped at the base, impairing their capacity to forage (forager impairment).

Image acquisition

In all three behavioral arenas, both nest and foraging cameras were acquired directly to a PC Desktop computer using custom Matlab scripts. For nest behavior, video frames were captured at 2 Hz for 5 seconds (10 frames total), saved to an external hard drive, and immediately processed using BEEtag (Video S1). After image processing was complete (typically after 2-5 minutes), the red LED panels were turned on using an Arduino micro controller controlled via Matlab, and - after a 10 second delay - another video sequence was recorded. The red LED panels were turned off during the image processing period, and thus the 10-second delay allowed for short-term habituation to the red lights. Bees, however, showed no noticeable response to turning on the red lights.

Foraging transits were recorded via motion capture by the foraging camera using custom Matlab scripts (Video S2). With both channels of the foraging tunnel in view, images were recorded whenever motion was detected within the camera's field of view and written directly to an external hard drive. At 22:30 each evening, after foraging had ceased for the day, motion capture image collection ceased and that day's foraging images were processed using BEEtag (Crall et al., 2015). Image collection began again after all images had been processed (always before 6 am the following morning).

Post-processing of tracking data

The BEEtag software records the location, orientation, and identity of any BEEtags located within a single frame (Crall et al., 2015) from either the nest or foraging cameras. We ignored any data from tags that were not from the know tag list of bees associated with each colony. To conservatively ensure that any included data weren't from bees that had died within the colony, we ignored all data after the last four instances of observable movement of individual tags.

After this initial pass, 2-dimensional spatial coordinates of each tag were corrected for lens distortion using the Camera Calibration toolbox in Matlab and the subsequently scaled. Missing coordinates "holes" within each nest video sequence were "healed" using linear interpolation.

Spatial mapping of nest elements

We manually mapped nest elements for each day and each colony using a semi-automated custom Matlab script (Video S3). This script first digitally removed moving bees from the nest scene by median averaging, providing a single image of the nest "background" for each day. The user then mapped the centroids for each of 7 elements of bumblebee nests: eggs, larvae, pupae, empty wax pots, filled wax pots, pollen pots, and wax cover. Subsequently, eggs, larvae, and pupae were categorized together as "brood", and wax pots were categorized together with pollen pots and wax covering (the latter two of which were uncommon in our experiments) as "wax pots." In the case of wax cover, eggs, and larvae, when there weren't discrete visual units, multiple points were marked covering the surface of the nest element. On days of experimental manipulations, forager removal, or when the nest was otherwise physical disturbed for any reason, nest elements were not mapped and nest behavior was not analyzed for these days.

Analysis of foraging data

We used tag tracking data from the camera over the foraging tunnel to estimate the foraging activity of individual bees. The split-tunnel design was intended to allow only unidirectional movement for bees through each side, which, in combination with tag orientation provided by BEEtag (Crall et al., 2015), provided two streams of directional information. Manual observation suggested that tag orientation was a more reliable indicator of movement direction than tunnel location, since bees were able to transit backward through the unidirectional valves. We therefore assessed the direction of movement of individual bees using their tag orientation output from the BEEtag tracking software, since tags were always oriented in the same direction with respect to the body (Video S2).

From these data on time, identity, and movement direction of tags from the foraging camera, we estimated foraging activity as the number of unique foraging transits taken by each bee. To reduce the effect of multiple, rapid movement in and out of the

hive, we removed any foraging transits separated by less than 3 minutes from previous transits (although this had no qualitative effect on any patterns reported here, over a range of time thresholds tested)

Analysis of nest behavior data

For every bee identified, we estimated several components of nest behavior for each 5-second video sequence (or "timestep"). For each timestep, we measured movement speed as the median of instantaneous frame-to-frame speed within a single video sequence. Movement speeds below a threshold of $10^{-4.3}$ m/s per second were considered to be stationary, based on the bimodal distribution of instantaneous movement speeds, the lower mode of which was assumed to result from noise in digital tracking (Fig S2). Moving velocity was calculated as the mean of movement speeds across all timesteps when the bee was moving, rather than stationary.

Next, we used the maps of nest components to assess spatial behavioral patterns of individual bees (Fig S3). For each frame where a bee's spatial position within the nest could be identified, we first calculated the instantaneous distance to each mapped nest element. Bees were considered to be located on the nest element closest to their position. If no nest elements were located within 1 cm (or approximately a worker bee's body length (Otterstatter & Thomson, 2007)), bees were not considered to be physically associated with any nest elements. If these spatial associations changed for an individual bee within a video sequence, the most common spatial association was assigned to that bee for that timestep.

We used this spatial association with nest elements, in combination with movement information, to group the behavior of individual workers at each timestep into four categories. Bees that were physically associated with eggs, larvae, or pupae were considered to be engaged in brood care, while bees physically associated with wax pots were considered engaged in food manipulation. Bees that were not associated with any nest elements were either considered inactive (not moving), or patrolling/cleaning (moving). Each of these four behaviors represents a cluster of previously-identified behaviors

bumblebees (Cameron, 1989). “Brood care,” for example, incorporates brood thermoregulation and larval feeding; “Food manipulation” includes inspecting and constructing wax pots; “Patrolling/cleaning” incorporates undertaking and other hygienic activity on the nest periphery, in addition to patrolling (and potentially transiting between nest structures or out of the nest); “Inactivity” incorporates guarding, resting, and inactivity. We tested repeatability of task allocation portions within individuals across experimental days via one-way ANOVAs, after accounting for the effects of body mass, colony, and experimental day with a linear mixed effects model.

To assess quantitative division of labor in experimental colonies, we calculated task repertoire size (i.e. the number of different tasks performed) for each bee daily (Fig 1G). In addition, we calculated individual specialization ($DOL_{individual \rightarrow task}$) and total division of labor (DOL_{total}) using the mutualized entropy method described in (Gorelick, Bertram, Killeen, & Fewell, 2004), and compared these values to reported values from *Temnothorax* ants(Dornhaus et al., 2009), bumblebees (Jandt et al., 2009), and halictine bees (Jeanson et al., 2005).

We characterized the spatial distribution of each bee within the nest in a variety of ways. First, we estimated two metrics of spatial distance from the nest center. We defined the “nest center” for each day, for each colony, as the mean spatial positions of all coordinates from all bees recorded on that day, as in (Jandt & Dornhaus, 2009). For each bee, we then measured (a) the “static” distance to the nest center as the distance between the mean position of each bee’s coordinates (i.e. a single point for each bee) and the nest center for that day, and (b) the “instantaneous” distance as the mean of all instantaneous distances of that bee to the nest center. These metrics were calculated separately for each day for daytime hours (between 6 am and 8 pm) and night time (between 8 pm and 6 am)

Next, we calculated a spatial probability distribution (spd) for each bee for each day by binning all spatial coordinates for each bee on a given day into a 2 cm grid and normalizing. We estimated the similarity between spatial probability distributions both (a) across individuals and (b) within individuals across days by calculating the correlation of occupancy across all spatial bins (from hereon “spatial correlation”).

We also used the spatial probability distributions for each individual bee for each day to calculate pairwise social interaction strength among all colony members for each day. Social interaction strength between two bees was calculated as the spatial correlation between their spatial probability distributions, a metric which incorporates both direct physical interactions, as well as indirect, stigmergic interactions (Richardson & Gorochowski, 2015). We then calculated a mean interaction strength for each worker by averaging the social interactions strengths of each worker to all other workers within the colony that day (Fig 2B). For each bee on each day, we also calculated interaction rates both waxpots and brood by multiplying spatial probability distributions by the number of identified nest elements identified in each spatial bin within the nest. For all spatial distribution metrics, estimates were only made for bees that had a sufficient quantity of spatial data (i.e. at least 100 tracked coordinates) to generate a spatial distribution.

To reduce the dimensionality of nest behavior metrics and examine the correlation structure between components of next behavior, we performed a principal components analysis on daily averages of all estimated metrics of nest behavior (Fig S1). Data were scaled and centered to reduce bias from metrics on different quantitative scales. We tested for significant repeatability of individual principle component scores across days by performing a one-way ANOVA on residual PC1 and PC2 scores (after accounting for effects of mass, colony, and experimental day with a Linear Mixed Effects model). From this and all other analyses of nest behavior, we removed data from bees on days that had less than 40 total timesteps (20 at night and 20 during the day) to assess nest behavior. This quality filter is unlikely to introduce bias into any analyses, since there was a weak relationship between number of observations and component of nest behavior (Fig S4).

To highlight the relationship of each principal component to patterns of information flow within nests, we calculated an overall Information Richness metric for each bee on each observational day, as the mean of social interaction strength, brood interaction rate, and waxpot interaction rate. We then calculated correlation strengths between residual principle component scores and residual Information Richness, based on

Linear Mixed Effects Models including colony as a random effect and mass as a fixed effect.

We quantified the inequality in foraging activity among workers within colonies by calculating the Gini coefficient in foraging transits across all individuals tracked within the nest on three equivalent days across all colonies, after allowing for a two day acclimation period. Gini coefficients were calculated in R as the relative area above the Lorenz curve, which plots the cumulative portion of foraging activity against an individual bee's foraging activity rank (Fig 3). Any colonies with insufficient foraging data on these days (less than 50 foraging transits) were excluded from this analysis. To estimate whether observed values were higher than random expectation, we generated simulated Gini coefficients based on two scenarios for each colony. In the first scenario, total foraging activity was randomly distributed across all individuals equally (1-group sim, Fig 3C), and in the second, foraging activity was randomly distributed among bees that were actively foraging during this time period (2-group sim, Fig 3C). We generated 100 simulations under each colony for each scenario, then calculated the average Gini coefficient under each simulation condition for each colony.

To examine colony responses to simulated predation, we either impaired (via wing clipping, simulating non-lethal damage from a predator)) or removed (simulating lethal predation) foragers randomly from colonies by monitoring outside the nest entrances and collecting up to the first 15 foragers entering or exiting the nest. While this technique does not explicitly select bees based on foraging activity, it tends to select for more active foragers by nature of their over-representing in foraging activity (Tenczar et al., 2014). We quantified colony-level foraging metrics (foraging bouts per bee, portion of bees foraging, and Gini coefficient) for the three days before and after simulated predation (Fig 3), as well as predicted foraging metrics based on which bees were removed or impaired, and assuming no change in foraging behavior of other bees within the colony. Due to low statistical power from treating whole colonies as experimental replicates, and since we were able to detect no significant difference in effect between the two treatments for any foraging metrics, these two treatments were combined.

To investigate the relationship between nest behavior and foraging activity, we built a series of generalized linear mixed effects model using the “lmer” function in the lme4 package (Bates, Mächler, Ben Bolker, & Walker, 2015) in R (Team, 2013). First, we tested the effect of nest behavior on probability of foraging in undisturbed colonies (i.e. all colonies before any experimental manipulations, “Correlation Model”, Fig 4), with PC1, PC2, and body mass as fixed effects, and colony and individual as random effects. Next, we tested the effect of nest behavior the day before simulated foraging on the probability of switching to foraging the day after disturbance, among bees that were previously not foraging (“Predictive Model”, Fig 4), again with PC1, PC2, and body mass as fixed effects, and colony as a random effect. Finally, to test the effects of switching to foraging on nest behavior, we tested the effects of switching to foraging after simulated predation on changes in nest behavior metrics with separate linear mixed effects models, with foraging activity (binary) as a fixed effect and colony as a random effect (Fig 4). Significance of fixed effects for all models were calculated using the “lmerTest”(Kuznetsova, Brockhoff, & Christensen, 2014) package in R.

References

Baracchi, D., & Cini, A. (2014). A Socio-Spatial Combined Approach Confirms a Highly Compartmentalised Structure in Honeybees. *Ethology*, *120*(12), 1167–1176. http://doi.org/10.1111/eth.12290

Bates, D., Mächler, M., Ben Bolker, & Walker, S. (2015). Fitting Linear Mixed-Effects Models Using lme4. *Journal of Statistical Software*, *67*(1). http://doi.org/10.18637/jss.v067.i01

Bengston, S. E. (2014). The development of collective personality: the ontogenetic drivers of behavioral variation across groups, 1–13. http://doi.org/10.3389/fevo.2014.00081/abstract

Berdahl, A., Torney, C. J., Ioannou, C. C., Faria, J. J., & Couzin, I. D. (2013). Emergent sensing of complex environments by mobile animal groups. *Science*, *339*(6119), 574–576. http://doi.org/10.1126/science.1225883

Beshers, S. N., & Fewell, J. H. (2001). Models of division of labor in social insects. *Annual Review of Entomology*, *46*(1), 413–440. http://doi.org/10.1146/annurev.ento.46.1.413

Bloch, G., & Robinson, G. E. (2001). Chronobiology. Reversal of honeybee behavioural rhythms. *Nature*, *410*(6832), 1048–1048. http://doi.org/10.1038/35074183

Boer, S. P. A. D., & Duchateau, M. J. H. M. (2006). A larval hunger signal in the bumblebee Bombus terrestris. *Insectes Sociaux*, *53*(3), 369–373. http://doi.org/10.1007/s00040-006-0883-8

Bonabeau, E., Theraulaz, G., & Deneubourg, J.-L. (1996). Quantitative Study of the Fixed Threshold Model for the Regulation of Division of Labour in Insect Societies. *Proceedings of the Royal Society B: Biological Sciences*, *263*(1376), 1565–1569. http://doi.org/10.1098/rspb.1996.0229

Buchanan, S. M., Kain, J. S., & de Bivort, B. L. (2015). Neuronal control of locomotor handedness in Drosophila. *Proceedings of the National Academy of Sciences of the United States of America*, *112*(21), 6700–6705. http://doi.org/10.1073/pnas.1500804112

Cameron, S. A. (1989). Temporal Patterns of Division of Labor among Workers in the Primitively Eusocial Bumble Bee, Bombus griseocollis (Hymenoptera: Apidae)1). *Ethology*, *80*(1-4), 137–151. http://doi.org/10.1111/j.1439-0310.1989.tb00735.x

Crall, J. D., Gravish, N., Mountcastle, A. M., & Combes, S. A. (2015). BEEtag: A Low-Cost, Image-Based Tracking System for the Study of Animal Behavior and Locomotion. *PLoS ONE*, *10*(9), e0136487–13. http://doi.org/10.1371/journal.pone.0136487

Dornhaus, A. (2005). Bumble bees (Bombus terrestris) store both food and information in honeypots. *Behavioral Ecology*, *16*(3), 661–666. http://doi.org/10.1093/beheco/ari040

Dornhaus, A., Holley, J. A., & Franks, N. R. (2009). Larger colonies do not have more specialized workers in the ant Temnothorax albipennis. *Behavioral Ecology*, *20*(5), 922–929. http://doi.org/10.1093/beheco/arp070

Fewell, J. H. (2003). Social insect networks. *Science*, *301*(5641), 1867–1870. http://doi.org/10.1126/science.1088945

Gordon, D. M. (1989). Dynamics of task switching in harvester ants. *Animal Behaviour*,

38(2), 194–204. http://doi.org/10.1016/s0003-3472(89)80082-x
Gordon, D. M. (2015). From division of labor to the collective behavior of social insects. *Behavioral Ecology and Sociobiology*, 1–8. http://doi.org/10.1007/s00265-015-2045-3
Gorelick, R., Bertram, S. M., Killeen, P. R., & Fewell, J. H. (2004). Normalized Mutual Entropy in Biology: Quantifying Division of Labor. *The American Naturalist*, *164*(5), 677–682. http://doi.org/10.1086/424968
Heinrich, B. (1975). Energetics of pollination. *Annual Review of Ecology and Systematics*, *6*(1), 139–170. http://doi.org/10.1146/annurev.es.06.110175.001035
Heinrich, B. (2004). Bumblebee Economics. Harvard University Press.
Henry, M., Beguin, M., Requier, F., Rollin, O., Odoux, J. F., Aupinel, P., et al. (2012). A Common Pesticide Decreases Foraging Success and Survival in Honey Bees. *Science*, *336*(6079), 348–350. http://doi.org/10.1126/science.1215039
Hölldobler, B., & Wilson, E. O. (2009). The Superorganism. W. W. Norton & Company.
Jandt, J. M., & Dornhaus, A. (2009). Spatial organization and division of labour in the bumblebee Bombus impatiens. *Animal Behaviour*, *77*(3), 641–651. http://doi.org/10.1016/j.anbehav.2008.11.019
Jandt, J. M., Bengston, S., Pinter-Wollman, N., Pruitt, J. N., Raine, N. E., Dornhaus, A., & Sih, A. (2013). Behavioural syndromes and social insects: personality at multiple levels. *Biological Reviews*, *89*(1), 48–67. http://doi.org/10.1111/brv.12042
Jandt, J. M., Huang, E., & Dornhaus, A. (2009). Weak specialization of workers inside a bumble bee (Bombus impatiens) nest. *Behavioral Ecology and Sociobiology*, *63*(12), 1829–1836. http://doi.org/10.1007/s00265-009-0810-x
Jeanson, R., & Weidenmüller, A. (2014). Interindividual variability in social insects–proximate causes and ultimate consequences. *Biological Reviews*, *89*(3), 671–687. http://doi.org/10.1111/brv.12074
Jeanson, R., Kukuk, P. F., & Fewell, J. H. (2005). Emergence of division of labour in halictine bees: contributions of social interactions and behavioural variance. *Animal Behaviour*, *70*(5), 1183–1193. http://doi.org/10.1016/j.anbehav.2005.03.004
Kurvers, R. H. J. M., Eijkelenkamp, B., van Oers, K., van Lith, B., van Wieren, S. E., Ydenberg, R. C., & Prins, H. H. T. (2009). Personality differences explain leadership in barnacle geese. *Animal Behaviour*, *78*(2), 447–453. http://doi.org/10.1016/j.anbehav.2009.06.002
Kuznetsova, A., Brockhoff, P. B., & Christensen, H. B. (2014). lmerTest: tests for random and fixed effects for linear mixed effect models (lmer objects of lme4 package), v. 2.0–25. … /cran. r-project. org/package= lmerTest.
LeBoeuf, A. C., & Grozinger, C. M. (2014). Me and we: the interplay between individual and group behavioral variation in social collectives. *Current Opinion in Insect Science*, *5*, 16–24. http://doi.org/10.1016/j.cois.2014.09.010
Mersch, D. P., Crespi, A., & Keller, L. (2013). Tracking individuals shows spatial fidelity is a key regulator of ant social organization. *Science*, *340*(6136), 1090–1093. http://doi.org/10.1126/science.1234316
Oster, G. F., & Wilson, E. O. (1978). Caste and Ecology in the Social Insects.
Otterstatter, M. C., & Thomson, J. D. (2007). Contact networks and transmission of an

intestinal pathogen in bumble bee (Bombus impatiens) colonies. *Oecologia*, *154*(2), 411–421. http://doi.org/10.1007/s00442-007-0834-8
Pinter-Wollman, N. (2015). Persistent variation in spatial behavior affects the structure and function of interaction networks. *Current Zoology*, *61*(1), 98–106. http://doi.org/10.1093/czoolo/61.1.98
Pinter-Wollman, N., Wollman, R., Guetz, A., Holmes, S., & Gordon, D. M. (2011). The effect of individual variation on the structure and function of interaction networks in harvester ants. *Journal of the Royal Society Interface*, *8*(64), 1562–1573. http://doi.org/10.1098/rsif.2011.0059
Quevillon, L. E., Hanks, E. M., Bansal, S., & Hughes, D. P. (2015). Social, spatial, and temporal organization in a complex insect society. *Scientific Reports*, *5*, 1–11. http://doi.org/10.1038/srep13393
Renner, M. A., & Nieh, J. C. (2008). Bumble bee olfactory information flow and contact-based foraging activation. *Insectes Sociaux*, *55*(4), 417–424. http://doi.org/10.1007/s00040-008-1021-6
Richardson, T. O., & Gorochowski, T. E. (2015). Beyond contact-based transmission networks: the role of spatial coincidence. *Journal of the Royal Society Interface*, *12*(111), 20150705–11. http://doi.org/10.1098/rsif.2015.0705
Richardson, T. O., Christensen, K., Franks, N. R., Jensen, H. J., & Sendova-Franks, A. B. (2011). Ants in a Labyrinth: A Statistical Mechanics Approach to the Division of Labour. *PLoS ONE*, *6*(4), e18416–12. http://doi.org/10.1371/journal.pone.0018416
Robinson, G. E., & Page, R. E. (1988). Genetic determination of guarding and undertaking in honey-bee colonies. *Nature*, *333*(6171), 356–358. http://doi.org/10.1038/333356a0
Robinson, G. E., & Page, R. E. (1989). Genetic basis for division of labor in an insect society. The genetics of social evolution. Westview.
Sendova-Franks, A. B., & Franks, N. R. (1994). Social resilience in individual worker ants and its role in division of labour. *Proceedings of the Royal Society B: Biological Sciences*, *256*(1347), 305–309. http://doi.org/10.1098/rspb.1994.0085
Sendova-Franks, A. B., & Franks, N. R. (1995). Spatial relationships within nests of the antLeptothorax unifasciatus (Latr.) and their implications for the division of labour. *Animal Behaviour*, *50*(1), 121–136. http://doi.org/10.1006/anbe.1995.0226
Sih, A., Bell, A., & Johnson, J. C. (2004). Behavioral syndromes: an ecological and evolutionary overview. *Trends in Ecology & Evolution*, *19*(7), 372–378. http://doi.org/10.1016/j.tree.2004.04.009
Skorupski, P., & Chittka, L. (2010). Photoreceptor Spectral Sensitivity in the Bumblebee, Bombus impatiens (Hymenoptera: Apidae). *PLoS ONE*, *5*(8), e12049–5. http://doi.org/10.1371/journal.pone.0012049
Team, R. C. (2013). R: A language and environment for statistical computing.
Tenczar, P., Lutz, C. C., Rao, V. D., Goldenfeld, N., & Robinson, G. E. (2014). Automated monitoring reveals extreme interindividual variation and plasticity in honey-bee foraging activity levels. *Animal Behaviour*, *95*, 41–48. http://doi.org/10.1016/j.anbehav.2014.06.006
Tofts, C. (1993). Algorithms for task allocation in ants. (A study of temporal polyethism:

Theory). *Bulletin of Mathematical Biology*, *55*(5), 891–918. http://doi.org/10.1007/BF02460691
Tofts, C., & Franks, N. R. (1992). Doing the right thing: Ants, honeybees and naked mole-rats. *Trends in Ecology & Evolution*, *7*(10), 346–349. http://doi.org/10.1016/0169-5347(92)90128-X
Weidenmüller, A. (2004). The control of nest climate in bumblebee (Bombus terrestris) colonies: interindividual variability and self reinforcement in fanning response. *Behavioral Ecology*, *15*(1), 120–128. http://doi.org/10.1093/beheco/arg101
Wilson, E. O. (1968). The Ergonomics of Caste in the Social Insects. *The American Naturalist*, *102*(923), 41–66. http://doi.org/10.1086/282522
Wilson, E. O. (1971). The Insect Societies. Belknap Press.
Wolf, M., & Weissing, F. J. (2012). Animal personalities: consequences for ecology and evolution. *Trends in Ecology & Evolution*, *27*(8), 452–461. http://doi.org/10.1016/j.tree.2012.05.001

Supplementary Figures

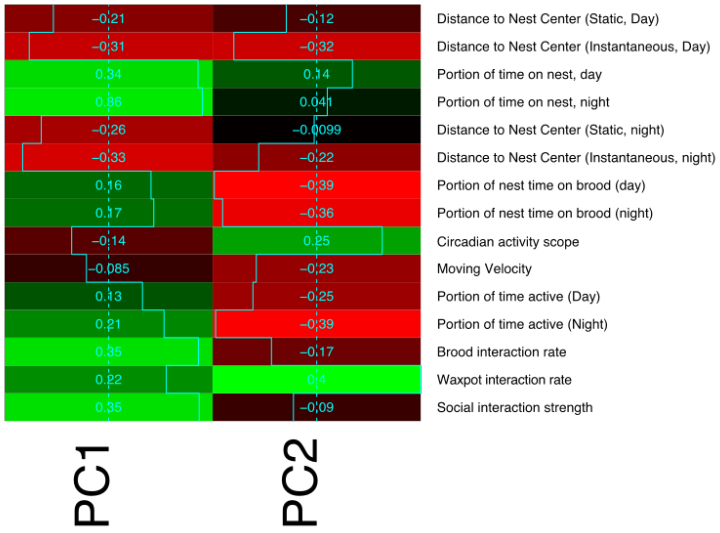

Figure S1. Loadings of nest behavior metrics on Principle Component 1 (left column) and Principle Component 2 (right column).

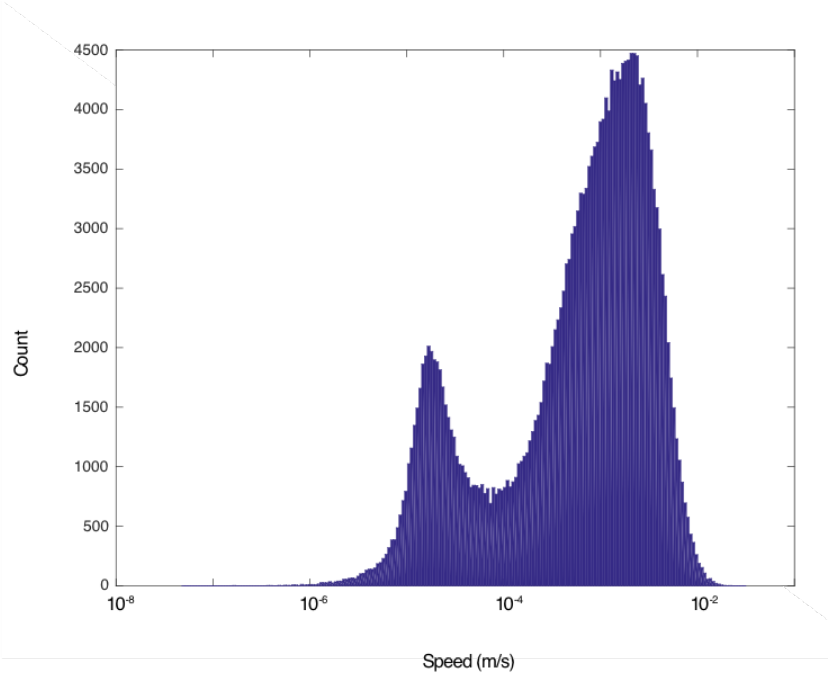

Figure S2. Bimodal distribution of instantaneous movement speeds with bumblebee nests, shown for a single representative colony.

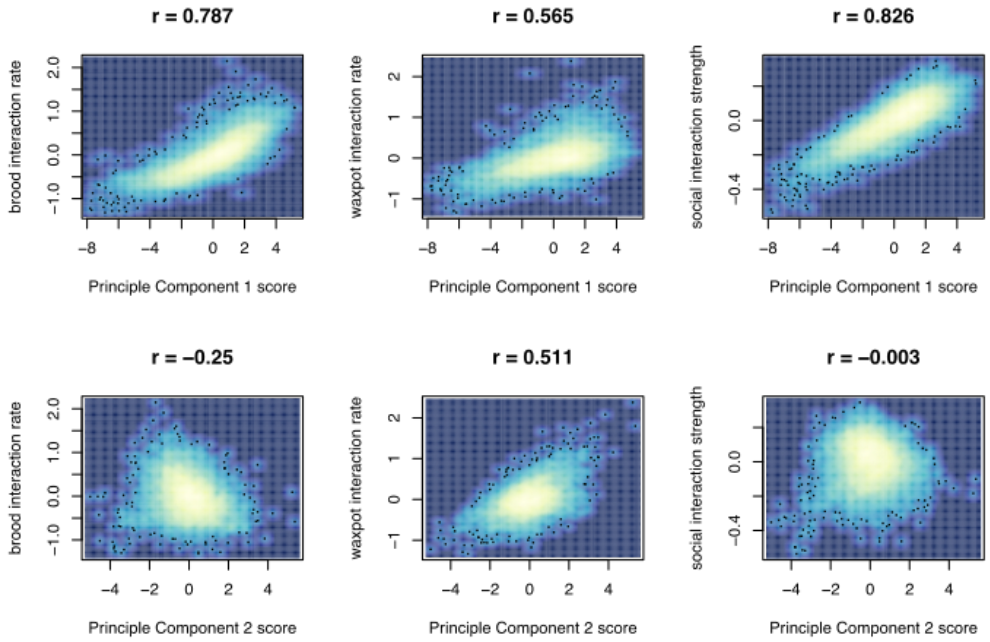

Figure S3. Pairwise correlations between PC1 scores (top row) and PC2 scores (bottom row), with brood interaction rate (left column), waxpot interaction rate (middle column), and social interaction strenght (right column).

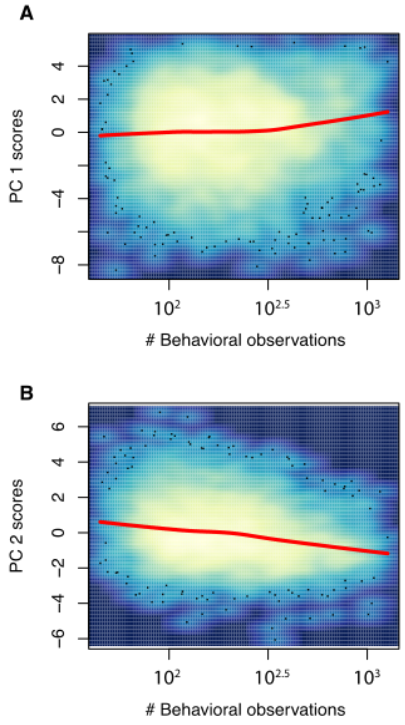

Figure S4. Relationship between the number of behaviorl observations and (A) PC1 and (B) PC2 scores. Red lines show Lowess smoothing of local trend lines.

Supplementary Videos

Video S1. Tracking of individual bumblebees within the nest. Dark green shows raw, and light green interpolated, locations of indiviudal bees.

Video S2. Tracking of individual foraging activity. Outwardly oriented bees are shown in green, and inwardly oriented bees in red.

Video S3. Spatial mapping of worker locations and brood elements in bumblebee colonies. Large transparent circle show mapped nest elements (yellow and red showing larvae and pupae, respectively, and green, purple, and blue showing empty waxpots, full waxpots, and wax coverings, respectively).

Chapter 6: A common neonicotinoid pesticide disrupts nest behavior and social network architecture in bee colonies

Title: A neonicotinoid pesticide disrupts nest behavior and social interactions in bee colonies

Authors: *James D. Crall[1], *Callin M. Switzer[1], Robert L. Oppenheimer[1], Stacey A. Combes[2]

[1] Department of Organismic and Evolutionary Biology, Harvard University, 26 Oxford St., Cambridge, Massachusetts, 02138, USA.
[2] Department of Neurobiology, Physiology, and Behavior, University of California, Davis, One Shields Avenue, Davis, California, 95616, USA.

Corresponding author: James D. Crall, 26 Oxford St., Cambridge, Massachusetts, 02138, USA, ph: 216-536-9279, email: james.crall@gmail.com

Keywords: imidacloprid, native bees, pollinators, social insects, automated tracking, bumblebees, ecotoxicology

Impact statement

In addition to affecting foragers, exposure to field-realistic, sub-lethal levels of a neonicotinoid pesticide (imidacloprid) impairs key aspects of social behavior and nest care in bumblebee colonies.

Abstract: Bees provide vital pollination services in both wild and agricultural ecosystems. Despite mounting evidence that neonicotinoid pesticides impair growth of bee colonies at sub-lethal levels of exposure, the mechanisms driving these effects remain unclear. While the receptors targeted by neonicotinoids are widespread within the insect central nervous system, potentially impacting a variety of key behaviors, previous work has focused largely on neonicotinoids' effects on individual bees foraging outside the nest (i.e. on learning and navigation). Here, we investigate the impacts of a common neonicotinoid pesticide (imidacloprid) on social behavior within the nests of bumblebee colonies (*Bombus impatiens*). Using an automated behavioral tracking system, we show that exposure to a single, field-realistic daily intake of imidacloprid has drastic effects on nest behavior in bumblebees: treated bees showed reduced rates of brood care and activity after treatment. Imidacloprid-treated bees also shifted occupancy patterns within the nest and had fewer social interactions with nestmates, altering the structure of the social network within colonies. Our results demonstrate that neonicotinoids impact a range of vital behaviors in bees and suggest a new avenue by which these pesticides may affect social behavior in bees, impair colony growth, and impact the health of bee populations.

Introduction

Animals pollinate the majority of angiosperm species, and insects (mostly bees) pollinate roughly one third of food consumed by humans (*1*). Because of their economic and ecological value (*1*-*3*), recent declines in honeybee populations (*4*, *5*) and wild bee abundance (*6*, *7*) have led to a surge in research efforts investigating the effects of pesticide exposure on the health of bee communities (*8*, *9*). There is now strong evidence that exposure to neonicotinoid pesticides, even at sub-lethal levels, nonetheless has negative impacts on bees (*10*, *11*), including reduced colony growth (*12*, *13*) and pollination services (*14*). While concerns over the environmental impacts of neonicotinoid pesticide application have led to the temporary ban of three neonicotinoid pesticides (imidacloprid, clothianidin, and thiamethoxam) in the European Union (*15*), and parts of Canada, these pesticides are still in wide use globally.

Despite mounting evidence for the negative impacts of neonicotinoids on bee populations, however, the mechanisms underlying these impacts are not well understood. Neonicotinoids target nicotinic acetylcholine receptors (nAChRs), which are widespread in the insect central nervous system, including in brain regions associated with sensory integration and learning such as the mushroom bodies (*16*). Previous work investigating the sub-lethal behavioral effects of neonicotinoids has focused almost exclusively on how neonicotinoid exposure affects foraging performance in bees. There is now strong evidence that sub-lethal exposure to neonicotinoids impairs key aspects of foraging behavior (i.e. navigation (*17*, *18*) and floral learning (*19*, *20*)), leading to reduced pollen foraging efficiency (*21*, *22*). Reduced growth rates in colonies of pesticide-exposed bees have thus been attributed to impacts on foraging behavior and associated reductions in pollen intake (*12*, *22*).

Foraging activity, however, represents only a fraction of the tasks necessary for colony growth and health in social insects, and the impacts of neonicotinoids on other key colony behaviors remain largely unexplored. For example, nest care (e.g. incubation, nest maintenance, and larval feeding) are also vital for the healthy development of bee colonies (*23*, *24*) and their impairment could partially explain observed patterns of decreased colony growth and queen production in bumblebees (*12*, *13*, *25*) in response to pesticide exposure. Nest workers are likely to be exposed to pesticides, as they feed on nectar and pollen collected by foragers that also contains neonicotinoids (*13*).

Despite their importance for colony health, however, the impacts of neonicotinoid exposure on nest care and social behavior in bee colonies remain almost entirely unexplored. Here, we use an automated behavioral tracking system (BEEtag (*26*)), to investigate the simultaneous impacts of neonicotinoid exposure on nest behavior and foraging activity of uniquely-identified workers in bumblebee colonies (*Bombus impatiens*), an important pollinator in both wild and cultivated plants.

Results

We tracked the nest behavior (Figures 1, S1,and S2, Video S1) and foraging activity (Figure S1, Video S2) of individual worker bees (n = 255, Figure 1) from four different colonies before and after exposure to either 0.1 ng (n = 84) or 1.0 ng (n = 85) of imidacloprid (a common neonicotinoid pesticide), or a control sucrose solution (n = 86). Imidacloprid doses were chosen to reflect the total consumption expected for a single bee at field-relevant concentrations in either a single feeding bout (0.1 ng) or a single day (1.0 ng). See Materials and Methods for discussion of the rationale behind dosage levels, as well as the method of exposure.

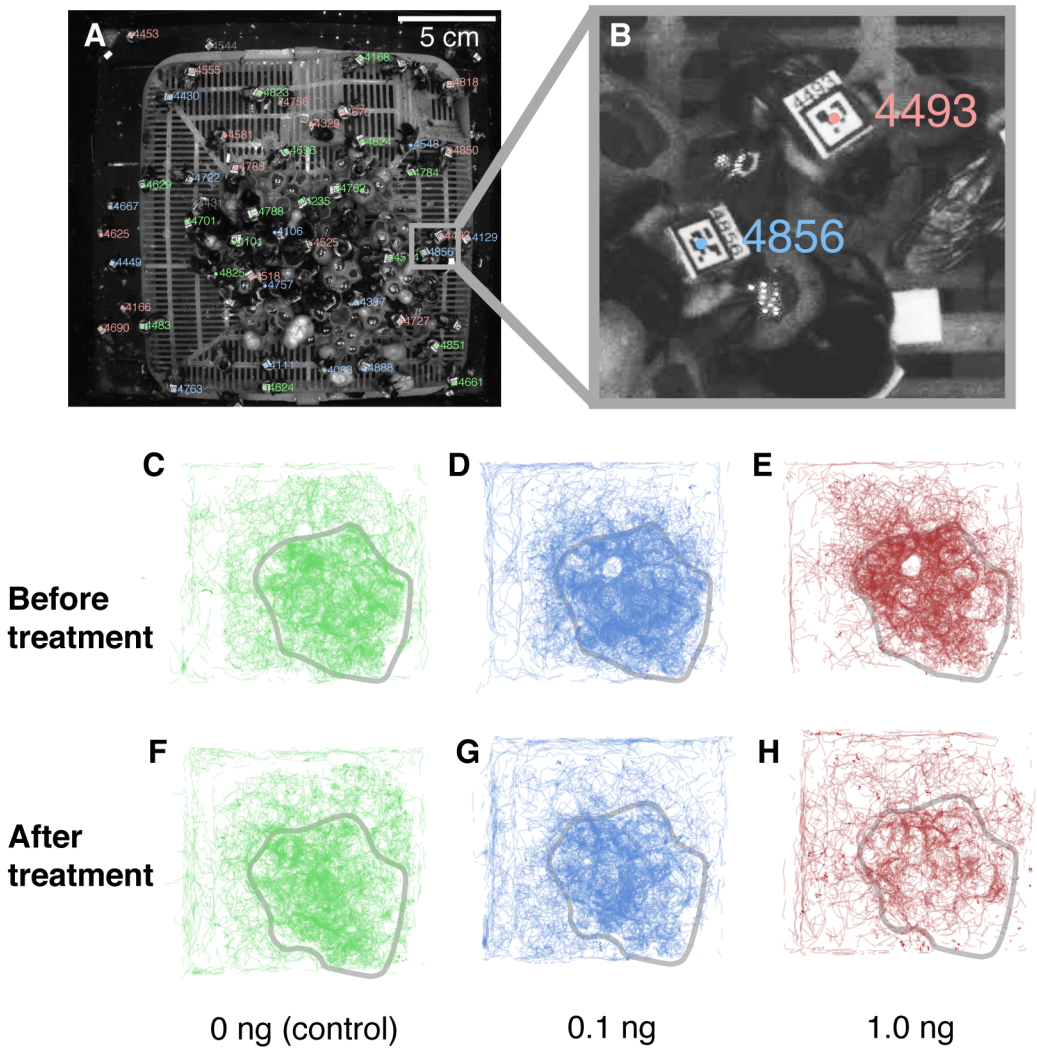

Figure 1. Automated behavioral tracking of individual bees within the nest. (A) Full view and (B) cropped inset showing individually identified bees within a bumblebee nest. In (A), color reflects treatment group, with bees in the control group in green, bees fed 0.1 ng imidacloprid in blue, and 1.0 ng in red. Gray indicates bees not removed from the nest for treatment. (C-E) Tracked positions of control (C: 0 ng) and imidacloprid-fed (D: 0.1 ng and E: 1.0 ng) bees during an hour of observation 24 hours before treatment. (F-H) Tracked positions of the same control (F) and imidacloprid-fed bees (G-H) 24 hours after treatment. In (C-H), convex hulls of nest structure (i.e. wax pots and developing brood) are outlined in gray.

We found strong evidence that imidacloprid affects nest behavior in bumblebees (Type II MANOVA, approx. $F_{(12, 490)} = 9.07$, $p << 0.0001$, $n_{nest, total} = 255$, $n_{nest,control} = 86$, $n_{nest,0.1\ ng} = 84$, $n_{nest,1.0\ ng} = 85$, Table 1, Supplementary File 1). Bees fed 1.0 ng of imidacloprid were less active; they spent less time moving (Figure 2A, Table 1, Supplementary File 1), and moved slower when they were moving (Figure 2B, Table 1, Supplementary File 1). Nearly all bees (94.6%) fed 1.0 ng of imidacloprid showed at at least partial activity after exposure (i.e. were active for more than 5% of the post-treatment observation period), and so reduced activity was not the result of complete immobility, which can occur in bees at relatively high levels of imidacloprid-exposure (*27*).

Workers fed 1.0 ng of imidacloprid spent significantly less time engaged in direct nest care compared to controls (Figure 2E, Table 1, Supplementary File 1). Bees fed 1.0 ng of imidacloprid also shifted spatial occupancy toward the nest periphery; they were further from the social center of the colony (Figure 2C, Table 1, Supplementary File 1) and from the queen (Figure 2D, Table 1, Supplementary File 1) compared to controls. Bees fed a low dose (0.1 ng) of imidacloprid did not differ significantly from controls in any aspects of nest behavior measured (Figure 2, $p > 0.05$ in all cases, Supplementary File 1).

Table 1. Results from the multivariate multiple regression for the 1.0 ng imidacloprid treatment group, relative to control group, while accounting for differences in colonies. N = 255.

Variable	Estimate	Std. Error	t	p
Δ Portion of time active	-0.27	0.039	-9.80	$< 2 \times 10^{-16}$
Δ Nest care rate	-0.27	.052	-5.05	8.6×10^{-7}
Δ Active velocity (m s-1)	-0.0011	2.7×10^{-4}	-4.06	6.6×10^{-5}
Δ Distance from nest center (m)	0.013	0.0031	4.08	6.0×10^{-5}
Δ Distance from queen (m)	0.014	0.0038	3.69	3.0×10^{-4}
Δ Degree centrality	-10.62	2.17	-4.91	1.7×10^{-7}

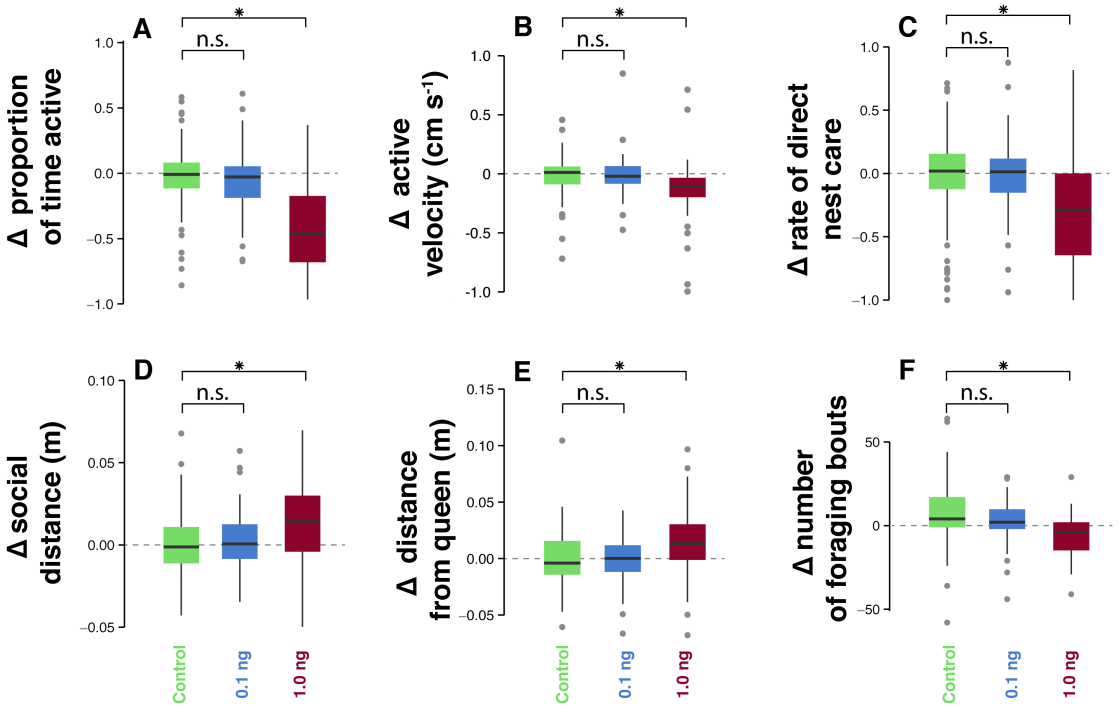

Figure 2. The effects of imidacloprid on nest behaviors. (A - E) Changes in five metrics of social behavior within the nest (n = 255) for individual workers before and after treatment with sucrose solution (control, green), 0.1 ng (blue), or 1.0 ng (red) of imidacloprid. (F) Change in the number of foraging bouts performed by each individual before and after treatment (n = 123), excluding bees that never foraged. Asterisks represent significant differences ($p < 0.001$) while accounting for differences in colonies. Boxes show the median and interquartile range (IQR), and whiskers show the highest and lowest values within 1.5*IQR. Filled dots represent outliers beyond 1.5*IQR.

Pesticide exposure also significantly altered patterns of social interaction, which play an important role in regulating the collective behavior of social insect colonies (*28*). We used physical proximity (i.e. whether bees were within 1 cm of each other) as a proxy for social interactions, since physical interactions bet ween bees play an important role in regulating foraging behavior in both honeybees (*29*) and bumblebees (*30*), as well as driving patterns of disease transmission (*31*). Bees fed 1.0 ng of imidacloprid showed a significant decrease in the number of interactions with nestmates compared to controls (i.e. lower degree centrality, Figure 3, Table 1, Supplementary File 1), whereas bees fed 0.1 ng of imidacloprid showed no difference in social interactions relative to controls (Supplementary File 1).

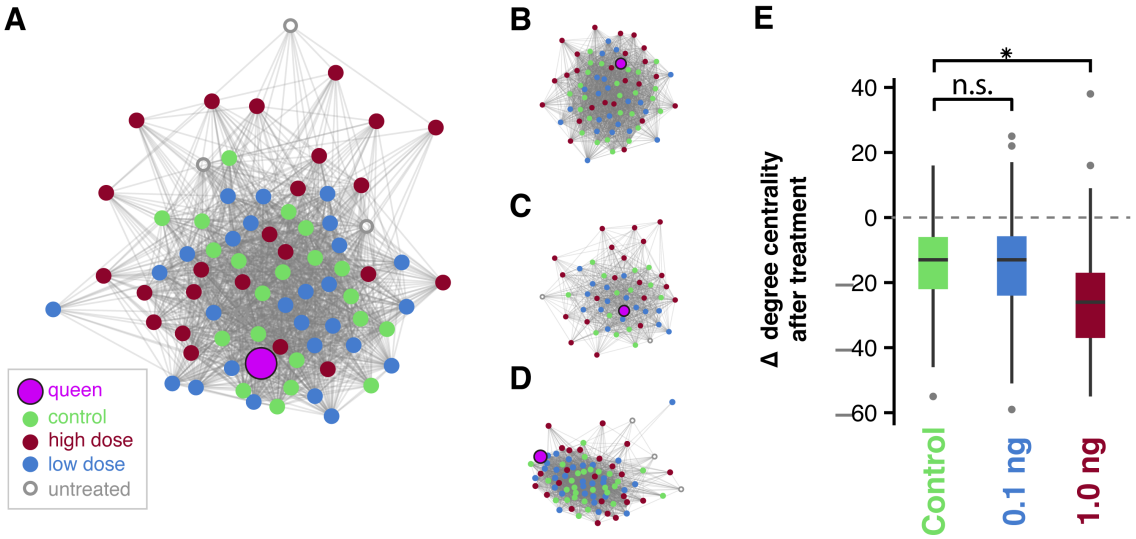

Figure 3. Effects of imidacloprid on social networks in bumblebees. (A-D) Fruchterman-Reingold plots of undirected network graphs based on proximity interactions of individual bumblebees in Colonies A (n = 77), B (n = 73), C (n = 53), and D (n = 87) after treatment, respectively. Circles represent individual bees, which are connected with a thin gray line if they physically interacted during one hour of observation. Filled circles show bees fed sucrose solution (control, green), 0.1 ng (blue) or 1.0 ng (red) of imidacloprid. Grey circles show workers that were not removed from the nest for treatment. Large, pink circles indicate queens. (E) Change in degree centrality (i.e. number of unique bees interacted with during 1-h of observation) of individual bees fed sucrose solution (control, green), 0.1 ng (blue) or 1.0 ng (red) of imidacloprid, after treatment. The asterisk represents a significant difference ($p < 0.001$) while accounting for differences in colonies (n = 255). Boxes show the median and interquartile range (IQR), and whiskers show the highest and lowest values within 1.5*IQR. Filled dots represent outliers beyond 1.5*IQR.

Foraging activity was also impacted by exposure to imidacloprid, with bees in the 1.0-ng group displaying a greater decrease in foraging after treatment than the control group (e.g., less foraging after treatment *vs*. before, Figure 2F, $t_{(117)} = 3.57$, two-sided $p = 0.0005$, $n_{forager,total} = 123$, $n_{forager,control} = 45$, $n_{forager,0.1\ ng} = 44$, $n_{forager,1.0\ ng} = 34$, Supplementary File 1). There was no significant difference between treatment groups in the probability of bees that had foraged before treatment continuing to forage after treatment ($\chi^2_{(2)} = 2.26$, $p = 0.32$, n = 100, Supplementary File 1). However, bees that did not forage before treatment and were fed 1.0 ng of imidacloprid were significantly less likely to begin foraging after treatment, as compared to bees in the control group (Overall model: $\chi^2_{(2)} = 12.32$, $p = 0.0021$, $n_{possible\ foragers,\ total} = 225$, $n_{possible\ forager,control} = 78$,

$n_{possible\ forager,0.1\ ng}$ = 74, $n_{possible\ forager,1.0\ ng}$ = 73; 1.0 ng group: z = 2.44, p = 0.015, Supplementary File 1).

Discussion

Previous work has suggested that reduced worker and queen production in neonicotinoid-exposed bee colonies (*12*, *13*) result from impaired foraging and decreased pollen intake (*25*, *32*). Our results provide clear evidence for an additional (non-exclusive) behavioral mechanism by which neonicotinoid pesticides negatively impact bee colony growth: exposure to neonicotinoids disrupts nest care and social behavior (Figs. 1-3; Table 1; Supplementary File 1) within bee colonies, leading to impaired larval development and decreased rates of colony growth. More broadly, our results suggest that neonicotinoids negatively affect pollinators through a variety of behavioral mechanisms in parallel, rather than impacting a narrow set of neural pathways associated with navigation or learning, consistent with the ubiquity of nAChRs in the central nervous systems of insects (*16*, *33*).

The effects of imidacloprid on social network architecture observed here also suggest that pesticide exposure could disrupt collective decision making by altering patterns of social interactions and network architecture within social insect colonies (*28*, *34*). We found that bees exposed to imidacloprid had reduced rates of social interaction with nestmates (Figure 3), and were less likely to switch to new foraging work, consistent with previous work demonstrating the importance of social interactions for regulation of foraging in bumblebee colonies (*30*). Our results show that pesticide-exposure may affect social network architecture even if only a portion of bees within the colony are exposed to neonicotinoids, reflected in decreased rates of social interaction after treatment, even in bees fed a control sucrose solution (Figure 3E). Interestingly, although neonicotinoids may impair immunity in bees (*35*), the decreased rates of social interaction after exposure to imidacloprid could mitigate rates of disease transmission among nestmates (*31*), suggesting a complex relationship between pesticide exposure and disease load in bee colonies.

Overall, our results highlight gaps in our understanding of the mechanisms by which neonicotinoid exposure affects bee behavior, colony growth, and abundance. It is unclear whether the behavioral effects demonstrated here extend to other neonicotinoid pesticides, or other bee species (since responses to neonicotinoids can

often be highly species-specific (*13*)). In addition, the relative importance of impacts on nest behavior and foraging remains unclear, and may depend on key factors such as resource abundance or other environmental stressors including disease load or climatic variation. Finally, whether the simultaneous impacts of neonicotinoid exposure on foraging and nest behavior are additive or interactive is not clear, and could be crucial for understanding the complex behavioral feedbacks that occur at the colony level in response to worker impairment (*36*). We suggest that future work harnessing techniques from quantitative behavioral analysis could help close these knowledge gaps and clarify the complex effects of agrochemical exposure on colony health and collective behavior in bees and other social insects.

Materials and Methods

Arena design and experimental timeline

Four bumblebee (*Bombus impatiens*) colonies (Class B) were acquired from BioBest® between Nov 1st and Dec 5th 2015. Colonies contained between 90 and 130 workers. Two colonies (Colonies A and C) had a small number of males (11 and 5, respectively), which were removed before any experimental trials began. While colony stage can have significant impacts on behavior (*37*), we found no evidence for different effects of pesticide exposure in these two colonies, reflected in a lack of interaction between colony and treatment (see "Analysis of nest behavior" below). Each colony was transferred to a custom nest box (Figure S1, 0.20 x 0.19 x 0.13 m). The walls and floor of the nest box were constructed from black, extruded acrylic (6.3 mm thick). The walls and floor both had 1.6 mm-wide perforations running along their length at 1-inch intervals to allow for air circulation but prevent bees from escaping. The top of the nest box was constructed from clear, laser-cut extruded acrylic (3.1 mm thick) to allow for imaging. A monochrome digital camera (DMK 24UJ003, USB 3.0, Imaging Source, 3856 x 2764 pixels) with a wide-angle lens (Fujinon, 2.8-8 mm) was mounted on aluminum construction rails (25 mm, Thorlabs®) above the clear top of the nest box. The nest was illuminated with two 6-inch square arrays of red LEDs (Knema Lighting®), which do not disturb nest behavior since bees have very poor sensitivity to red light (*38*). After bees were settled within the nest box, they displayed normal patterns of nest behavior (aside from a brief period of increased grooming after tag attachment), and were never observed flying within the nest. The nest box, camera, and lighting array were covered with black cloth to exclude non-red light (Figure S1).

After transferring all bees and the nest structure (including brood and honeypots, which were removed from shipping boxes by detaching the plastic platform on which the colonies built their nest), colonies were allowed to acclimate to the nest box for 72 hours, where they were provided with *ad libitum* pollen and nectar directly within the nest.

After the acclimation period, colonies were given access to a clear plastic tunnel that ran roughly 0.5 meters from the nest to the foraging chamber (Figure S1), which was a 0.8 m x 0.6 m x 0.6 m screened enclosure within the lab. Bees could access the tunnel through a 1 cm (diameter) hole in one wall of the nest box. The foraging chamber

was illuminated with four 150-watt incandescent lights maintained on 12h light, 12h dark cycle from 9 am to 9 pm.

An artificial feeder constructed of white, laser-cut extruded acrylic (3.1 mm thick) was located on the far wall of the foraging chamber, supplying the bees with *ad libitum* access to artificial nectar (Biogluc®) and pollen (Koppert®). The feeder was divided by a 2 cm-high wall that separated the nectar supply on one side from the pollen supply on the other. The feeder could be refilled from outside of the enclosure (Figure S1); the nectar supply was replenished when necessary, and the pollen feeder was cleaned and refilled daily. Bees had direct access to the pollen supply and access to the nectar via a wick. A monochrome digital camera (Chameleon3, USB 3.0, Point Grey®, 1288 x 964 pixels, Fujinon 2.8-8 mm lens) was mounted roughly 15 cm above the feeder. Once colonies had access to the foraging chamber, they were no longer supplied with nectar or pollen within the nest.

Colonies were allowed to acclimate to the foraging chamber for an additional 72 hours, after which all bees were removed from the foraging chamber and the nest and cold-anaesthetized at 4°C for 1-2 hours. Bees that remained active were cooled at -11°C for about 1 minute prior to tagging. Each bee, including the queen, was outfitted with a unique BEEtag (*26*) printed on waterproof, tear-resistant paper. Tags measured 3x4 mm and weighed roughly 2.4 mg each. Tags were affixed to the mesoscutum of each bee with cyanoacrylate glue (super glue gel, ACE, Oak Brook Il). Each bee was then weighed and returned to the nest box.

After being returned to the nest, bees were allowed to forage undisturbed for 48 hours, during which time initial (i.e. pre-treatment) nest behaviors and foraging activity were recorded (see below). After 48 hours, all tagged bees (excluding the queen, newly eclosed workers, or bees that had lost their tags) were removed from the nest box and foraging chamber and cold-anaesthetized for 30 minutes at 4°C, then separated into individual, breathable plastic containers and starved for 2 hours to encourage subsequent feeding. Individual bees were then hand-fed (using a micropipette) 10 μL of artificial nectar containing one of three randomly assigned dosages (see below). Bees were maintained in separate chambers for an additional hour to ensure full consumption of nectar/imidacloprid solutions and to prevent regurgitation of treatment solutions into shared honeypots within the nest. Following this additional starvation period, all bees

were returned to the nest box, except for the few bees that died during starvation (less than 3% of bees treated).

Colonies were then given undisturbed access to the foraging chamber for an additional 48 hours, during which time post-treatment nest behavior and foraging activity were recorded. After 48 hours, all bees were removed from the hive, individuals were recorded as dead if they displayed no signs of voluntary movement, and all bees were frozen.

The same process was repeated for subsequent colonies, after cleaning the nest box, foraging tube, and artificial feeder with water.

Preparation of solutions

We dissolved 0.0040 g of imidacloprid (Pestanal, Sigma-Aldrich, St. Louis, Missouri) in 20 mL of deionized water to produce an initial concentration of 0.2 g L^{-1}. We then performed a series of 1/10 dilutions to arrive at concentrations of 200 μg L^{-1} and 20 μg L^{-1}. We stored these solutions in the dark, because imidacloprid is broken down by aquatic photolysis (*39*). Immediately before treating bees, we mixed the imidacloprid solutions with sugar water (Biogluc®, BioBest, Westerlo, Belgium) in equal parts. Thus, the final concentrations fed to bees were 100 μg L^{-1} and 10 μg L^{-1} imidacloprid mixed in sugar water. The density of a 50% Biogluc®/50% water solution is approximately 1.15 kg L^{-1}, which allows us to convert the concentrations to ppb (w/w). The final concentrations of imidacloprid fed to bumblebees were approximately 8.7 ppb (μg kg^{-1}) and 87 ppb.

We fed each bee 10 μL of solution containing one of three doses of imidacloprid. The control dose was 50% Biogluc® and 50% water with no imidacloprid. The treated bees consumed 10 μL of either 100 μg L^{-1} or 10 μg L^{-1} imidacloprid in sugar water, which translates to each bee consuming either 0.1 ng or 1 ng of imidacloprid.

Rationale for dosages

Neonicotinoids and their metabolites are regularly found in plant tissues, including nectar and pollen (*10*, *13*). When applied to the soil, imidacloprid can be incorporated into nectar for up to ~230 days after application (*40*). A recent review (*10*)

found typical environmental concentrations of neonicotinoids in pesticides to be between 2-6 ng/g, but the amount of imidacloprid found in pollen and nectar varies, with measurements of 10 ppb in nectar and 14 ppb in pollen from squash (*41*), 16 ppb in nectar of buckwheat (*42*), and 12.8 ng mL^{-1} in nectar of citrus trees (*40*). In the citrus experiment, Byrne et al. (*40*) found that when imidacloprid was applied at the full, manufacturer-recommended rate, the highest reported value in nectar was 21.9 ng mL^{-1}; however, taking into account the total residues of imidacloprid plus its metabolites, the highest amount reported was 37.1 ng mL^{-1}. Furthermore, the highest amount of total residues in uncapped nectar from the hive comb of nearby honeybees was found to be 95.2 ng mL^{-1} (*40*).

Reported lethal doses (LD_{50}) for bees have significant variation. For honeybees (*A. mellifera*), Schmuck et al. (*43*) reported three 48-hour LD_{50} values from three collaborating facilities in the UK, the Netherlands, and Germany as 3.7 ng, >21ng, and 40.9 ng per bee, respectively. Decourtye et al. (*44*) reported a 48-hour LD_{50} of 30 ng per honeybee. The LD_{50} for bumblebees has been reported as 40 ng per bee (24-hour) and 20 ng per bee (72-hour) (*45*).

While there is disagreement on the reversibility of the effects of neonicotinoids, some studies have suggested that honeybees and bumblebees can clear non-lethal doses of imidacloprid from their bodies – with honeybees clearing 2 ng per day, and bumblebees clearing 7 ng per day (*46*).

Studies disagree about whether a single, concentrated dose or a chronic, low dose of imidacloprid is more harmful to bees. Cresswell et al. (*46*) suggest that an acute, concentrated dose would have a larger deleterious effect on bees, while Suchail et al. (*47*) claimed that chronic exposure to honeybees was toxic at a dose that was 60-6000 times lower than the acute dose required to produce the same effect.

Experiments involving chronic exposure (i.e., *ad libitum* access to contaminated nectar) may more accurately mimic field-realistic conditions that bumblebees experience, but measuring the exact amount of pesticide ingested is extremely difficult in these studies. We chose to instead treat bees with a precise amount of imidacloprid, equivalent to the amount they are likely ingest in the field when feeding on contaminated nectar over various periods of time. However, bees were allowed a 24-hour recovery period before recording after-treatment behaviors, allowing for any potential clearing (*46*) or reversibility (*48*) of toxic effects.

Estimates of the amount of nectar that a foraging bee eats in a day vary widely. One study states that honeybees need about 11 mg of sugar per day (*49*), which translates to about 22 μl of 50% sucrose (*50*), whereas another study estimates that honeybees consume this much sugar (11 mg) in just an hour during flying (*51*). Some sources suggest that bumblebees burn up to 20 mg of sugar per hour of flight (*52*), and because they are slightly larger on average than honeybees, bumblebees probably drink more nectar per day. In one study, *Bombus terrestris* workers consumed between 125 and 233 μL of sugar syrup (50% w/v) per day (*53*). Bertsch (*54*) found that male bumblebees (*Bombus lucorum*) that foraged for 4 hours per day were consuming an average of 180 μl of 50% sugar solution in 24 hours. Laycock et al. (2012) reported *Bombus terrestris* workers consuming over 400 mg of sugar syrup – at 10 μg L^{-1} imidacloprid, workers consumed around 3 ng imidacloprid in a day.

Taken together, these reports suggest that a *B. impatiens* worker, foraging for a full day, could consume 100 - 400 μl of nectar (50 % w/w sugar) per day. If this nectar were contaminated with a field-realistic concentration of imidacloprid (5.5 μg L^{-1}) (*13*), this would result in consumption of 0.55 – 2.2 ng of imidacloprid.

Image acquisition and tracking software

On the day before and the day after treS3atment, nest behavior and foraging activity were recorded via digital cameras situated in the nest box and the foraging chamber.

For nest behavior, a single, 1-hour video was recorded to a laptop computer (Dell Latitude E6530, 2.60 GHz i7 Intel Processor, 8 GB RAM) at 2 Hz using IC Capture (Imaging Source®). Video recordings were started at 2 pm on each day of data collection, and red lights were turned on for at least 20 minutes before recording began to allow bees to habituate. Each video frame was analyzed using BEEtag (*26*), and the identities and coordinates of every tag in the frame were recorded (Figure S2) ignoring identified numbers that were not associated with the list of tagged bees (i.e. false positives). Spatial coordinates for each bee were corrected for lens distortion using the Camera Calibration toolbox and scaled during post-processing in Matlab. Gaps of missing coordinates of up to 5 seconds (or 10 frames) were “healed” with a linear interpolation.

Foraging behavior was continuously monitored when lights were on in the foraging chamber (9 am to 9 pm) using the camera mounted directly above the feeder. A video feed from the camera was monitored using custom scripts in Matlab on the same Dell laptop computer described above. Each time motion was detected on the feeder, a single image was recorded to memory and processed using BEEtag (~2-3 seconds per image). The identity and coordinates of any identified tags were recorded and the motion capture was started again after a 5-second delay (Figure S1).

Analysis of nest behavior

We performed six measurements of in-nest behavior. First, we calculated the proportion of time each bee was active by dividing number of frames in which a bee was moving by the number of time steps over which its movement speed could be calculated (i.e. when a bee's tag was identified in two subsequent video frames). Bees were considered to be "inactive" if the movement speed of their tag was below $10^{-3.9}$ m s^{-1}. This threshold was chosen based on the clearly bimodal distribution of instantaneous speeds within the nest, the lower of which is almost certainly associated with digital noise involved with image tracking rather than real movement of bees (Figure S4). Second, we calculated the proportion of time each bee was on the nest by dividing the number of frames a bee was detected on the nest by the total number of frames in which that bee was identified. Bees were considered to be on the nest if they were found within 1 cm (roughly one body length) of any part of the nest structure. Coordinates of the nest structure were digitized by hand, and then corrected for lens distortion and scaled following the same procedure performed for all bee spatial coordinates within the nest. Rate of direct nest care was defined as the portion of time bees were found located on the nest structure (a strong predictor of direct nest care, see below and Figure S3) during the observation period. Third, we measured the active velocity by calculating the average velocity of each bee, over the frames when they were active (i.e. when their instantaneous velocity was above $10^{-3.9}$ m s^{-1}). Fourth, we measured the distance of each bee from the queen by calculating the average distance of a bee from the queen, over the frames in which that bee was identified. Fifth, we measured distance of each bee from the hive center, by first calculating an average "social center" of the hive (i.e. the mean of all x and y coordinates of all bees found within the nest across all time points), and then averaging each bee's instantaneous

distances from that center. Last, we calculated degree centrality, or the number of unique bees that each bee interacted with, using the igraph package in R (*55*). Bees were considered to have interacted if their tags were located within 1 cm of each other at any point during the trial period. Bees that had a low detection frequency (i.e. were found in less than 250 seconds out of 3600 seconds of video) were removed from network analyses to avoid unreliable estimates of interaction frequency, although this affected only a small portion of the dataset (20 out of 310 bees) and did not qualitatively affect any results. For all variables, we calculated each bee's change from before to after treatment – for instance, if a bee moved more slowly after treatment as compared to before, the change in its average velocity would be negative.

We performed multivariate multiple regression with six dependent variables – change in proportion of time active, change in rate of direct nest care, change in active velocity, change in distance to the queen, change in distance from the social center, and change in degree centrality. This analysis was appropriate because the in-nest measurements had approximate multivariate normality. We initially included treatment, colony, and body weight as covariates, as well as an interaction terms, weight*treatment and treatment*colony. Likelihood ratio tests confirmed that weight*treatment, treatment*colony, and weight did not contribute significantly to the models, so our final model included only colony and treatment as independent variables.

We evaluated the assumptions of multivariate multiple regression in several ways. We first checked to see that none of the predictor variables were highly correlated using Variance Inflation Factor with the R package, car (*56*). We checked for multivariate outliers by computing Mahalanobis distances using the R package, mvoutlier (*57*). We removed obvious outliers, reran the analysis, and observed no qualitative changes to results; thus we report the final model, including multivariate outliers. We graphically assessed multivariate normality using a Q-Q plot of squared Mahalanobis distances, and found that it was approximately correctly distributed – again, we found that the outliers do not change our results significantly. We found no evidence that the variance-covariance matrices were heterogeneous, using Box's M test for equality of covariance ($p > 0.001$). Since this test is very sensitive, the level of significance for Box's M test should be taken as 0.001(*58*). We acknowledge that data within each hive may not be completely independent – *e.g.* treated bees may stop

performing colony duties, causing other non-treated bees to change their behavior. However, this non-independence should not affect any conclusions concerning differences between treatment groups.

Manual tracking of nest behavior

To confirm that spatial position within the nest predicted patterns of nest care, we manually identified behaviors from 1,079 short video sequences from 91 different bees from Colony A. Each video sequence consisted of a brief 5-second clip from the same video used for automated tracking. In each video sequence, the behavior of individual bees were scored following established ethograms (*24*, *59*), using a custom Matlab script. In addition to this focal 5 second clip, the individual performing manual scoring was able to view a contextual 30 second video clip surrounding the focal segment in to aid behavioral identification. Focal segments were spaced 1 minute apart, and so contextual clips were non-overlapping.

We used this dataset to estimate the portion of time spent in different behaviors when bees were in different spatial locations (i.e. on the nest or off the nest, Figure S3). We then calculated the total portion of video segments where bees were performing direct nest care and maintenance (i.e. inspecting, incubating, working honey pots, or probing honey pots) when individuals were either on the nest (92.6%, Figure S3) or off the nest (2.7%, Figure S3). Interestingly, we observed no direct larval feeding in these sequences, which may result from a combination of our relatively conservative definition of larval feeding (clear opening of a larval pot and regurgitation of food), and the relatively short observation periods.

Analysis of foraging behavior

For each bee observed foraging, we quantified the total number of nectar- and pollen-foraging bouts observed. We classified observations as a single bout of foraging if a bee was identified on a feeder without being absent for more than two minutes; if the bee left the foraging area for at least two minutes and returned, this was classified as a new foraging bout. Because almost all bees that foraged visited both the nectar and pollen feeder during the same visit, we combined pollen and nectar foraging bouts. We calculated the change in the number of foraging bouts for each individual by subtracting the number of pre-treatment foraging bouts from the number of post-

treatment bouts, for all bees who were observed foraging before or after treatment. Though the resulting variable (change in number of foraging bouts) was not continuous, we approximated it as a continuous, normal variable for analysis. We used a linear model with change in the number of foraging bouts as the dependent variable, and we included colony and treatment as independent variables.

In addition, we used two logistic regressions to determine if the imidacloprid treatment predicted whether bees would either cease foraging or begin foraging after treatment. For the regression predicting whether bees would begin foraging after treatment, we excluded all bees that were observed foraging prior to treatment. For the regression predicting whether bees were likely to cease foraging, we included only bees that were observed foraging prior to treatment. Since the number of new bees that foraged after treatment was very small, we re-analyzed the data with bias-reduced logistic regression (*60*). We found no significant difference between the two methods, so we reported the logistic regression without bias reduction.

Significance Level Adjustment

While we do not report multiple-comparison adjustments, doing so would not have affected any of our nest behavior results, although we may have failed to reject the results of the logistic regression predicting the probability of becoming a new forager after treatment.

Acknowledgements: The authors thank Nora E. Mishanec for aid in manual scoring of behaviors. Associated data and custom scripts are deposited on zenodo.org [Accession number: PLACEHOLDER]. This material is based upon work supported by the National Science Foundation Graduate Research Fellowship to J.D.C., the National Defense Science & Engineering Graduate Fellowship (NDSEG 32 CFR 168a) Program to C.M.S., and by the National Science Foundation (CAREER IOS-1253677) to S.A.

References

1. A. M. Klein *et al.*, Importance of pollinators in changing landscapes for world crops. *Proceedings of the Royal Society B: Biological Sciences*. **274**, 303–313 (2007).

2. M. M. Kwak, O. Velterop, J. Andel, Pollen and gene flow in fragmented habitats. *Applied Vegetation Science*. **1**, 37–54 (1998).

3. N. Myers, Environmental services of biodiversity. *Proc Natl Acad Sci USA*. **93**, 2764–2769 (1996).

4. G. K. Meffe, The potential consequences of pollinator declines on the conservation of biodiversity and stability of food crop yields. *Conservation Biology*. **12**, 8–17 (1998).

5. D. van Engelsdorp *et al.*, Colony Collapse Disorder: A Descriptive Study. *PLoS ONE*. **4**, e6481–17 (2009).

6. J. C. Biesmeijer *et al.*, Parallel declines in pollinators and insect-pollinated plants in Britain and the Netherlands. *Science*. **313**, 351–354 (2006).

7. I. Koh *et al.*, Modeling the status, trends, and impacts of wild bee abundance in the United States. *Proc Natl Acad Sci USA*. **113**, 140–145 (2016).

8. D. Goulson, E. Nicholls, C. Botias, E. L. Rotheray, Bee declines driven by combined stress from parasites, pesticides, and lack of flowers. *Science*. **347**, 1255957–1255957 (2015).

9. O. Lundin, M. Rundlöf, H. G. Smith, I. Fries, R. Bommarco, Neonicotinoid Insecticides and Their Impacts on Bees: A Systematic Review of Research Approaches and Identification of Knowledge Gaps. *PLoS ONE*. **10**, e0136928 (2015).

10. H. C. J. Godfray *et al.*, A restatement of recent advances in the natural science evidence base concerning neonicotinoid insecticides and insect pollinators. *Proc. Biol. Sci.* **282**, 20151821 (2015).

11. H. C. J. Godfray *et al.*, A restatement of the natural science evidence base concerning neonicotinoid insecticides and insect pollinators. *Proc. Biol. Sci.* **281**, 20140558–20140558 (2014).

12. P. R. Whitehorn, S. O'Connor, F. L. Wackers, D. Goulson, Neonicotinoid pesticide reduces bumble bee colony growth and queen production. *Science*. **336**, 351–352 (2012).

13. M. Rundlöf *et al.*, Seed coating with a neonicotinoid insecticide negatively affects wild bees. *Nature*. **521**, 77–80 (2015).

14. D. A. Stanley *et al.*, Neonicotinoid pesticide exposure impairs crop pollination services provided by bumblebees. *Nature*. **528**, 548–550 (2015).

15. European Commission, “Bee Health: EU-wide restrictions on Pesticide use to enter into

force on 1 December" (2013), pp. 1–2.

16. P. Déglise, B. Grünewald, M. Gauthier, The insecticide imidacloprid is a partial agonist of the nicotinic receptor of honeybee Kenyon cells. *Neurosci. Lett.* **321**, 13–16 (2002).

17. J. Fischer *et al.*, Neonicotinoids Interfere with Specific Components of Navigation in Honeybees. *PLoS ONE*. **9**, e91364–10 (2014).

18. M. Henry *et al.*, A Common Pesticide Decreases Foraging Success and Survival in Honey Bees. *Science*. **336**, 348–350 (2012).

19. D. A. Stanley, K. E. Smith, N. E. Raine, Bumblebee learning and memory is impaired by chronic exposure to a neonicotinoid pesticide. *Sci. Rep.* **5**, 16508–10 (2015).

20. K. Tan *et al.*, A neonicotinoid impairs olfactory learning in Asian honey bees (Apis cerana) exposed as larvae or as adults. *Sci. Rep.* **5**, 1–8 (2015).

21. R. J. Gill, N. E. Raine, Chronic impairment of bumblebee natural foraging behaviour induced by sublethal pesticide exposure. *Funct Ecol*. **28**, 1459–1471 (2014).

22. H. Feltham, K. Park, D. Goulson, Field realistic doses of pesticide imidacloprid reduce bumblebee pollen foraging efficiency. *Ecotoxicology*. **23**, 317–323 (2014).

23. K. E. Gardner, R. L. Foster, S. O'Donnell, Experimental analysis of worker division of labor in bumblebee nest thermoregulation (Bombus huntii, Hymenoptera: Apidae). *Behav Ecol Sociobiol*. **61**, 783–792 (2006).

24. S. A. Cameron, Temporal Patterns of Division of Labor among Workers in the Primitively Eusocial Bumble Bee, Bombus griseocollis (Hymenoptera: Apidae)1). *Ethology*. **80**, 137–151 (1989).

25. R. J. Gill, O. Ramos-Rodriguez, N. E. Raine, Combined pesticide exposure severely affects individual- and colony-level traits in bees. *Nature*. **490**, 105–108 (2012).

26. J. D. Crall, N. Gravish, A. M. Mountcastle, S. A. Combes, BEEtag: A Low-Cost, Image-Based Tracking System for the Study of Animal Behavior and Locomotion. *PLoS ONE*. **10**, e0136487–13 (2015).

27. C. Moffat *et al.*, Neonicotinoids target distinct nicotinic acetylcholine receptors and neurons, leading to differential risks to bumblebees. *Sci. Rep.* **6**, 24764 (2016).

28. J. H. Fewell, Social insect networks. *Science*. **301**, 1867–1870 (2003).

29. J. C. Nieh, The stop signal of honey bees: reconsidering its message. *Behav Ecol Sociobiol*. **33**, 51–56 (1993).

30. M. A. Renner, J. C. Nieh, Bumble bee olfactory information flow and contact-based foraging activation. *Insect. Soc.* **55**, 417–424 (2008).

31. M. C. Otterstatter, J. D. Thomson, Contact networks and transmission of an intestinal

pathogen in bumble bee (Bombus impatiens) colonies. *Oecologia*. **154**, 411–421 (2007).

32. H. Feltham, K. Park, D. Goulson, Field realistic doses of pesticide imidacloprid reduce bumblebee pollen foraging efficiency. *Ecotoxicology*. **23**, 317–323 (2014).

33. M. J. Palmer *et al.*, Cholinergic pesticides cause mushroom body neuronal inactivation in honeybees. *Nat Commun*. **4**, 1634 (2013).

34. D. P. Mersch, A. Crespi, L. Keller, Tracking individuals shows spatial fidelity is a key regulator of ant social organization. *Science*. **340**, 1090–1093 (2013).

35. G. Di Prisco, V. Cavaliere, D. Annoscia, (2013).

36. C. J. Perry, E. Søvik, M. R. Myerscough, A. B. Barron, Rapid behavioral maturation accelerates failure of stressed honey bee colonies. *Proc Natl Acad Sci USA*. **112**, 3427–3432 (2015).

37. G. Bloch, A. Hefetz, Regulation of reproduction by dominant workers in bumblebee (Bombus terrestris) queenright colonies. *Behav Ecol Sociobiol*. **45**, 125–135 (1999).

38. P. Skorupski, L. Chittka, Photoreceptor Spectral Sensitivity in the Bumblebee, Bombus impatiens (Hymenoptera: Apidae). *PLoS ONE*. **5**, e12049–5 (2010).

39. W. Zheng, W.-P. Liu, Y.-Z. Wen, S.-J. Lee, Photochemistry of insecticide imidacloprid: direct and sensitized photolysis in aqueous medium. *J Environ Sci (China)*. **16**, 539–542 (2004).

40. F. J. Byrne *et al.*, Determination of exposure levels of honey bees foraging on flowers of mature citrus trees previously treated with imidacloprid. **70**, 470–482 (2013).

41. K. A. Stoner, B. D. Eitzer, Movement of Soil-Applied Imidacloprid and Thiamethoxam into Nectar and Pollen of Squash (Cucurbita pepo). *PLoS ONE*. **7**, e39114–5 (2012).

42. V. A. Krischik, A. L. Landmark, G. E. Heimpel, Soil-applied imidacloprid is translocated to nectar and kills nectar-feeding Anagyrus pseudococci (Girault) (Hymenoptera: Encyrtidae). *Environ. Entomol.* **36**, 1238–1245 (2007).

43. R. Schmuck, R. Schöning, A. Stork, O. Schramel, Risk posed to honeybees (Apis mellifera L, Hymenoptera) by an imidacloprid seed dressing of sunflowers. *Pest. Manag. Sci.* **57**, 225–238 (2001).

44. A. Decourtye, E. Lacassie, M.-H. Pham-Del gue, Learning performances of honeybees (Apis mellifera L) are differentially affected by imidacloprid according to the season. *Pest. Manag. Sci.* **59**, 269–278 (2003).

45. F. Marletto, A. Patetta, A. Manino, Laboratory assessment of pesticide toxicity to bumblebees. *Bulletin of Insectology*. **56**, 155–158 (2003).

46. J. E. Cresswell, F.-X. L. Robert, H. Florance, N. Smirnoff, Clearance of ingested neonicotinoid pesticide (imidacloprid) in honey bees (Apis mellifera) and bumblebees (

Bombus terrestris). *Pest. Manag. Sci.* **70**, 332–337 (2013).

47. S. Suchail, D. Guez, L. P. Belzunces, Discrepancy between acute and chronic toxicity induced by imidacloprid and its metabolites in Apis mellifera. *Environ. Toxicol. Chem.* **20**, 2482–2486 (2001).

48. H. M. Thompson, S. Wilkins, S. Harkin, S. Milner, K. F. Walters, Neonicotinoids and bumblebees (Bombus terrestris): effects on nectar consumption in individual workers. **71**, 946–950 (2014).

49. Z. Y. Huang, E. Plettner, G. E. Robinson, Effects of social environment and worker mandibular glands on endocrine-mediated behavioral development in honey bees. *J Comp Physiol A*. **183**, 143–152 (1998).

50. Z. Huang, Honey bee nutrition. *American Bee Journal*. **150**, 773–776 (2010).

51. R. Beutler, D. Loman, Time and Distance in the Life of the Foraging Bee. *Bee World*. **32**, 25–27 (2015).

52. B. Heinrich, Energetics of pollination. *Annual Review of Ecology and Systematics*. **6**, 139–170 (1975).

53. L. A. Malone, E. Phyllis, J. Burgess, D. Stefanovic, H. S. Gatehouse, Effects of four protease inhibitors on the survival of worker bumblebees, Bombus terrestris L. *Apidologie*. **31**, 25–38 (2000).

54. A. Bertsch, Foraging in male bumblebees (Bombus lucorum L.): maximizing energy or minimizing water load? *Oecologia*. **62**, 325–336 (1984).

55. G. Csárdi, T. Nepusz, *The igraph software package for complex network research. InterJournal Complex Systems 1695 (2006)* (Springer Berlin Heidelberg, Berlin, Heidelberg, 2014).

56. J. Fox, S. Weisberg, *An R Companion to Applied Regression* (SAGE, 2010).

57. P. Filzmoser, M. Gschwandtner, *mvoutlier: Multivariate outlier detection based on robust methods* (R package version, 2012).

58. J. P. Verma, *Repeated Measures Design for Empirical Researchers* (John Wiley & Sons, 2015).

59. J. M. Jandt, E. Huang, A. Dornhaus, Weak specialization of workers inside a bumble bee (Bombus impatiens) nest. *Behav Ecol Sociobiol*. **63**, 1829–1836 (2009).

60. G. Heinze, M. Ploner, D. Dunkler, H. Southworth, *logistf: Firth's bias reduced logistic regression* (R package version, 2013).

Supplementary Material

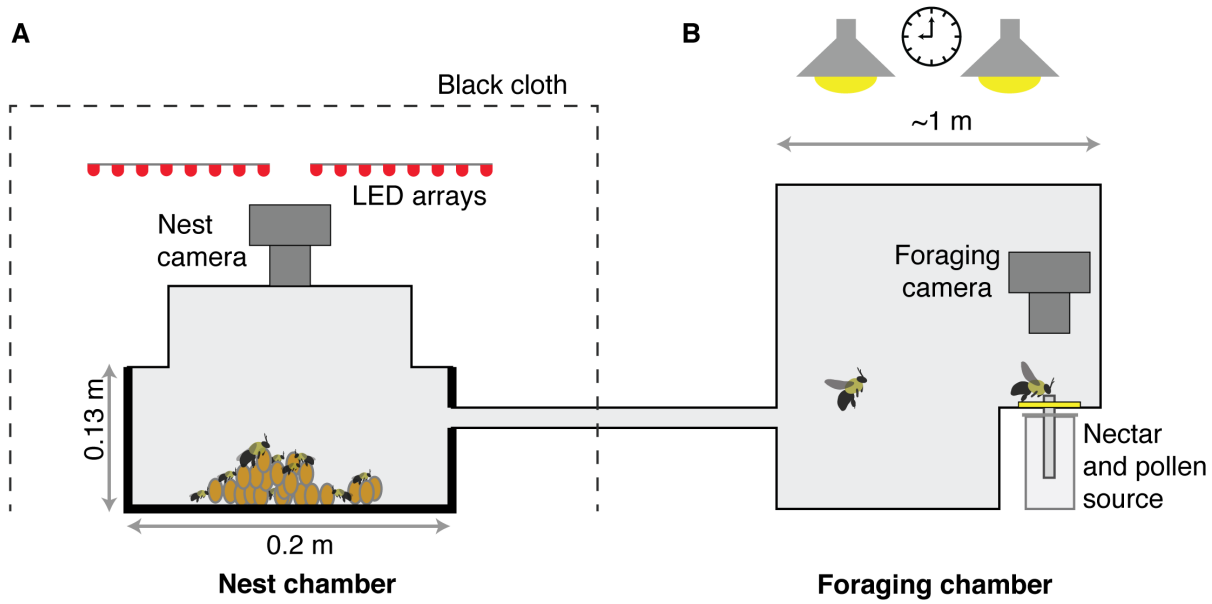

Figure S1. Schematic of experimental tracking arena. (A) Nest chamber. Thick black lines show opaque, black plastic nest box, and thin lines show transparent plastic cover. Dotted line indicated black drop cloth draped over nest chamber and cameras. (B) Foraging chamber, showing relative positions of lights, foraging camera, and nectar and pollen source. Drawing is not to scale.

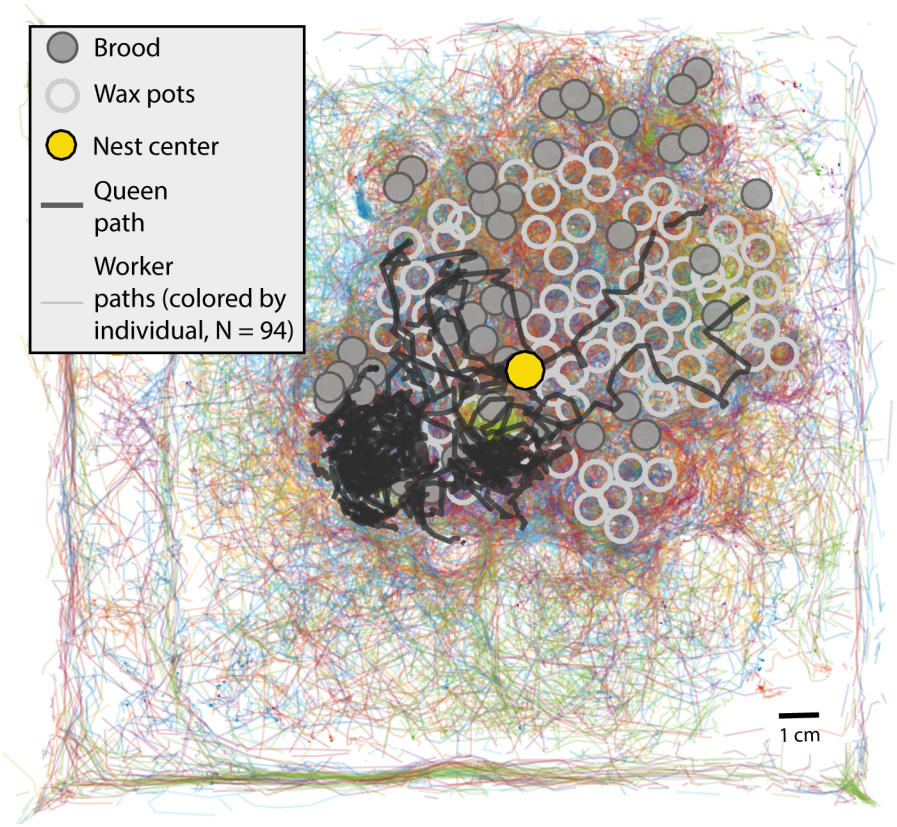

Figure S2. Mapping of individual movement patterns and relevant nest elements from Colony A. Thin, transparent lines represent the paths of individual workers (N = 94, each identified with a unique color) within the nest over the course of an hour. Filled gray circles indicate positions of developing brood (eggs, larvae, and pupae), while empty gray circle represent the position of honeypots. Thick black line represents the path of the queen and the large yellow circle shows the position of the social center of the colony.

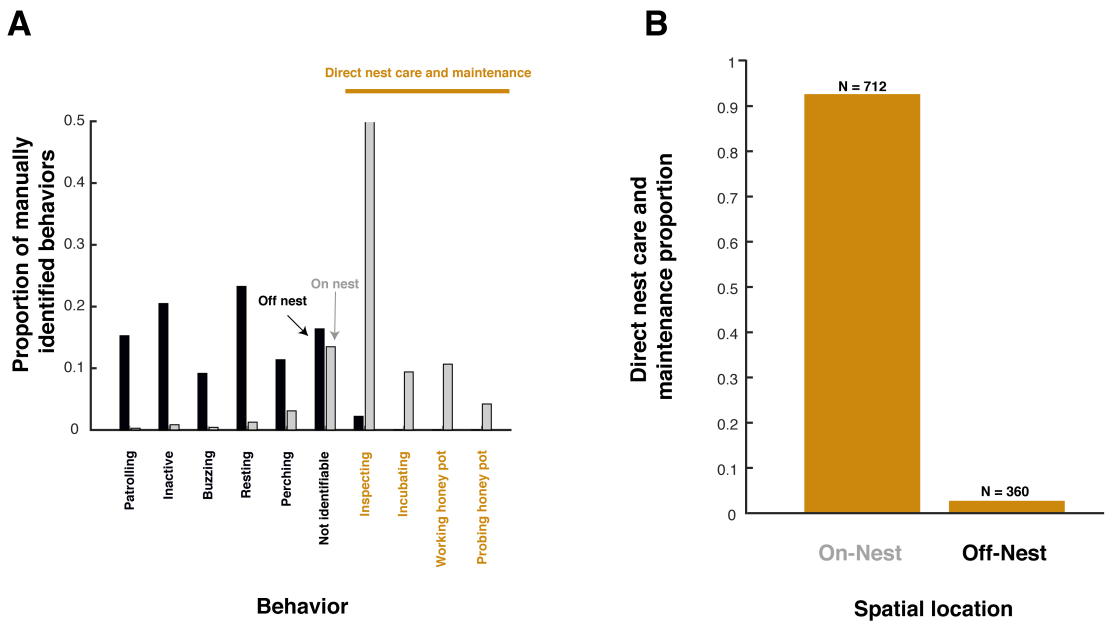

Figure S3. Spatial location is a strong predictor of direct nest care and maintenance. (A) Proportions of video sequences manually identified as each behavioral category when bees were located either on the nest (gray bars) or off the nest (black bars), based on automated tracking and spatial mapping of nest structure. Behaviors associated with direct nest and brood care are shown in orange (inspecting, incubating, working honey pot, and probing honey pot). Behaviors that did not represent at least 2% of all observed behaviors were removed from this analysis. (B) Total proportion of time engaged in direct nest care and maintenance when bees were located on or off the nest, based on automated tracking. Sample sizes reflect the number of focal video sequences scored for each category.

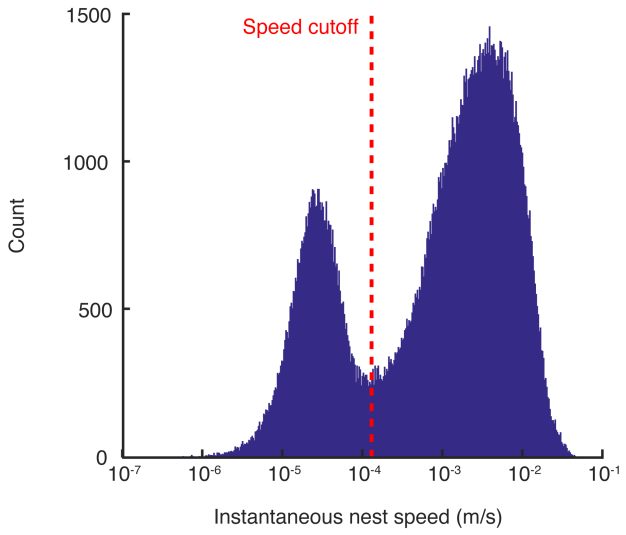

Figure S4. Histogram of all instantaneous measured speeds (N = 197,981) for all individuals within Colony A before treatment over an hour of observation. Dotted red line indicates the speed cutoff used throughout. Instantaneous speeds below this cutoff (10^{-4} m s^{-1}, or 0.12 mm s^{-1}) were assumed to result from digital noise, rather than real movements of bees.

Video S1. Tracking of BEEtags within a *B. impatiens* nest after treatment. Colors indicate treatment group, with bees in the control, low dose (0.1 ng bee^{-1}), and high dose (1.0 ng bee^{-1}) groups shown in green, blue, and red, respectively. Bees shown in grey were not removed from the nest for treatment. Frames were recorded at 2 frames per second (fps), but are shown at 15 fps in the video, or sped up roughly 7.5x.

Video S2. Tracking of foraging behavior of bumblebee (*B. impatiens*) workers. Time-lapse video shows location and identity (in red for all treatment groups) of foragers visiting a nectar feeder (left) and pollen feeder (right) over the course of 55 minutes.

Appendix: Social context modulates idiosyncrasy of behavior in the gregarious cockroach *Blaberus discoidalis*

Reprinted from:
Crall, J. D., Souffrant, A. D., Akandwanaho, D., Hescock, S. D., Callan, S. E., Coronado, W. M., et al. (2016). Social context modulates idiosyncrasy of behaviour in the gregarious cockroach Blaberus discoidalis. *Animal Behaviour*, *111*(C), 297–305. http://doi.org/10.1016/j.anbehav.2015.10.032

Animal Behaviour 111 (2016) 297–305

Contents lists available at ScienceDirect

Animal Behaviour

journal homepage: www.elsevier.com/locate/anbehav

Social context modulates idiosyncrasy of behaviour in the gregarious cockroach *Blaberus discoidalis*

James D. Crall [a, b, *, 1], André D. Souffrant [a, 1], Dominic Akandwanaho [a, 1], Sawyer D. Hescock [a, 1], Sarah E. Callan [a, 2], W. Melissa Coronado [a, 2], Maude W. Baldwin [a], Benjamin L. de Bivort [a, c, *]

[a] *Department of Organismic and Evolutionary Biology, Harvard University, Cambridge, MA, U.S.A.*
[b] *Concord Field Station, Harvard University, Bedford, MA, U.S.A.*
[c] *Center for Brain Science, Harvard University, Cambridge, MA, U.S.A.*

ARTICLE INFO

Article history:
Received 24 June 2015
Initial acceptance 21 July 2015
Final acceptance 29 September 2015
Available online 12 December 2015
MS. number: A15-00542R

Keywords:
animal personality
behaviour
cockroach
collective behaviour
group composition
individuality
phototaxis
sociality

Individuals are different, but they can work together to perform adaptive collective behaviours. Despite emerging evidence that individual variation strongly affects group performance, it is less clear to what extent individual variation is modulated by participation in collective behaviour. We examined light avoidance (negative phototaxis) in the gregarious cockroach *Blaberus discoidalis*, in both solitary and group contexts. Cockroaches in groups exhibited idiosyncratic light-avoidance performance that persisted across days, with some individual cockroaches avoiding a light stimulus 75% of the time, and others avoiding the light just above chance (i.e. ~50% of the time). These individual differences were robust to group composition. Surprisingly, these differences did not persist when individuals were tested in isolation, but returned when testing was once again done in groups. During the solo testing phase cockroaches exhibited individually consistent light-avoidance tendencies, but these differences were uncorrelated with performance in any group context. Therefore, we have observed not only that individual variation affects group-level performance, but also that whether or not a task is performed collectively can have a significant, predictable effect on how an individual behaves. That individual behavioural variation is modulated by whether a task is performed collectively has major implications for understanding variation in behaviours that are facultatively social, and it is essential that ethologists consider social context when evaluating individual behavioural differences.

In animal groups, individuals with different phenotypes can nevertheless coordinate their behaviours to solve problems and increase individual fitness. Group living increases the chance of encountering a mate (Uzsák & Schal, 2013), provides security from predators (Treherne & Foster, 1980; Uzsák & Schal, 2013), and enhances access to other key resources such as food and shelter (Parrish & Edelstein-Keshet, 1999). Group dynamics are important for understanding how animals use collective decision making to solve problems and attain high levels of fitness.

To understand group dynamics, we need to examine the relationship between individual variation and collective behaviour. This relationship is complex, however, and is currently a frontier of research in animal behaviour (Bengston & Jandt, 2014; Jandt et al., 2014; Jeanson & Weindenmuller, 2014; LeBoeuf & Grozinger, 2014). It is clear that individual variation (arising through a number of mechanisms, including genetic diversity (Bengston & Jandt, 2014), or differences in experience (Ravary et al., 2007)) can give rise to variation between groups through a variety of processes, such as founder effects or interactions with conspecifics, etc. (Bengston & Jandt, 2014; LeBoeuf & Grozinger, 2014). Increasingly, however, there is also evidence that the presence of conspecifics can drive individual behavioural variation (LeBoeuf & Grozinger, 2014), for example through social niche differentiation (Bergmüller & Taborsky, 2010). Individual variation can thus affect, but also be affected by, group behaviour.

* Correspondence: J. D. Crall, B. L. de Bivort, Department of Organismic and Evolutionary Biology, Harvard University, Cambridge, MA 02138, U.S.A.
E-mail addresses: james.crall@gmail.com (J. D. Crall), debivort@oeb.harvard.edu (B. L. de Bivort).
[1] These authors contributed equally.
[2] These authors contributed equally.

http://dx.doi.org/10.1016/j.anbehav.2015.10.032
0003-3472/

There is strong empirical evidence for individual variation in collectively behaving animals. Schools of fish (Marras & Domenici, 2013), flocks of homing pigeons (Hoffman, 1958), and even human groups (Vindenes, Engen, & Sæther, 2008) are populated by highly varied individuals, which can have important effects on group performance (Brown & Irving, 2013). Among invertebrates, castes within eusocial insects are a classical example of behavioural differentiation within a group context (O'Donnell, 1998; Winston & Michener, 1977). These differences can emerge even when all individuals are genetically identical (Freund et al., 2013), suggesting that individual variation in behaviour could be an emergent property of group membership. Yet, eusociality is not a prerequisite for behavioural differences between individuals. Indeed, several non-eusocial insects exhibit conspicuous individual differences even when genetically identical (Buchanan, Kain, & de Bivort, 2015; Kain, Stokes, & de Bivort, 2012; Petrovskii, Mashanova, & Jansen, 2011; Schuett et al., 2011; Stamps, Saltz, & Krishnan, 2013), probably reflecting developmental noise rather than an emergent property.

As an intermediate case between eusocial and solitary lifestyles, gregarious insects represent an interesting case for the consideration of individuality in the group context. Clonal, gregarious aphids exhibit individuality in both escape (Schuett et al., 2011) and exploratory locomotion behaviours (Petrovskii et al., 2011). Canonge, Sempo, Jeanson, Detrain, and Deneubourg (2009) showed that American cockroaches, *Periplaneta americana*, exhibit individual differences in resting site preferences. Planas-Sitjà, Deneubourg, Gibon, and Sempo (2015) found (in the same species) that behavioural variation between individuals can affect group dynamics and collective shelter-seeking behaviour. However, the interplay between individual variation and collective behaviour in gregarious insects remains a nascent research area.

There is emerging evidence that such individual variation plays an important role in determining collective behaviour (Hui & Pinter-Wollman, 2014; Modlmeier, Keiser, Shearer, & Pruitt, 2014) and group success (Modlmeier, Liebmann, & Foitzik, 2012; Pruitt & Riechert, 2011). Individual variation in social spider groups (*Stegodyphus dumicola*) plays a larger role in determining group success than the size of the group (Keiser & Pruitt, 2014). Hoffman (1958) showed that even in humans, the individual variation within a group significantly contributes towards that group's success. The effect of individual differences on group behaviour can be distributed evenly across individuals or concentrated in specific members. Key individuals in a group can have a particularly strong influence on the collective behaviour of their group (Modlmeier, Keiser, Watters, Sih, & Pruitt, 2014).

Despite increasing evidence that individuality plays a large role in determining collective behaviour, we have only recently begun to understand the potential effects of group membership in modulating individual variation. In social spiders, group membership can increase individual behavioural variation (Laskowski & Pruitt, 2014; Modlmeier, Laskowski, et al., 2014). In social insects, there has been increasing interest in understanding how feedback between individual behaviour and social context may dynamically produce stable, individually specific behavioural patterns (Bengston & Jandt, 2014; Jandt et al., 2014; Jeanson & Weindenmuller, 2014; LeBoeuf & Grozinger, 2014). In honeybees, for example, colony context has a clear effect on at least some behaviours, with clonal subpopulations of bees exhibiting different behavioural patterns depending on the genetic homogeneity of the entire colony (Gempe, Stach, Bienefeld, & Beye, 2012; Hunt, Guzman-Novoa, Uribe-Rubio, & Prieto-Merlos, 2003). Outside of social insects, there is also evidence that social context can modulate behavioural traits typically associated with 'personality' (i.e. risk-taking behaviour: Schuett and Dall, 2009; van Oers, Klunder, & Drent, 2005; 'boldness': Keiser, Modlmeier, Singh, Jones, & Pruitt, 2014). However, the extent to which such group effects are pervasive outside of highly social arthropods is largely unknown.

Our broad goal was to use cockroach light-avoidance behaviour to examine (1) how individual behavioural differences correlate with collective behaviour in a system that allows rapid quantification and robust tracking of individuals across contexts and (2) the effect that group membership has on individual variation. Cockroach light-avoidance is likely a predator-evasion and shelter-seeking response. Performance (defined as the fraction of time spent in the shade) of this behaviour improves with the size of the group, and thus can be considered a collective behaviour (Canonge, Deneubourg, & Sempo, 2011; Salazar, Deneubourg, & Sempo, 2013; Sempo et al., 2009). When searching for a suitable shelter, cockroaches are able to use social cues to reach a consensus and aggregate in a single suitable shelter (Sempo et al., 2009). However, the consensus decision is influenced by the individual variation within a group (Sempo et al., 2009). Thus we also expected to find that individual variation in light-avoidance performance contributes to differences at the group level.

Using a new two-dimensional bar-coding system (Crall, Gravish, Mountcastle, & Combes, 2015), we tracked individual cockroaches as they performed a collective light-avoidance behaviour, in a variety of group configurations, to test the following hypotheses. First, we hypothesized that individual animals would display different behaviours with respect to the light stimulus. Specifically, some individuals would be better at avoiding the light than others. We also hypothesized that these differences between individuals would emerge from social niche construction occurring after the formation of those experimental groups. We reassigned individual roaches from their original random groups to groups based on similarity in their individual light-avoidance performance. If social niche construction acts on days-long timescales, individual variation in performance would re-emerge even in groups initially composed of individuals with little variation. These experiments assess the stability of individual differences across changes in group membership. Next, using solitary light-avoidance assays, we tested the hypothesis that any stable individual differences observed across the first two experiments would persist when animals were assayed individually. Finally, by restoring the animals to experimental groups, we tested the hypothesis that any discrepancy between individual behaviours in the group and solitary contexts could be explained by drift in individual behavioural biases over time.

METHODS

We developed a system for automatically tracking cockroach position in a circular arena, in which a downward-facing projector delivered a moving light/shade stimulus, and cockroach position was imaged using light invisible to the cockroaches. Cockroaches were permanently tagged with optical codes whose positions could be extracted from the frames of a video using pattern recognition software (Crall et al., 2015). Combining these two techniques, we were able to determine a cockroach's position and speed, and whether it was in the light or in the shade. The use of permanent tags enabled us to track the performance of individual cockroaches over a month of successive experiments, even while varying the membership of the groups.

Scripts and processed cockroach position data are available at: http://lab.debivort.org/social-context-modulates-idiosyncrasy and Zenodo (doi:10.1101/028571).

Study Organism and Animal Care

Blaberus discoidalis animals were purchased from Backyard Brains (Ann Arbor, MI, U.S.A.) and were approximately 8 months old

on arrival. We selected 60 males from a mixed-sex population that were free of conspicuous external damage and used them as experimental individuals. Cockroaches were housed in opaque black plastic containers with translucent white perforated lids. Houses contained egg-carton cardboard enrichment. Food pellets (Rat and Mouse Food, Carolina Biological Supply, Burlington, NC, U.S.A.) and water-soaked paper towels were replaced weekly. Containers were cleaned weekly.

The test cockroaches were tagged with BEEtag codes for automated video tracking (Crall et al., 2015). Tags were printed on waterproof paper and measured ~8 × 8 mm. Each cockroach was anaesthetized using CO_2. While anaesthetized, we abraded the pronotum of the cockroach with fine grit sandpaper and attached the BEEtags to the pronotum using cyanoacrylate glue. Cockroaches were given a minimum of 48 h to recover after anaesthetization before the start of experimental trials. During this time, two out of ~80 tagged individuals shed their tags, and were not retained for experiments.

Experimental Set-up and Stimulus

We constructed a circular arena with walls made from high-density polyethylene by cutting the top and bottom off a 5-gallon (18.93-litre) liquid waste container. The circular arena was 28.2 cm in diameter and ~30 cm tall. A mounting base for the arena was constructed with black 5.6 mm acrylic. The arena walls could be slotted into a ~5 mm wide circular groove cut into this base, holding the walls in place. For trials, we covered the base by a sheet of Absorbent Lab Paper (VWR-51138-500, VWR, Radnor, PA, U.S.A.), which was changed between trials, to minimize odorant contamination. An Optoma S316 DLP (digital light processing) projector and 5MP monochromatic digital camera with a global shutter (Blackfly model, Point Grey, Richmond, BC, Canada) were mounted on an aluminium extrusion rig above the arena. Recordings were collected at seven frames/s, with an exposure time of 8 ms. This exposure time was chosen to minimize motion blur within each frame, as well as to synchronize with the vertical scan of the DLP projector. The projector delivered a computer-controlled stimulus (at 30 frames/s) onto the base and the interior walls of the arena. The camera lens was covered by a 590 nm long-pass red filter (Thorlabs, Newton, NJ, U.S.A.). The camera recorded a video of the entire base of the arena for the duration of each trial.

For tagging control experiments (see Supplementary Fig. S1), the projected stimulus was magenta on the top half and red on the bottom half. Control experiments were conducted with individual cockroaches ($N = 21$ untagged, 19 tagged) and in groups of three randomly selected individuals ($N = 6$ untagged groups, 5 tagged groups). For all other experiments, the projected stimulus was alternating red and magenta quadrants (Fig. 1). The quadrants rotated at 0.05 Hz and randomly reversed rotation direction with a probability of 0.033 per frame, resulting in an average rotational direction persistence of 1 s. The stimulus also included two small black wedges at the centre of the red sectors, which allowed us to use machine vision to identify the position of the sectors in the same image that we used to track the BEEtags. These colours were chosen because cockroaches do not sense red light, so the red segments of the stimulus would appear to be dark to them, while the magenta stimulus would appear bright (Walther, 1958). Before each trial, we transferred experimental animals to an empty plastic container in darkness. We then initiated the stimulus and gently poured the cockroaches into the arena (Supplementary Movie S1). Recordings lasted either 10 min or 5 min.

Trial Structure

We conducted four different experiment phases (Rounds), varying the composition of housing and experimental groups (cohorts).

Round 1

In the first round of trials, we randomly placed 60 individuals into six cohorts of 10 cockroaches each. To ensure that cohort composition was not influenced by the relative ease of picking up some cockroaches compared to others, we took a population of 80 tagged cockroaches and divided them into five groups of equal size. Cockroaches were placed in these temporary groups in the order in which they were picked up (the first 16 cockroaches picked up went into group 1, the second 16 cockroaches went into group 2, etc.). From each group we randomly selected two cockroaches to be in each of the experimental cohorts. The cockroaches were allowed to acclimate to their new housing group for 48 h. Each 10-individual cohort then underwent one experimental trial each day on 6 consecutive days, in which the entire cohort was introduced into the arena for a 10 min trial (Fig. 1c, d). Here and in all analyses, tracking performance was defined as the percentage of time that each individual spent in the red zones. Only the first 5 min was considered because the cockroaches habituated to the stimulus (see below).

Round 2

After the last experiment of Round 1, we placed the cockroaches in new housing and experimental cohorts ('re-cohorted') based on their ranked individual tracking performance in the first round. Rank 1 individuals were all added to the first new cohort. Rank 2 individuals were randomly split between the first and second Round 2 cohorts, so that the first cohort had 10 members, etc. We continued this procedure to populate all Round 2 cohorts (Fig. 1d). We then gave the cockroaches 48 h to acclimate to their new housing groups. Experiments in Round 2 proceeded as in Round 1, with each cohort of 10 individuals being tested six times.

Round 3

After the last Round 2 experiment, the cockroaches were re-cohorted randomly into six new cohorts with the use of a six-sided die. The cockroaches were then given 48 h to acclimate to their new housing groups. For experiments, we introduced each individual into the arena alone (Supplementary Movie S2) and recorded its movements for 5 min. The stimulus presentation during trials was identical except for the random timing of quadrant reversals. Each day we tested cockroaches from two cohorts, and we repeated this until each individual was tested four times in this Round, which consequentially lasted for 12 days (Fig. 1d).

Round 4

After the last Round 3 experiment, the cockroaches were re-cohorted randomly into six new cohorts with the use of a six-sided die. The cockroaches were then given 48 h to acclimate to their new housing groups. These cohorts underwent group trials similar to the trials described in the first and second rounds of trials. Each cohort of 10 individuals was tested three times each over the course of Round 4.

Thus, in terms of fully independent units (i.e. the sample sizes), we tested six cohorts of 10 roaches each in Rounds 1, 2 and 4, and 60 individual roaches in Round 3. The number of replicate experiments per Round 1–4 was, respectively, 6, 6, 4 and 3. During the 31 days of experiments, three cockroaches died, the first between trials 1 and 2 of the first round of experiments. This individual was replaced with a randomly chosen individual from the remaining pool of tagged cockroaches. The subsequent cockroaches were not replaced, so at any time, up to two experimental and housing cohorts had nine individuals rather than 10 individuals.

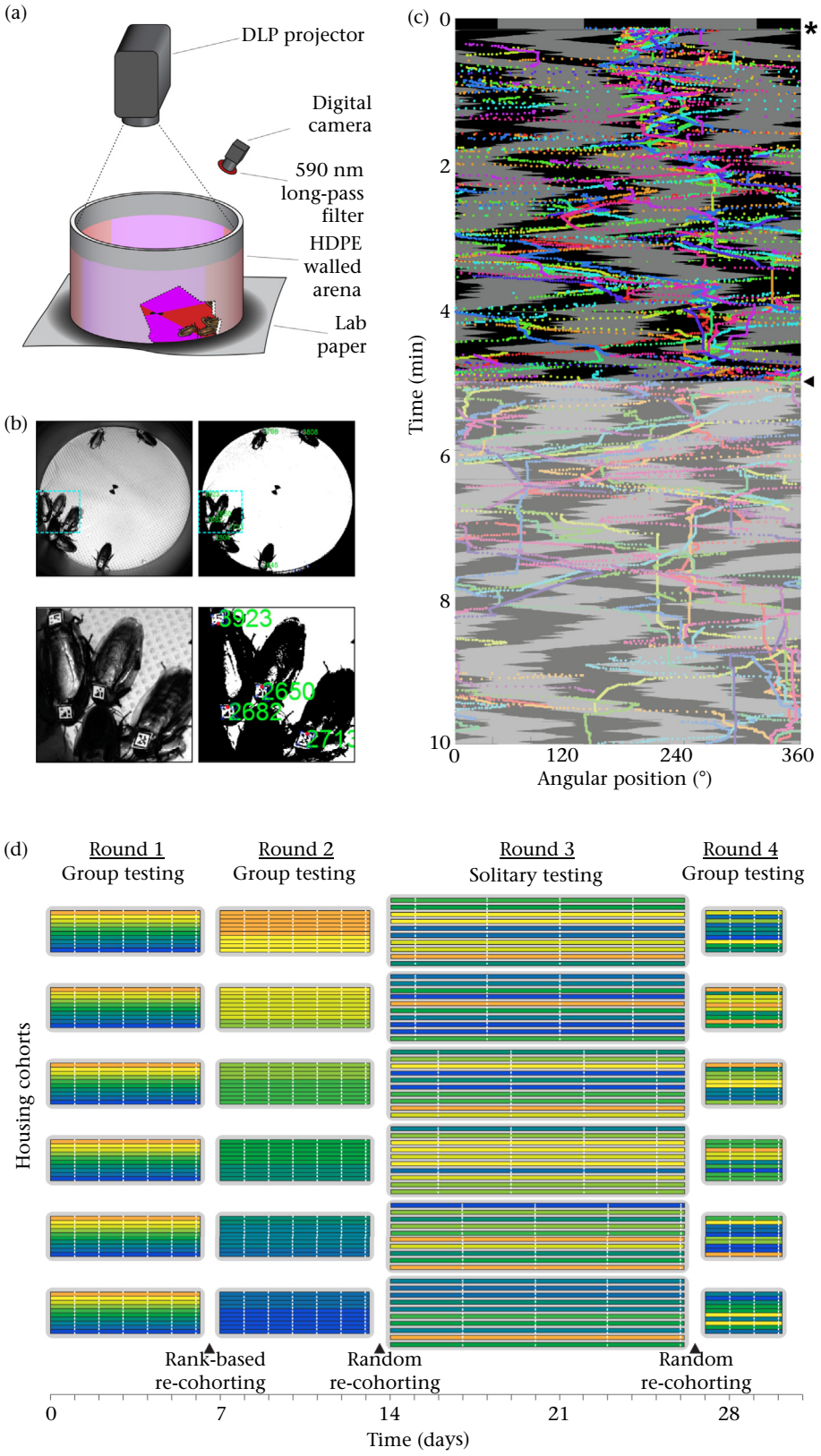

Figure 1. An automated tracking system monitored individual cockroach behaviour during group phototaxis. (a) Diagram of experimental set-up. Circular arena resting on absorbent laboratory paper directly under a projector that projected the moving stimulus onto the arena. A digital camera was positioned to capture the entire arena; the camera was filtered with a 590 nm long-pass filter to allow digital tracking through both light conditions. (b) Upper row: a still frame of the tracking video during a group trial (left) and the same image showing the number and location of identified tags. Lower row: inset images from each of the upper-row panels. (c) Kymograph with time running along the vertical axis, depicting cockroach angular position in the arena as it relates to the angular position of shaded and lit regions over time. The black region corresponds to the red zone of the arena and the grey region corresponds to the magenta zone. Each cockroach has a unique colour trail throughout the timeline of the kymograph. Note that only the top half, or the first 5 min, of the kymograph was used in the analysis. (d) Cohort composition during each of the four rounds of trials. Round 2 cohorts were determined based on tracking performance in Round 1; cohorts for Rounds 1, 3 and 4 were randomly selected. Colours illustrate hypothetical tracking performance.

Automated Behavioural Analysis

All recordings were saved in raw monochromatic .avi format and processed using custom scripts in MatLab (Mathworks, Natick, MA, U.S.A.). For control experiments comparing tagged and untagged cockroaches, we imported movies and collected 50 evenly spaced frames throughout the recording. We combined the frames using a median filter to generate an image of the empty arena for background subtraction. We thresholded the subtracted images and reduced noise by eroding and dilating above threshold pixels until only the outlines of the cockroaches remained. In solitary control trials, we considered the centre of a convex hull surrounding the cockroach's outline to be the animal's position. In three animal trials, we calculated the aggregation index as the area enclosed by the convex hull surrounding all outlines.

We extracted BEEtag positions from thresholded images using published code (Crall et al., 2015). For each trial, we marked the centre of the arena manually upon running the MATLAB script. To determine an optimal image threshold for tag identification, we chose a sample of frames from throughout the recording and then systematically varied the thresholds. The threshold identifying the greatest number of tags from those sample frames was used for the whole movie. Based on the indicated centre of the arena, we translated the cockroach positions into polar coordinates, and chose the angular coordinate as the focus for analysis. Sometimes tracking of the position of the red sectors generated errors (e.g. when a cockroach walked over the small black targeting sectors). To address this, we used an interpolation script to make a 'best guess' estimate of the sector positions for each frame. Individuals were untrackable on some frames due to motion blur, foreshortening of the BEEtags, being obscured by other cockroaches, being flipped upside down, or (rarely) walking through the unilluminated black targeting sectors. We replaced these missing values with values linearly interpolated across the gap of missing values (Movie S3). We calculated average instantaneous speeds for each cockroach as a proxy for activity. Average velocity within a trial was highly correlated with portion of time spent moving, since cockroaches had a relatively characteristic speed when moving, and we therefore only included average speed in our analyses here.

Statistics

We calculated ANOVAs and regression analyses in MatLab or R (R Foundation for Statistical Computing, Vienna, Austria) with built-in functions. For all ANOVAs, individual cockroaches provided the independent grouping variables. We estimated repeatability of individual behaviour within rounds with the intraclass correlation coefficient (ICC) in the ICC package in R (Wolak, Fairbairn, & Paulsen, 2011).

RESULTS

In control experiments, we found that both tagged and untagged cockroaches preferred the shaded portion of the arena, showing no conspicuous differences in either tracking performance (Fig. S1a) or speed (Fig. S1b). The tagging treatment caused no significant differences in the distribution of aggregation index scores of groups of three animals (Fig. S1c). Thus, the application of BEEtags did not appear to significantly alter naturalistic behaviour.

We measured the shade-tracking performance of each of the six experimental cohorts in Round 1 six times each over successive days (Fig. 1d). Cockroaches tracked the shaded sectors (Fig. 1c, Movie S1), although they exhibited habituation to the stimulus over the course of 10 min (Supplementary Fig. S2). We chose a cutoff of 5 min for further trials to capture the highest shade-tracking performance.

Cockroaches showed significant interindividual variation in tracking performance (one-way ANOVA: $F_{60,291} = 3.599$, $P < 10^{-6}$; repeatability (estimated ICC (95% CI)) = 0.31 (0.20–0.44); Fig. 2a, Supplementary Table S1). The best-tracking cockroaches avoided the light ~75% of the time, while the poorest trackers avoided it ~55% of the time. The distribution of tracking performance appeared to be roughly Gaussian. Individual shade-tracking performance was stable across the six trials within Round 1, which spanned 6 days (Fig. 2b). Notably, individual tracking performance, averaged across trials, was not correlated with the speed of individuals, averaged across trials (Pearson correlation: $r_{60} = 0.13$, $P = 0.31$; Supplementary Fig. S3). Because of this individual variation in tracking performance, cohorts also varied in their mean tracking performance across trials (Fig. S4).

For Round 2, the cockroaches were placed in new experimental cohorts, based on their ranked tracking performance within their respective Round 1 cohorts (Fig. 1d). The best-performing individuals from each Round 1 cohort were placed together into a single Round 2 cohort, etc. As in Round 1, consistent interindividual variation in tracking was observed in Round 2 (one-way ANOVA: $F_{58,295} = 2.443$, $P < 10^{-6}$; repeatability (95% CI) = 0.20 (0.10–0.32); Supplementary Fig. S5a, Table S1), which persisted across days (Supplementary Fig. S5b). Likewise, cohorts in Round 2 varied in their average tracking performance (Supplementary Fig. S4b). Individual tracking performance in Round 2 was significantly correlated with individual tracking performance in Round 1 (Pearson correlation: $r_{58} = 0.58$, $P < 0.0001$; Fig. 3a). Individuals that tracked well in Round 1 continued to track well in Round 2, and individuals that tracked poorly in Round 1 continued to track poorly in Round 2. The overall tracking performance of each cohort in Round 2 was not significantly different from a prediction based on the average performance of its members in Round 1 (multiple comparisons corrected t test: $2.37 > t_{18} > 0.062$, $0.16 < P < 0.99$; Fig. 3b). Thus, individual tracking performance in a group context appears to be robust to group composition.

In Round 3, individuals were tested alone to see if the observed idiosyncratic behaviour, evident in groups, appears in a solitary context. All individuals were randomly assigned to six new housing groups of 10 individuals (Fig. 1d). From these housing cohorts, individuals were removed and tested alone under the same stimulus conditions as the earlier group tests (Movie S2). Concordant with previous results on collective light-avoidance behaviour in cockroaches, the average tracking performance in solitary trials was significantly lower than in-group trials (Supplementary Fig. S6).

Cockroaches in Round 3 demonstrated consistent interindividual variation in tracking performance in the solitary trials (one-way ANOVA: $F_{58,176} = 1.821$, $P = 0.0015$; repeatability (95% CI) = 0.17 (0.05–0.32); Fig. 4a, Supplementary Table S1), which persisted over days (Supplementary Fig. S5c). Individual tracking performance (average of four Round 3 trials) in the solitary context was uncorrelated with tracking performance in the group context (average of six Round 2 trials) (Pearson correlation: $r_{58} = 0.094$, $P = 0.48$; Fig. 4b). Thus, the individual shade-tracking performance observed in group contexts disappeared during solitary trials. In its place, new, consistent individual tracking performance levels appeared during solitary trials. As expected, the average tracking performance was lower in the solitary context than in the group context (Fig. 4a).

The final experiments (Round 4) examined whether individual tracking performance levels would re-emerge when animals were restored to the group context during experiments. This was an important control when considering the possibility that over time and repeated manipulation the behaviour of the cockroaches may

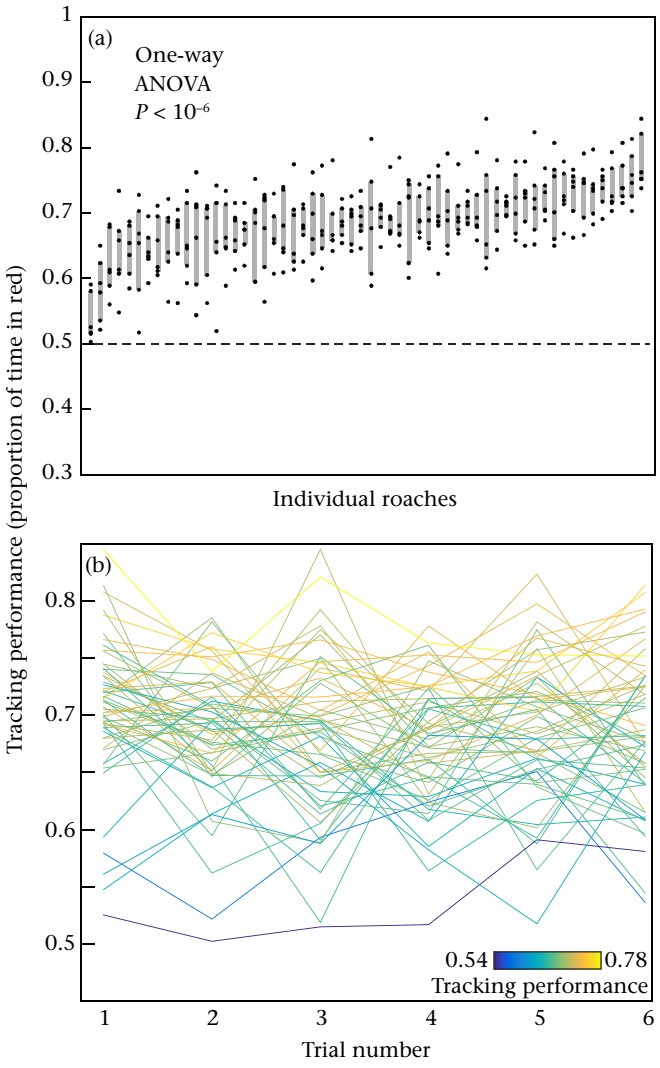

Figure 2. (a) Proportion of time that each cockroach spent in the shaded region (i.e. tracking performance) for each of the six Round 1 trials. A shaded region indicate the interquartile range. The cockroaches are sorted by average tracking performance. Dotted line shows the null expectation of a tracking performance of 0.5. (b) Each cockroach's tracking performance across all six trials of Round 1. Line colours indicate average tracking performance for that individual.

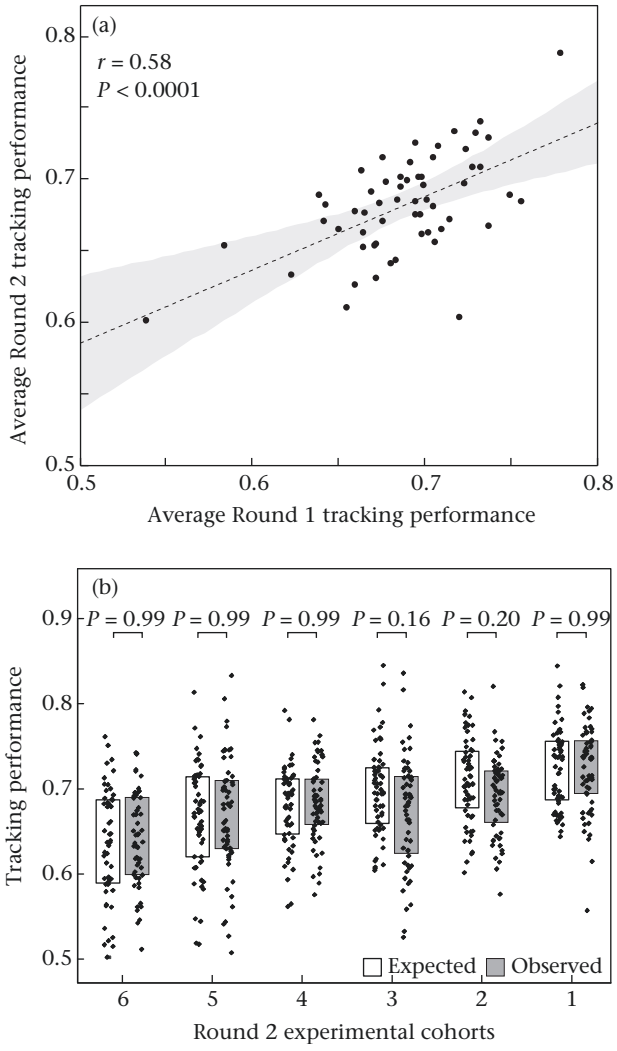

Figure 3. (a) Scatterplot of average individual performance in Round 2 versus Round 1. Dotted line indicates linear fit. Shaded region indicates the 95% confidence interval on the linear regression. (b) Expected (white) and observed (grey) distributions of individual trial tracking performance, by experimental cohort. Expected values are based on the per-trial performance of each cohort's members in Round 1. P values were corrected for $k = 6$ multiple comparisons using the formula $p^* = 1 - (1 - p)^k$.

have drifted (Ridgel, Ritzmann, & Schaefer, 2003), which could trivially explain the lack of correlation between tracking performance between Round 3 and earlier Rounds. When individuals were randomly assigned to new experimental cohorts (Fig. 1d), the observed individual tracking performances from Round 2 re-emerged. Average tracking performance was significantly correlated between Rounds 2 and 4 across individuals ($r_{57} = 0.39$, $P = 0.0023$; Fig. 5). Individual tracking performance in Round 4 was significantly correlated with Round 1 performance as well. Thus, all pairwise comparisons between Rounds of individual tracking performance in the group context were significantly correlated (Table 1). Conversely, the individual tracking performance in the solitary context was not significantly correlated with individual performance in any other Rounds (Table 1). As before, tracking performance showed significant interindividual variation (one-way ANOVA: $F_{1,57} = 1.834$, $P = 0.0032$; repeatability = 0.22 (0.06–0.40); Supplementary Fig. S5d, Table S1) and persistence across days (Supplementary Fig. S5e). As expected, cohorts in Round 4 differed in their average tracking performance (Supplementary Fig. S4c).

DISCUSSION

Our results demonstrate that cockroaches have individually consistent variation in shade-tracking performance (Figs. 1 and 2). We show that this idiosyncratic cockroach behaviour is robust to group composition (Fig. 3) and is consistent over the course of several weeks (Fig. 5), but surprisingly does not persist when cockroaches are tested in isolation from a group (Fig. 4). Overall, these findings show that idiosyncratic behaviour is modulated by social context in cockroaches. While previous work has investigated how individual behavioural variation affects group performance in different classes of organisms (Briffa, 2013; Burns, Herbert-Read, Morrell, & Ward, 2012; Marras & Domenici, 2013; Millor, Amé, Halloy, & Deneubourg, 2006; Pruitt & Keiser, 2014), it is less well understood how group membership influences individual behavioural performance.

These results have important implications for understanding the dynamics of collective decision making in animals. Despite increasing focus on both collective decision making (Arganda, Pérez-Escudero, & de Polavieja, 2011; Planas-Sitjà et al., 2015)

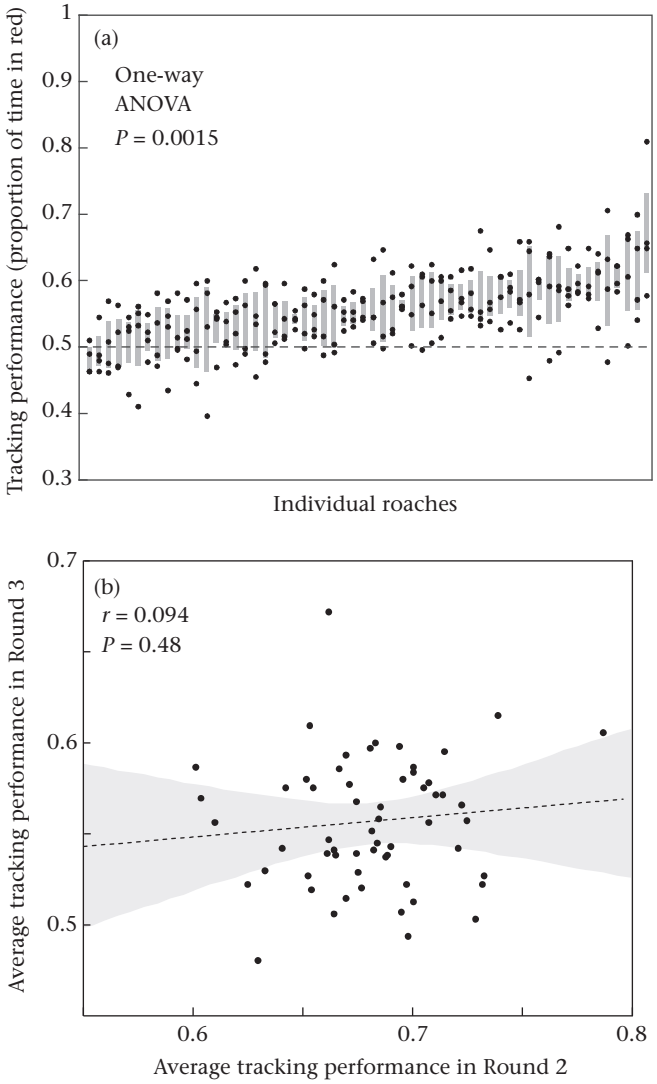

Figure 4. (a) Tracking performance for each of the six Round 3 trials. Shaded regions show interquartile range. (b) Scatterplot of average individual performance in Round 3 versus Round 2. Dotted line indicates linear fit. Shaded region indicates the 95% confidence interval on the linear regression.

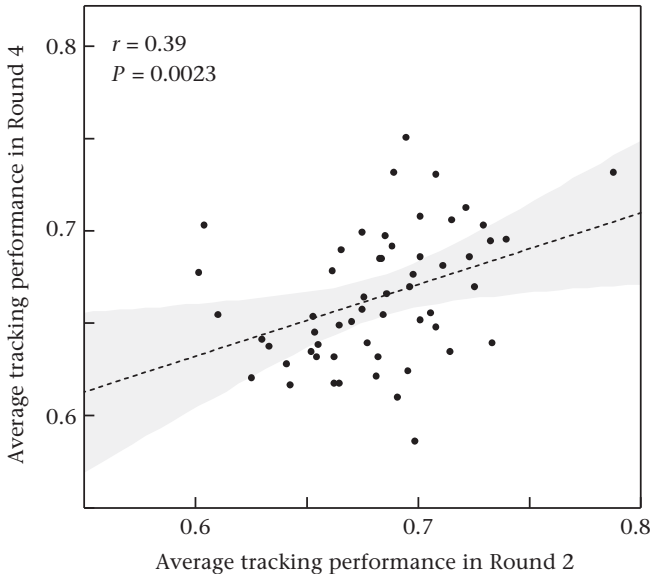

Figure 5. Scatterplot of average individual tracking performance in Round 4 versus Round 2. Dotted line indicates linear fit. Shaded region indicates the 95% confidence interval on the linear regression.

Table 1
Pairwise Pearson correlation coefficients (r) across tracking performances of individual cockroaches (averaged across trials) between all rounds

	Round 2	Round 3	Round 4
Round 1			
r	0.58	0.10	0.38
P	<0.001	0.45	0.003
Round 2			
r		0.094	0.39
P		0.48	0.002
Round 3			
r			0.19
P			0.15

and consistent interindividual variation (i.e. personality; Burns et al., 2012; Santos, Neupert, Lipp, Wikelski, & Dechmann, 2014) in animals, the role of group heterogeneity in collective decision making of animals, particularly in gregarious insects, remains a nascent research area. Where attempts have been made to understand the role of group heterogeneity in collective behaviour, this has typically been done by measuring personalities when individuals are separated (Briffa, 2013; Brown & Irving, 2013; Pruitt & Keiser, 2014). This approach might not always be valid, however, because our results show that individual differences can be substantially modified by group context.

What drives individual behavioural variation in cockroach groups? One hypothesis for this variation could be the dichotomy between bold and shy (Frost, Winrow-Giffen, Ashley, & Sneddon, 2007; Sinn, Gosling, & Moltschaniwskyj, 2008) or sitter–rover (de Belle & Sokolowski, 1987) personalities present in a wide variety of animals (Sih, Bell, & Johnson, 2004), since both higher activity level and higher portion of time in light could be considered characteristics of bold individuals. Especially for a mobile stimulus as used here, it is possible that more active individuals would perform better at tracking since they must actively search out the preferred stimulus. In our experiments, however, there was no relationship between activity level (i.e. velocity) and tracking performance (Supplementary Fig. S3, Movie S2).

Individual variation may also be produced dynamically in the presence of a social group, either by the presence of social hierarchies (Chase, 1980), or by social niche differentiation (Bergmüller & Taborsky, 2010). However, this does not appear to be the case in the experiments described here, since individuals did not shift behaviour in response to group composition shuffling (Fig. 3) as would be expected from individual behavioural variation that emerges dynamically from the establishment of social hierarchies (Bell, Gorton, Tourtellot, & Breed, 1979).

Although it is still possible that social niche differentiation plays a role in increasing behavioural variation among individual cockroaches, this effect would have to occur on a timescale of at least several weeks, since cockroaches housed together in new groups with lower behavioural variation (Round 2 above) for 1 week continuously showed no significant shift in their individual tracking performance. Alternatively, there may be a critical window for social niche construction, so that if an individual joins a niche sufficiently early in life, it will stay in that niche permanently even if re-grouped among individuals in the same niche. Even in this case, however, this social niche construction would seem to apply only in social contexts, since it disappeared when individuals were tested in isolation.

Another potential source of individual variation could be individual experience (Ravary et al., 2007), for example arising from microenvironmental differences. However, for two reasons, we believe that environmental differences are unlikely to explain the sudden change in individual behaviours seen when animals were transferred to the solitary context. First, we were careful to match their environmental circumstances during the experiments (i.e. matching their social conditions with constant group size housing; matching their visual experience by storing them in dark containers when not conducting experiments; making sure that all experimental handling was done by each experimenter across the whole cohort, rather than across subsets of animals). Second, the re-emergence in Round 4 of the individual behaviours observed in Rounds 1 and 2 would be statistically improbable if environmental fluctuations explained the behavioural differences that occurred between Rounds 3 and 4.

As we observed, the correlation in individual shade-tracking performance between solitary and group contexts was very weak, and could plausibly be less than zero ($r_{58} = 0.094$ between rounds 2 and 3; bootstrap resampling: 95% CI = −0.19–0.37). The weaker correlation between solitary and group performance cannot be explained by sampling error alone, as all within-condition correlations (e.g. between pairs of Rounds 1, 2, 4) were above the 95% CI of the solitary∗group correlation.

A possible mechanism at play is that individuals vary in social cohesion (i.e. are more or less likely to stay next to other cockroaches), and this drives interindividual variation in tracking performance, but only in the group context. Attraction to conspecifics is important in many aspects of social behaviour (e.g. collective motion: Berdahl, Torney, Ioannou, Faria, & Couzin, 2013; habitat selection: Stamps, 1988), and interindividual variation in social cohesion can be important in structuring social behaviour (see, e.g. Wey & Blumstein, 2010). Since group-tracking performance was generally much higher than tracking performance of separated individuals (Supplementary Fig. S6), individuals that are more likely to stay with a group are also more likely to have higher average tracking performance than individuals that ignore the presence of others. However, the intensity of social cohesion among individual cockroaches would have no necessary bearing on performance when alone. This might explain the lack of correlation between individual performance levels in the solitary and group contexts (Fig. 4). One way of testing this hypothesis in future work might be to examine interindividual variation in levels of social cohesion, for example by measuring the amount of time cockroaches spend in proximity to a constrained group of other cockroaches in a behavioural arena. This test could be done in either the presence or the absence of a light stimulus to investigate the interaction between social and visual stimuli.

This hypothesis highlights an important result of our experiments, namely that parameters driving individual behavioural performance in isolation may not have simple relationships to the parameters relevant for the same task when performed in a group. For example, in the group context, the probability of stopping next to another cockroach might be the single most important factor in determining tracking performance, while in isolation other behavioural parameters (e.g. velocity differences when in versus out of the shade stimulus, etc.) may be much more relevant. If the correlation between individual performance in the group and solitary contexts is strictly zero, or negative, this implies that the cues driving shade tracking in both the solitary and group contexts (such as visual information) interact nonlinearly with the cues present only in the group context (such as conspecific odour or tactile cues). If the interaction were linear, better-than-average exploitation of solitary cues would invariably be helpful in the group context, imparting a positive correlation. A slightly positive correlation could arise if significantly more linear weight were given to group-only cues; alternatively, the presence of group-only cues could gate the processing of solitary cues. In humans, social context modulates numerous sensory channels including nociception (Krahé, Springer, Weinman, & Fotopoulou, 2013) and vision–touch integration (Heed, Habets, Sebanz, & Knoblich, 2010).

In agreement with previous findings (Canonge et al., 2011; Salazar et al., 2013), we found that cockroach groups outperformed individuals at tracking a shade stimulus (Supplementary Fig. S6). We hypothesize that this difference is due to the lack of information sharing typically associated with the presence of conspecifics and aggregation behaviour. The presence of conspecifics enhances public information sharing, which has been shown to be important for a variety of collective decision-making tasks (Miller, Garnier, Hartnett, & Couzin, 2013), including locating shelters in cockroaches (Canonge et al., 2011).

One important consideration when interpreting the results of any longitudinal behaviour study in animals is the potential for time and physical injury to have influenced behaviour. Ageing has been associated with neural degradation that affects not only gait mechanics but also the neural pathways associated with escape behaviours (Ridgel et al., 2003). While not statistically significant, our experiments showed a tendency towards lower tracking performance in Round 4 when compared to Rounds 1 and 2 (Fig. S6), as well as weaker correlations between individual performance in Round 4 and Rounds 1 and 2 than was first observed between experimental Rounds 1 and 2 (Fig. 5). These results suggest there may be at least weak levels of both behavioural drift and performance degradation.

Interestingly, cockroaches displayed the least individual consistency (i.e. the lowest repeatability) in the solitary context (Supplementary Table S1). This result is consistent with the emergence of more stable individual behavioural patterns within a group context, as has been observed in solitary ant queens and suggested to play an important role in division of labour in insect colonies (Fewell & Page, 1999).

Most broadly, our results highlight the importance of considering group context when examining behaviour in animals. For animals exhibiting any degree of social behaviour, from occasionally gregarious animals to the highly eusocial insects, groups are not only composed of individuals of different types, but may also play an active role in modulating and creating individual variation in collective behaviours.

Acknowledgments

We thank Clark Magnan, Ed Soucy and Joel Greenwood for help with implementing experiments.

Supplementary Material

Supplementary material associated with this article can be found, in the online version, at http://dx.doi.org/10.1016/j.anbehav.2015.10.032.

References

Arganda, S., Pérez-Escudero, A., & de Polavieja, G. G. (2011). A common rule for decision making in animal collectives across species. *Proceedings of the National Academy of Sciences of the United States of America, 109*(50), 20508–20513.

Bell, W. J., Gorton, R. E., Tourtellot, M. K., & Breed, M. D. (1979). Comparison of male agonistic behaviour in five species of cockroaches. *Insect Sociaux, 26*(3), 252–263.

de Belle, J. S., & Sokolowski, M. B. (1987). Heredity of rover/sitter: alternative foraging strategies of *Drosophila melanogaster* larvae. *Heredity, 59*, 73–83.

Bengston, S. E., & Jandt, J. M. (2014). The development of collective personality: the ontogenetic drivers of behavioural variation across groups. *Frontiers in Ecology and Evolution, 2*, 81. http://dx.doi.org/10.3389/fevo.2014.00081.

Berdahl, A., Torney, C. J., Ioannou, C. C., Faria, J. J., & Couzin, I. D. (2013). Emergent sensing of complex environments by mobile animal groups. *Science, 339*(6119), 574–576. http://dx.doi.org/10.1126/science.1225883.

Bergmüller, R., & Taborsky, M. (2010). Animal personality due to social niche specialisation. *Trends in Ecology & Evolution, 25*(9), 504–511.

Briffa, M. (2013). The influence of personality on a group-level process: shy hermit crabs make longer vacancy chains. *International Journal of Behavioral Biology, 119*(11), 1014–1023.

Brown, C., & Irving, E. (2013). Individual personality traits influence group exploration in a feral guppy population. *Behavioral Ecology, 25*(1), 95–101.

Buchanan, S. M., Kain, J. S., & de Bivort, B. L. (2015). Neuronal control of locomotor handedness in *Drosophila*. *Proceedings of the National Academy of Sciences of the United States of America, 112*, 6700–6705. http://dx.doi.org/10.1073/pnas.1500804112.

Burns, A., Herbert-Read, J., Morrell, L., & Ward, A. (2012). Consistency of leadership in shoals of mosquitofish (*Gambusia holbrooki*) in novel and in familiar environments. *PLoS One, 7*(5), e36567.

Canonge, S., Deneubourg, J. L., & Sempo, G. (2011). Group living enhances individual resources discrimination: the use of public information by cockroaches to assess shelter quality. *PLoS One, 6*(6), e19748.

Canonge, S., Sempo, G., Jeanson, R., Detrain, C., & Deneubourg, J. L. (2009). Self-amplification as a source of interindividual variability: shelter selection in cockroaches. *Journal of Insect Physiology, 55*(11), 976–982.

Chase, I. (1980). Social process and hierarchy formation in small groups: a comparative perspective. *American Sociological Review, 45*(6), 905–924.

Crall, J., Gravish, N., Mountcastle, A. M., & Combes, S. A. (2015). BEEtag: a low cost image based tracking system for the study of animal behaviour and locomotion. *PLoS One, 10*(9), e0136487.

Fewell, J. H., & Page, R. E., Jr. (1999). The emergence of division of labour in forced associations of normally solitary ant queens. *Evolutionary Ecology Research, 1*, 537–548.

Freund, J., Brandmaier, A. M., Lewejohann, L., Kirste, I., Kritzler, M., Krüger, A., et al. (2013). Emergence of individuality in genetically individual mice. *Science, 340*(6133), 756–759.

Frost, J., Winrow-Giffen, A., Ashley, P., & Sneddon, L. (2007). Plasticity in animal personality traits: does prior experience alter the degree of boldness. *Proceedings of the Royal Society B: Biological Sciences, 274*, 333–339.

Gempe, T., Stach, S., Bienefeld, K., & Beye, M. (2012). Mixing of honeybees with different genotypes affects individual worker behaviour and transcription of genes in the neuronal substrate. *PLoS One, 7*(2), e31653.

Heed, T., Habets, B., Sebanz, N., & Knoblich, G. (2010). Others' actions reduce crossmodal integration in peripersonal space. *Current Biology, 20*(15), 1345–1349.

Hoffman, R. L. (1958). Homogeneity of member personality and its effect on group problem-solving. *58*(1), 27–32.

Hui, A., & Pinter-Wollman, N. (2014). Individual variation in exploratory behaviour improves speed and accuracy of collective nest selection by Argentine ants. *Animal Behaviour, 93*, 261–266.

Hunt, G. J., Guzman-Novoa, E., Uribe-Rubio, J. L., & Prieto-Merlos, D. (2003). Genotype–environment interactions in honeybee guarding behaviour. *Animal Behaviour, 66*, 459–467.

Jandt, J. M., Bengston, S., Pinter-Wollman, N., Pruitt, J. N., Raine, N. E., Dornhaus, A., et al. (2014). Behavioural syndromes and social insects: personality at multiple levels. *Biological Reviews, 89*, 48–67.

Jeanson, R., & Weindenmuller, A. (2014). Interindividual variability in social insects: proximate causes and ultimate consequences. *Biological Reviews, 89*, 671–687.

Kain, J. S., Stokes, C., & de Bivort, B. L. (2012). Phototactic personality in fruit flies and its suppression by serotonin and white. *Proceedings of the National Academy of Sciences of the United States of America, 109*(48), 19834–19839.

Keiser, C. N., Modlmeier, A. P., Singh, N., Jones, D. K., & Pruitt, J. N. (2014). Exploring how a shift in the physical environment shapes individual and group behavior across two social contexts. *Ethology, 120*(8), 825–833. http://dx.doi.org/10.1111/eth.12256.

Keiser, C. N., & Pruitt, J. N. (2014). Personality composition is more important than group size in determining collective foraging behaviour in the wild. *Proceedings of the Royal Society B: Biological Sciences, 281*(1796), 20141424.

Krahé, C., Springer, A., Weinman, J., & Fotopoulou, A. (2013). The social modulation of pain: others as predictive signals of salience, a systematic review. *Frontiers in Human Neuroscience, 7*, 386.

Laskowski, K. L., & Pruitt, J. N. (2014). Evidence of social niche construction: persistent and repeated social interactions generate stronger personalities in a social spider. *Proceedings of the Royal Society B: Biological Sciences, 281*(1783), 20133166. http://dx.doi.org/10.1098/rspb.2013.3166.

LeBoeuf, A. C., & Grozinger, C. M. (2014). Me and we: the interplay between individual and group behavioural variation in social collectives. *Current Opinion in Insect Science, 5*, 16–24.

Marras, S., & Domenici, P. (2013). Schooling fish under attack are not all equal: some lead, others follow. *PLoS One, 8*(6), e65784.

Miller, N., Garnier, S., Hartnett, A., & Couzin, L. (2013). Both information and social cohesion determine collective decisions in animal groups. *Proceedings of the National Academy of Sciences of the United States of America, 110*(13), 5263–5268.

Millor, J., Amé, J. M., Halloy, J., & Deneubourg, J. L. (2006). Individual discrimination capability and collective decision-making. *Journal of Theoretical Biology, 239*(3), 313–323.

Modlmeier, A. P., Keiser, C. N., Shearer, T. A., & Pruitt, J. N. (2014). Species-specific influence of group composition on collective behaviors in ants. *Behavioral Ecology and Sociobiology, 68*(12), 1929–1937. http://dx.doi.org/10.1007/s00265-014-1799-3.

Modlmeier, A. P., Keiser, C. N., Watters, J., Sih, A., & Pruitt, J. N. (2014). The keystone individual concept: an ecological and evolutionary overview. *Animal Behaviour, 89*, 53–62.

Modlmeier, A. P., Laskowski, K. L., DeMarco, A. E., Coleman, A., Zhao, K., Brittingham, H. A., et al. (2014). Persistent social interactions beget more pronounced personalities in a desert-dwelling social spider. *Biology Letters, 10*(8), 20140419. http://dx.doi.org/10.1098/rsbl.2014.0419.

Modlmeier, A. P., Liebmann, J. E., & Foitzik, S. (2012). Diverse societies are more productive: a lesson from ants. *Proceedings of the Royal Society B: Biological Sciences, 279*(1736), 2142–2150.

O'Donnell, S. (1998). Reproductive caste determination in eusocial wasps (Hymenoptera: Vespidae). *Annual Review of Entomology, 43*, 323–346.

van Oers, K., Klunder, M., & Drent, P. J. (2005). Context dependence of personalities: risk-taking behavior in a social and a nonsocial situation. *Behavioral Ecology, 16*(4), 716–723.

Parrish, P. K., & Edelstein-Keshet, L. (1999). Complexity, pattern, and evolutionary trade-offs in animal aggregation. *Science, 284*(5411), 99–101.

Petrovskii, S., Mashanova, A., & Jansen, V. A. A. (2011). Variation in individual walking behavior creates the impression of a lévy flight. *Proceedings of the National Academy of Sciences of the United States of America, 108*(21), 8704–8707.

Planas-Sitjà, I., Deneubourg, J. L., Gibon, C., & Sempo, G. (2015). Group personality during collective decision-making: a multi-level approach. *Proceedings of the Royal Society B: Biological Sciences, 282*, 20142515. http://dx.doi.org/10.1098/rspb.2014.2515.

Pruitt, J. N., & Keiser, K. N. (2014). The personality types of key catalytic individuals shape colonies' collective behaviour and success. *Animal Behaviour, 93*, 87–95.

Pruitt, J. N., & Riechert, S. E. (2011). How within-group behavioural variation and task efficiency enhance fitness in a social group. *Proceedings of the Royal Society B: Biological Sciences, 278*(1709), 1209–1215.

Ravary, F., Lecoutey, E., Kaminski, G., Châline, N., & Jaisson, P. (2007). Individual experience alone can generate lasting division of labor in ants. *Current Biology, 17*(15), 1308–1312.

Ridgel, A., Ritzmann, R., & Schaefer, P. (2003). Effects of aging on behaviour and leg kinematics during locomotion in two species of cockroaches. *Journal of Experimental Biology, 206*(24), 4453–4465.

Salazar, M. O. L., Deneubourg, J. L., & Sempo, G. (2013). Information cascade ruling the fleeing behaviour of a gregarious insect. *Animal Behaviour, 85*(6), 1271–1285.

Santos, C. D., Neupert, S., Lipp, H. P., Wikelski, M., & Dechmann, D. K. N. (2014). Temporal and contextual consistency of leadership in homing pigeon flocks. *PLoS One, 9*(7), e10277.

Schuett, W., & Dall, S. R. X. (2009). Sex differences, social context and personality in zebra finches, *Taeniopygia guttata*. *Animal Behaviour, 77*, 1041–1050.

Schuett, W., Dall, S. R. X., Baeumer, J., Kloesener, M. H., Nakagawa, S., Beinlich, F., et al. (2011). 'Personality' variation in a clonal insect: the pea aphid, *Acyrthosiphon pisum*. *Developmental Psychobiology, 53*(6), 631–640.

Sempo, G., Canonge, S., Detrain, C., & Deneubourg, J. L. (2009). Complex dynamics based on a quorum: decision-making process by cockroaches in a patchy environment. *Ethology, 115*, 1150–1161.

Sih, A., Bell, A., & Johnson, J. C. (2004). Behavioral syndromes: an ecological and evolutionary overview. *Trends in Ecology & Evolution, 19*(7), 372–378.

Sinn, D. L., Gosling, S. D., & Moltschaniwskyj, N. A. (2008). Development of shy/bold behaviour in squid: context-specific phenotypes associated with developmental plasticity. *Animal Behaviour, 75*, 433–442.

Stamps, J. A. (1988). Conspecific attraction and aggregation in territorial species. *American Naturalist, 131*(3), 329–347.

Stamps, J. A., Saltz, J. B., & Krishnan, V. V. (2013). Genotypic differences in behavioural entropy: unpredictable genotypes are composed of unpredictable individuals. *Animal Behaviour, 86*, 641–649.

Treherne, J. E., & Foster, W. A. (1980). The effects of group size on predator avoidance in a marine insect. *Animal Behaviour, 28*(4), 1119–1122.

Uzsák, A., & Schal, C. (2013). Social interaction facilitates reproduction in male German cockroaches, *Blattella germanica*. *Animal Behaviour, 85*, 1501–1509.

Vindenes, Y., Engen, S., & Sæther, B. E. (2008). Individual heterogeneity in vital parameters and demographic stochasticity. *American Naturalist, 171*(4), 455–467.

Walther, J. B. (1958). Changes induced in spectral sensitivity and form of retinal action potential of the cockroach eye by selective adaptation. *Journal of Insect Physiology, 2*(2), 142–151.

Wey, T. W., & Blumstein, D. T. (2010). Social cohesion in yellow-bellied marmots is established through age and kin structuring. *Animal Behaviour, 79*, 1343–1352.

Winston, M. L., & Michener, C. D. (1977). Dual origin of highly social behaviour among bees. *Proceedings of the National Academy of Sciences of the United States of America, 74*(3), 1135–1137.

Wolak, M. E., Fairbairn, D. J., & Paulsen, Y. R. (2011). Guidelines for estimating repeatability. *Methods in Ecology and Evolution, 3*(1), 129–137. http://dx.doi.org/10.1111/j.2041-210X.2011.00125.x.